

9. SITE 702¹

Shipboard Scientific Party²

HOLE 702A

Date occupied: 13 April 1987
Date departed: 13 April 1987
Time on hole: 14 hr
Position: 50°56.786' S, 26°22.127' W
Bottom felt (rig floor; m; drill-pipe measurement): 3093.9
Distance between rig floor and sea level (m): 10.50
Water depth (drill-pipe measurement from sea level; corrected m): 3083.4
Total depth (rig floor; corrected m): 3127.0
Penetration (m): 33.1
Number of cores: 4
Total length of cored section (m): 33.1
Total core recovered (m): 34.21
Core recovery (%): 103
Oldest sediment cored:
Depth sub-bottom (m): 33.1
Nature: nannofossil ooze
Age: late Eocene
Measured velocity (km/s): 1.64 at 32.10 mbsf

HOLE 702B

Date occupied: 13 April 1987
Date departed: 15 April 1987
Time on hole: 2 days, 7 hr
Position: 50°56.786' S, 26°22.117' W
Bottom felt (rig floor; m; drill-pipe measurement): 3094.2
Distance between rig floor and sea level (m): 10.50
Water depth (drill-pipe measurement from sea level; corrected m): 3083.7
Total depth (rig floor; corrected m): 3388.5
Penetration (m): 294.3
Number of cores: 32
Total length of cored section (m): 294.3
Total core recovered (m): 195
Core recovery (%): 66
Oldest sediment cored:
Depth sub-bottom (m): 294.3
Nature: silicified limestone
Age: late Paleocene
Measured velocity (km/s): 4.46 at 287.83 mbsf

Principal results: Site 702 is located on the central part of the Islas Orcadas Rise (50°56.786' S, 26°22.117' W; water depth of 3083.4 m), a north-northwest-trending aseismic ridge more than 500 km long, 50–100 km wide, and over 1000 m above the adjacent seafloor. The Islas Orcadas Rise and Meteor Rise were once conjugate features, prior to seafloor spreading that separated them in the Eocene. The major objectives of this site were: (1) to determine the age, nature, and subsidence history of the Islas Orcadas Rise and (2) to investigate the influence of the shallow Islas Orcadas and Meteor rises on oceanic water-mass communication between the southern high-latitude region and the South Atlantic. The objectives of this site originally were intended to be addressed by drilling on the Meteor Rise; however, the basal stratigraphic sequence and basement of these once conjugate features were considered more accessible at Site 702 on the Islas Orcadas Rise. Bad weather and problems with deep holes during Leg 114 precipitated the cautious decision to pursue these objectives at sites on both the Islas Orcadas and Meteor Rise. An additional consideration for selecting this site was the prospect of reaching basement to test the Navidrill coring system.

Site 702 consists of two holes: Hole 702A, with four cores taken with the advanced hydraulic piston corer (APC) to a depth of 33.1 m below seafloor (mbsf) for 100% recovery, and Hole 702B, with 3 APC cores and 29 cores taken with the extended core barrel (XCB) system to 294.3 mbsf, with 195.2 m recovered (66.3%). Sediment recovery was good (87%) to a depth of 205 mbsf, but dropped sharply below this depth because of the occurrence of frequent chert stringers. The Navidrill was deployed and tested on a silicified limestone encountered at 294 mbsf, but no material was retrieved, and the site was abandoned because of insufficient time to trip the drill string to deploy the rotary coring system.

The stratigraphic section at Hole 702B consists of a thin layer of diatom ooze and nannofossil-diatom ooze above a thick sequence of pelagic carbonates, with increasing lithification downhole. The dominant lithologies and ages of the stratigraphic sequence are as follows:

0–6.65 mbsf: diatom ooze and mud with frequent dropstones, manganese nodules and staining; late Miocene to Quaternary age;
6.65–22.15 mbsf: nannofossil-diatom ooze with dropstones, manganese nodules and dispersed ash layers; late Miocene age;
22.15–33.1 mbsf: nannofossil ooze; late Miocene age;
33.1–202.45 mbsf: nannofossil chalk; early Eocene age;
202.45–294.3 mbsf: indurated nannofossil chalk with thin chert layers and a basal silicified limestone; early late Paleocene to early Eocene age.

Most of the older sedimentary sequence of the Islas Orcadas Rise–Meteor Rise aseismic ridge system was obtained at Site 702. This predominantly lower upper Paleocene–upper Eocene section represents a ~20-m.y. history of pelagic carbonate sedimentation during a period that precedes and postdates the rifting of these aseismic ridges. Although basement was not reached, the age of the Islas Orcadas Rise was further constrained to be older than ~62 Ma. A Late Cretaceous age for the rise is suggested by reworked planktonic foraminifers and calcareous nannofossils present in the basal 20 m of the section, about 150 m above basement. An early Eocene episode of extension generated numerous small half-grabens over much of the rise, and a major post-late Eocene to pre-late middle Miocene tectonic event formed a north-trending horst through the Site 702 location.

Site 702 is the fifth site on Leg 114 to recover a significant representation of Eocene and Paleocene sediments. Sites 698–702 recov-

¹ Ciesielski, P. F., Kristoffersen, Y., et al., 1988. *Proc. ODP, Init. Repts.*, 114: College Station, TX (Ocean Drilling Program).

² Shipboard Scientific Party is as given in the list of Participants preceding the contents.

ered 1027 m of Paleocene to Eocene sediments, providing the most complete stratigraphic representation of this interval yet obtained from the Southern Ocean.

A relatively complete succession of magnetic polarity zones was identified between approximately 20 and 205 mbsf. Good core recovery (86%) and relatively little core disturbance in this interval resulted in identification of early to late Eocene Chrons C22R through C16N. This magnetostratigraphic framework adds to our previous paleomagnetic representation of the Late Cretaceous–earliest Paleocene, late Oligocene, late Miocene, and Pliocene to Quaternary. These sections will make a significant contribution toward age calibration of high-latitude biozones and paleoenvironmental history.

Sedimentation rates at Site 702 were about 10 m/m.y. during the late Paleocene to early middle Eocene and increased to 14 m/m.y. during the rest of the middle Eocene. A major hiatus of ~29–33 m.y. (~24 mbsf) spans the uppermost Eocene to upper Miocene. Additional hiatuses of yet undetermined duration occur in the 24-m-thick upper Miocene to Quaternary section.

Calcareous microfossils are abundant throughout the Eocene section, where the carbonate content is generally 85% to 95%, but are less abundant in the upper Miocene, where the carbonate content declines to no more than 40% to 70%. Siliceous microfossils are abundant in the Neogene, persist down to the upper lower Eocene, and are absent in the remainder of the sequence, except for the lower upper Paleocene where they are again present. As was the case at the previous sites, Paleogene sequences without biosiliceous microfossils were attributed to dissolution of biosiliceous opal and its downward diffusion to form zeolites, chert, or porcellanite.

Calcareous microfossils record a similar history of surface-water cooling, as reported in more detail in the preceding site chapters. Assemblages reveal relative warmth during the late Paleocene, a brief but not severe cooling near the Paleocene/Eocene boundary, maximum warmth during the early Eocene, cooling during the middle Eocene, and the establishment of even cooler conditions during the late Eocene when assemblages developed a true high-latitude affinity. Benthic foraminifers suggest a Paleocene water depth of 1000–2000 m; however, sediments of this age contain transported shallow-water organisms such as bivalves, echinoid spines, and ostracodes. If the Islas Orcadas Rise is Cretaceous in age, as reworked faunas and floras suggest, intermediate- to deep-water exchange of antarctic waters with the South Atlantic may have been severely inhibited during the Late Cretaceous to early Paleogene by the Falkland Plateau and Falkland Fracture Zone, the Islas Orcadas and Meteor rises, and the Agulhas Plateau and Agulhas Fracture Zone.

BACKGROUND AND OBJECTIVES

Site 702 is located on the central part of the Islas Orcadas Rise, an aseismic ridge more than 500 km long and 90 to 180 km wide, with a strike of ~330° and a maximum relief of ~2 km. The rise, named after the ship of discovery *ARA Islas Orcadas*, forms the eastern boundary of the Georgia Basin (Fig. 1) and intersects the eastern terminus of the Falkland Fracture Zone at 49.5°S, 28°W (LaBrecque and Hayes, 1979). The Islas Orcadas Rise is thought to have been generated during the early Paleogene at the site of a propagating rift that also produced the once conjugate Meteor Rise. Eocene rifting and seafloor spreading separated the Islas Orcadas and Meteor rises, forming a deep passageway that allowed less-restricted communication of deep water between the high latitudes and the South Atlantic to the north (Fig. 2).

Site 702 is at 50°56.786' S, 26°22.117' W, in a water depth of 3083.4 m. The setting of the site is in the middle of the broadest portion of the Islas Orcadas Rise, where a ~80-km-wide basin occurs between the western flank and a long north-northwest-trending basement high bordering its eastern margin (Fig. 3). Large areas of the central part of the rise are relatively smooth, and the seismic data show an up to 0.8-s-thick (two-way travel-time—TWT) section characterized by an upper 300-ms-thick unit with acoustic stratification, a middle transparent unit (200 ms thick), and a basal 250-ms-thick unit with two distinct parallel bands of reflections (Fig. 4). The selected drill site is on the

upper flank of a basement high in the central basin where sediments are attenuated, which would allow for more rapid penetration of the older sedimentary sequence and basement (Fig. 4). Site 702 had two main objectives: (1) to determine the age, nature, and subsidence history of the rise and (2) to interpret the influence of the shallow Islas Orcadas Rise, Meteor Rise, and adjacent fracture zones and plateaus on Paleogene oceanic communication between the Southern Ocean and the South Atlantic.

The influence of surface waters on deposition at Site 702 is similar to that at the other Leg 114 sites, which are between 51° and 51.5°S. The present-day position of the Antarctic Convergence Zone (ACZ), or polar front, lies across the northern portion of the Islas Orcadas Rise, approximately 60 km north of Site 702 (Gordon et al., 1977). Because of the close proximity of the site to the ACZ, its location is well within the range of seasonal fluctuations of the front, which separates subantarctic and antarctic surface waters. During Pliocene-Quaternary glacial episodes, the position of the site would have been within the antarctic surface waters to the south of the convergence. Variations in the position of the ACZ relative to Site 702 were expected to have influenced the relative contributions of ice-rafted detritus, as well as the deposition of siliceous and carbonate sediments. Ice-rafted sediment is more commonly deposited south of the ACZ, where ice bergs are entrained in the Antarctic Circumpolar Current (ACC). In areas above the carbonate compensation depth (CCD) and north of the ACZ, sediments are increasingly calcareous, as a result of changes in the abundance of silica- and carbonate-producing planktonic organisms. Prior to the late Miocene, the position of the ACZ was to the south of Site 702 (Ciesielski and Weaver, 1983); therefore, older sediments are expected to be predominantly calcareous, with an increasing biosiliceous component in the Miocene as a consequence of a closer proximity to the convergence.

The seafloor of the broad central region of the Islas Orcadas Rise, where Site 702 is located, is bathed by Circumpolar Deep Water (CPDW) originating from the Pacific and Indian Oceans (Reid et al., 1977). The CPDW is entrained within the ACC, which has a strong easterly flow, particularly near the axis of the ACC at Site 702. Previous studies of rises in the southwest Atlantic sector of the Southern Ocean—the Maurice Ewing Bank, Northeast Georgia Rise, and Islas Orcadas Rise—have shown that Neogene sediments are punctuated by numerous disconformities caused by episodes of intense CPDW flow (Ciesielski, 1978; Ciesielski and Wise, 1977; Ciesielski et al., 1982). Periods of nondeposition and erosion are particularly pronounced where the strong, eastward-flowing CPDW impinges directly upon parts of the rises that are unprotected by higher topography to the west. Piston cores taken on the Islas Orcadas Rise in the vicinity of Site 702 reveal that the upper Neogene section is highly condensed and contains numerous disconformities (Fig. 5). In several locations, piston cores penetrated upper Oligocene and upper Miocene sediments, suggesting deep erosion of the rise by CPDW.

The specific objectives for Site 702 were as follows:

1. to determine the age, nature, and early subsidence history of the Islas Orcadas Rise;
2. to obtain basement of this aseismic ridge to examine the geochemical development of oceanic crust along a flow line that commences with the initial rifting of oceanic crust and the generation of dual aseismic ridges and proceeds to steady-state seafloor spreading;
3. to examine the evolution of Paleogene latitudinal water-mass temperature gradients and their influence on the migration and evolution of planktonic biota;

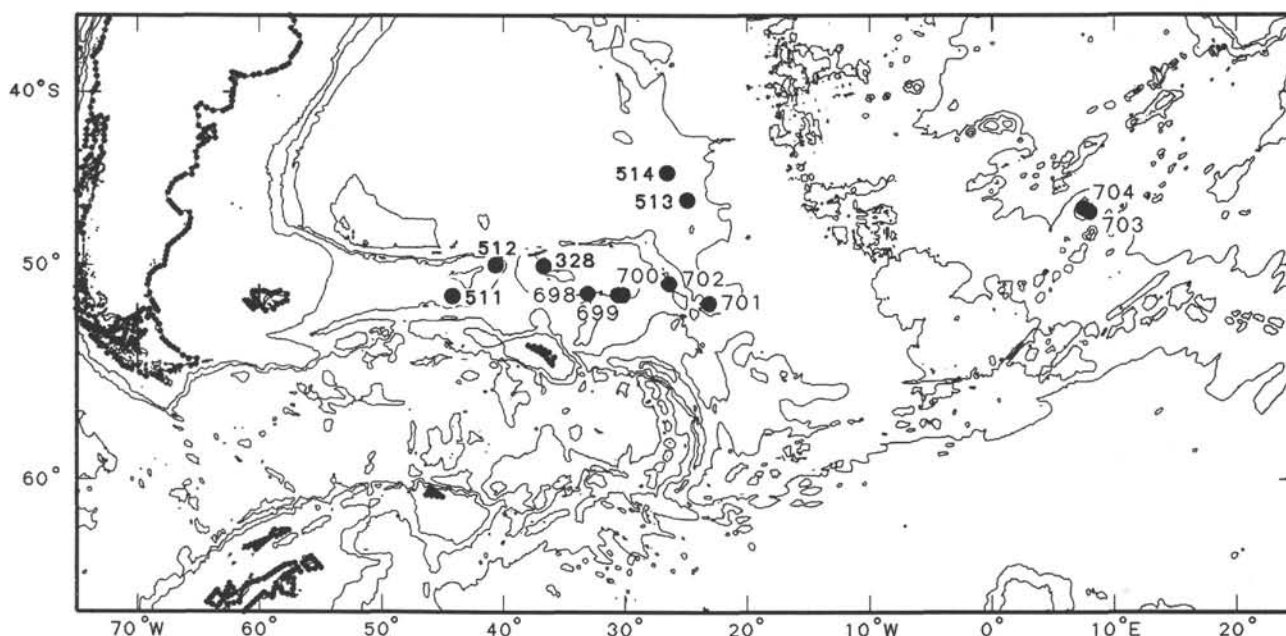


Figure 1. Bathymetric chart of the subantarctic South Atlantic showing the location of Site 702 and other Leg 114 sites. Contour interval 1500 m.

4. to interpret the evolution of Paleogene vertical water-mass structure through comparisons with the previous and subsequent sites;

5. to calibrate the subantarctic microfossil zonal scheme and datums with the geomagnetic polarity time scale (GPTS);

6. to test the experimental Navidrill coring system.

The original operational plan of Leg 114 called for drilling of one site on the Islas Orcadas Rise–Meteor Rise aseismic ridge couple. Sites on the Meteor Rise were selected as primary sites, with Site 702 on the Islas Orcadas Rise as a lower priority site. Plans were modified at sea to occupy Site 702 for the following reasons: (1) there was ample time in the remaining schedule, (2) the thickness of the Meteor Rise sedimentary sequence (800–1000 m) made it unlikely that the deeper portion of the section and basement could be reached because bad weather and other problems had prevented deep penetration at previous Leg 114 sites, (3) a thinner sequence could be rapidly drilled at Site 702 that would be similar to the deep section on Meteor Rise, and (4) Site 702 would provide the best chance to test the experimental Navidrill system.

The drilling plan was to drill a shallow hole at Site 702 to basement and to proceed to the Meteor Rise to attempt to obtain a minimum depth that would achieve stratigraphic overlap with Site 702. A APC/XCB hole was drilled to refusal, and the experimental Navidrill system unsuccessfully tested prior to termination of the hole. The hole was not logged because of its shallow depth and the uniform nature of the lithology.

OPERATIONS

We dropped the beacon at Site 702 at 0200 hr on 13 April 1987, retrieved the gear, and by 0355 hr the vessel was operating in dynamic positioning mode.

Two objectives of coring at this site were to core to basement and to test the Navidrill coring system. Both of these goals had been elusive throughout the cruise, and it appeared that our only chance of reaching basement and/or finding a shallow formation hard enough to allow a Navidrill test would be at this site. We intended to drill one hole at this site using the APC and XCB systems down to hard rock or basement and then proceed with the Navidrill.

Hole 702A was spudded at 1110 hr, 13 April 1987 (Table 1). The formation was extremely firm near the surface, so operations progressed slowly and cautiously to avoid breaking off a bottom-hole assembly (BHA). The fourth piston core required 25,000 lb to pull free of the formation, which is unusually high for this depth of penetration. Incredibly, the fifth core barrel required 125,000 lb to pull out of the sediment, an increase of 100,000 lb over the previous core. The pin thread failed on the 12¼-in. inner barrel sub, leaving the core barrel stuck in the formation. Altogether, only four APC cores were taken, with a 100.3% recovery. The bit was pulled clear of the seafloor at 1545 hr to end Hole 702A.

After offsetting 10 m to the east, Hole 702B was spudded at 1616 hr. The APC coring depth for this hole was staggered by 2 m to overlap the initial cores taken from Hole 702A. This time, only three APC cores were taken before switching to the XCB system. The next eight cores were cut with caution because we needed to penetrate approximately 90 m before all of the drill collars were buried below the mud line. Coring continued remarkably well for the next 200 m. Exceptionally good weather and the associated sea state contributed to efficient handling of the XCB system and a marked absence of problems. Cores were recovered every 40–50 min for the first 200 m, which is an exceptional rate for this water depth (3100 m). The advantages of the XCB system in chalk formations also were demonstrated by an excellent 89.5% recovery.

The lower 100 m of the section proved to be difficult to recover. We frequently encountered chert layers of 7–14 cm thickness. Sometimes several chert layers were recovered in one core. Penetration rates slowed significantly and then increased as the layer was penetrated. Recovery in this part of the formation dropped to 26%. The use of diamond cutting shoes did little to improve overall recovery; however, the diamond shoes were able to cut through and recover some of the chert layers, whereas the other shoes would not cut.

While cutting Core 114-704C-32X, the penetration stalled with literally no advancement for 10 min. The decision was made to rig down the XCB tools and to attempt the first Navidrill system coring. At 0330 hr on 15 April 1987, the Navidrill was run in the hole, but the deployment was unsuccessful, and the hole was filled with weighted mud and the drill pipe was

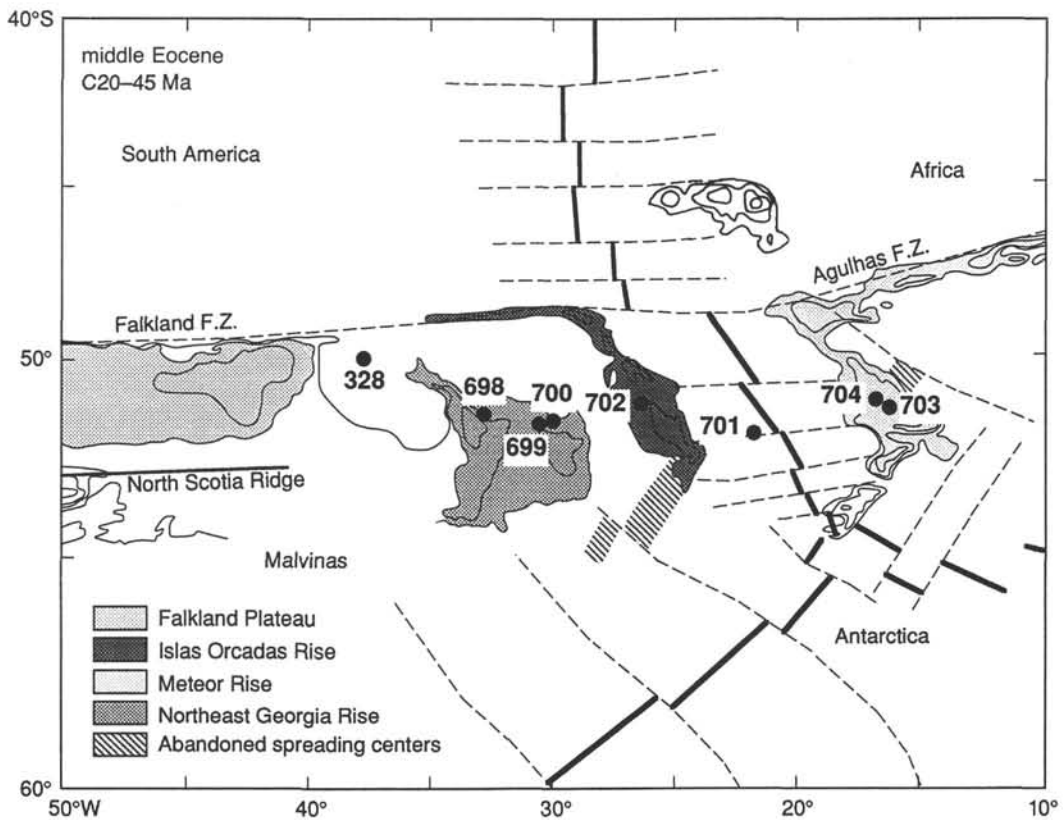
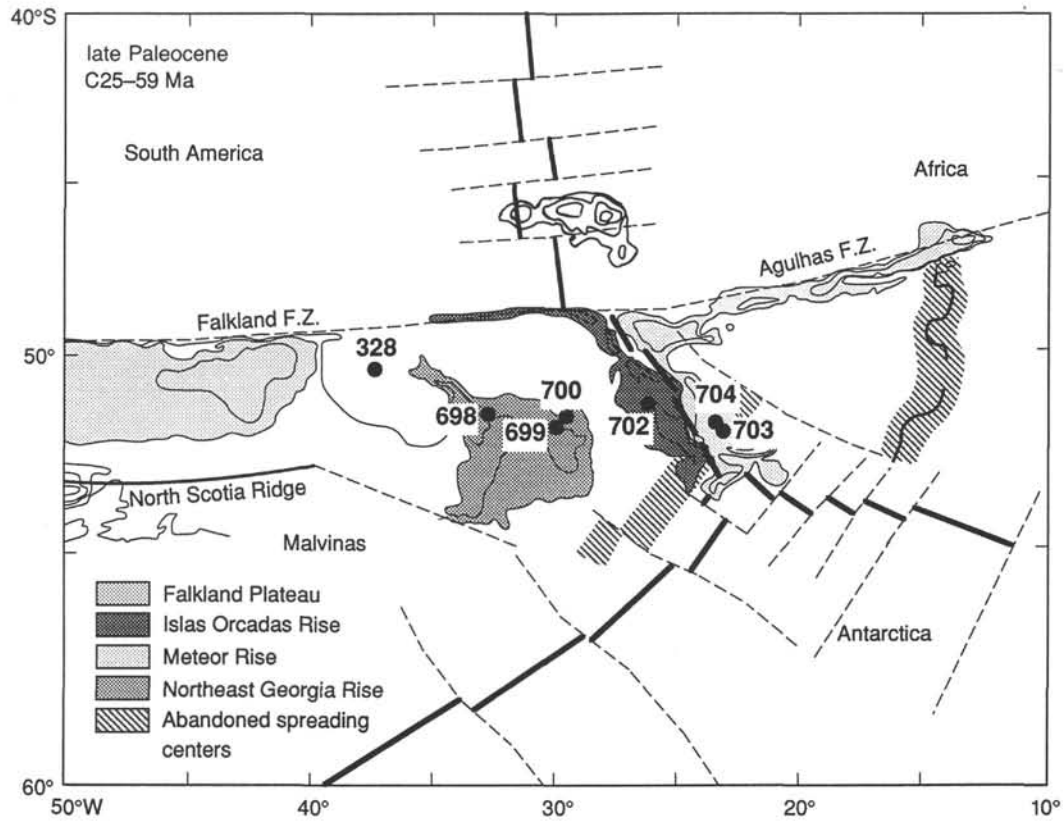


Figure 2. Plate tectonic reconstruction of the subantarctic South Atlantic for the late Paleocene and middle Eocene, showing the position of Site 702 and other Leg 114 sites. Spreading-center locations based on magnetic anomaly locations and SEASAT gravity field. Supporting data are presented in the OMD Region 13 synthesis (LaBrecque, 1986).

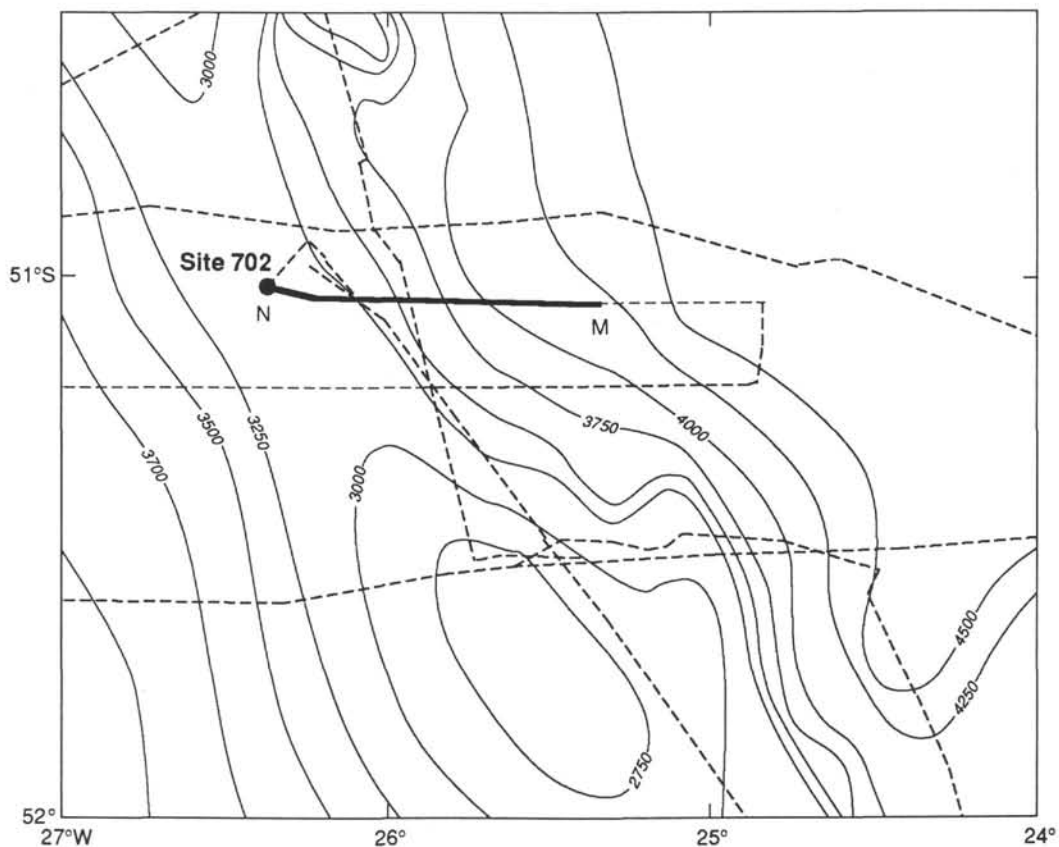


Figure 3. GEBCO bathymetry in the vicinity of Site 702 with the plotted ship tracks of previous geophysical survey lines. The bold line between *M* and *N* represents the 1986 single-channel seismic line of the *Polar Duke* upon which Site 702 is located (see Fig. 4). Note that the GEBCO bathymetry (in meters) does not reflect the newly acquired data from the *Polar Duke*, and consequently, the broad central basin of Figure 4 is not evident.

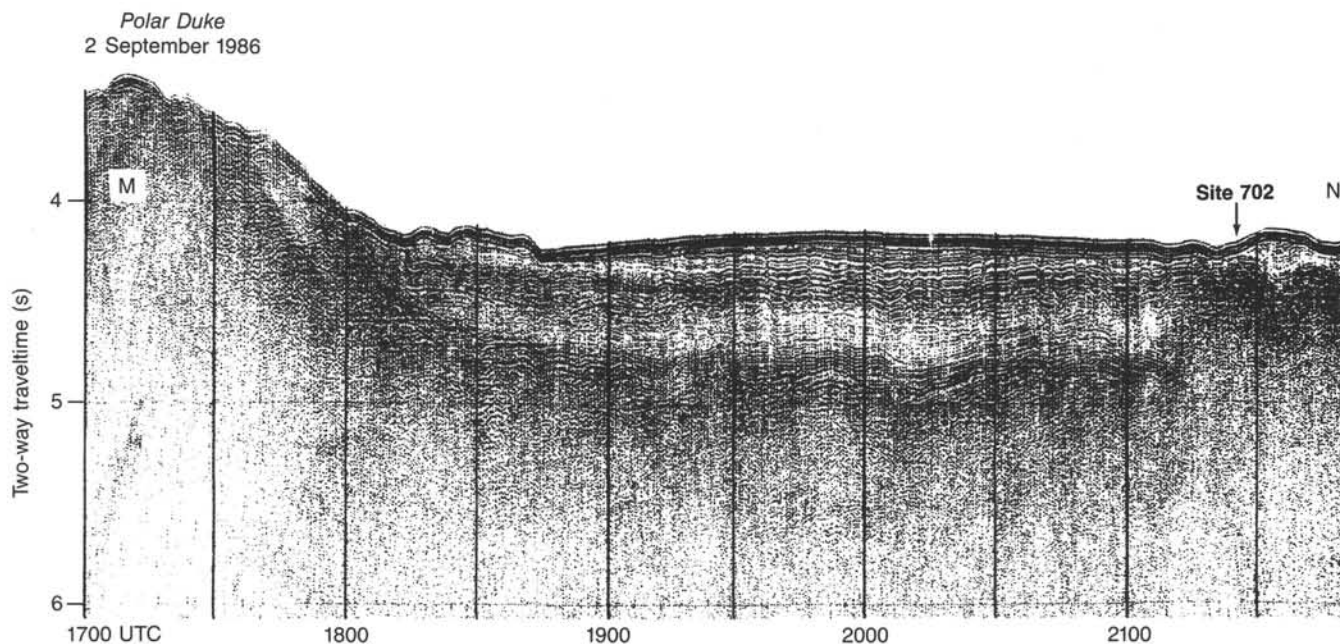


Figure 4. Single-channel seismic-reflection profile along the *M-N* line shown in Figure 3. Site 702 is on the flank of the basement high near the end-point *M*. The seismic line was acquired on the 1986 site survey cruise of the *Polar Duke* (courtesy of C. Raymond, 1987).

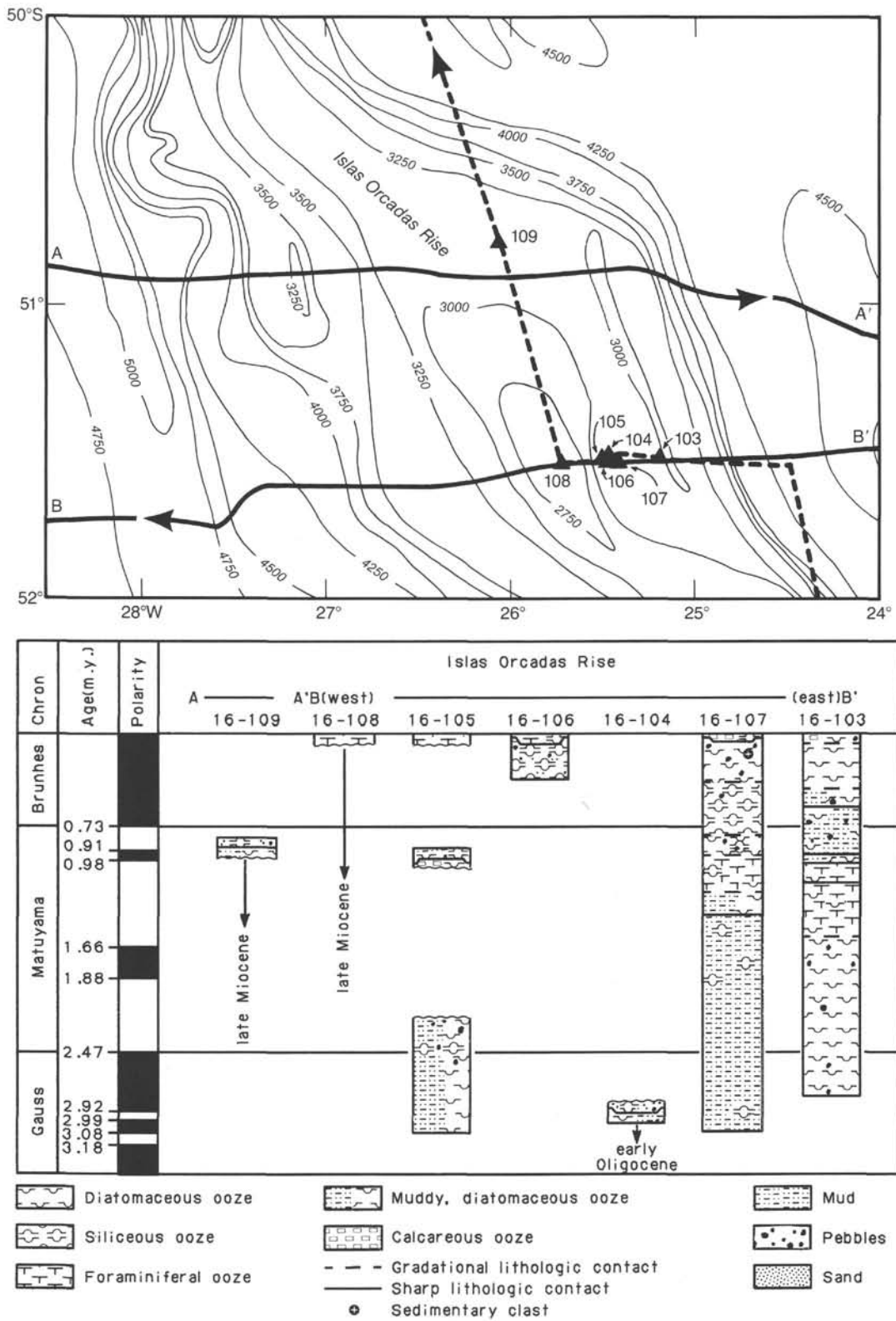


Figure 5. Locations, ages, and lithologies of piston cores taken in the vicinity of Site 702 by P. F. Ciesielski.

Table 1. Site 702 coring summary.

Core no.	Date (April 1987)	Local time (hr)	Depths (mbsf)	Cored (m)	Recovered (m)	Recovery (%)
Hole 702A:						
1H	13	1130	0.0-4.6	4.6	4.61	100.0
2H	13	1222	4.6-14.1	9.5	9.45	99.5
3H	13	1310	14.1-23.6	9.5	10.12	106.5
4H	13	1350	23.6-33.1	9.5	10.03	105.6
				33.1	34.21	
Hole 702B:						
1H	13	1636	0.0-6.3	6.3	6.34	100.0
2H	13	1720	6.3-15.8	9.5	9.65	101.0
3H	13	1815	15.8-25.3	9.5	9.40	98.9
4X	13	1934	25.3-34.8	9.5	8.37	88.1
5X	13	2025	34.8-44.3	9.5	8.26	86.9
6X	13	2145	44.3-53.8	9.5	3.20	33.7
7X	13	2245	53.8-63.3	9.5	2.54	26.7
8X	13	2325	63.3-72.8	9.5	9.53	100.0
9X	14	0025	72.8-82.3	9.5	8.70	91.6
10X	14	0125	82.3-91.8	9.5	9.55	100.0
11X	14	0237	91.8-101.3	9.5	9.49	99.9
12X	14	0320	101.3-110.8	9.5	9.65	101.0
13X	14	0355	110.8-120.3	9.5	7.82	82.3
14X	14	0445	120.3-129.8	9.5	9.55	100.0
15X	14	0540	129.8-139.3	9.5	9.28	97.7
16X	14	0630	139.3-148.8	9.5	9.54	100.0
17X	14	0715	148.8-158.3	9.5	9.68	102.0
18X	14	0840	158.3-167.8	9.5	8.76	92.2
19X	14	0925	167.8-177.3	9.5	9.44	99.3
20X	14	1010	177.3-186.8	9.5	8.37	88.1
21X	14	1050	186.8-196.3	9.5	4.78	50.3
22X	14	1230	196.3-205.8	9.5	6.56	69.0
23X	14	1355	205.8-215.3	9.5	1.26	13.2
24X	14	1435	215.3-224.8	9.5	3.87	40.7
25X	14	1545	224.8-234.3	9.5	1.47	15.5
26X	14	1700	234.3-243.8	9.5	1.47	15.5
27X	14	1845	243.8-253.3	9.5	1.70	17.9
28X	14	1950	253.3-262.8	9.5	0.85	9.0
29X	14	2057	262.8-272.3	9.5	0.77	8.1
30X	14	2210	272.3-277.3	5.0	2.73	54.6
31X	14	2340	277.3-286.8	9.5	1.43	15.0
32X	15	0140	286.8-294.3	7.5	1.09	14.5
				294.3	195.10	

tripped out of the hole. At 2300 hr the same day, the bit cleared the rotary table, the rig floor was secured, and the ship got underway for Site 703.

LITHOSTRATIGRAPHY

Hole 702A (Cores 114-702A-1H through 114-702A-4H) reached a total depth of 34.2 m below seafloor (mbsf) and recovered sediments of late Eocene to Quaternary age. Because of coring difficulties, Hole 702A was abandoned, and a new hole was begun nearby.

Hole 702B was drilled using the APC and XCB systems to recover 32 cores to a total depth of 294.3 mbsf. A total of 195.10 m was recovered, resulting in a recovery rate of 66.06%.

The sedimentary sequence consists of pelagic carbonates, overlain by a thin veneer of diatom muds and siliceous and calcareous oozes. The carbonates grade from nannofossil oozes near the top of the hole through nannofossil chalks to "micritic," indurated nannofossil chalks at the bottom of the hole. Chert nodules increase in abundance near the bottom of the hole. Ice-rafted debris occurs only in a gravelly layer near the surface as a lag deposit. The entire sequence is subdivided into two units, as shown in Tables 2 and 3 and Figure 6. Smear slide results are summarized in Figures 7 and 8. Recovery at this site was generally excellent down to Core 114-702B-21X (lower Eocene), but significantly decreased below 192 mbsf.

Table 2. Lithostratigraphic units, Hole 702A.

Unit/subunit	Lithology	Depth (mbsf)	Age
IA	Diatom mud	0-6.65	late Miocene to Quaternary
IB	Nannofossil-diatom ooze	6.65-22.15	late Miocene
IIA	Nannofossil ooze	22.15-33.0	middle Miocene to late Miocene

Table 3. Lithostratigraphic units, Hole 702B.

Unit/subunit	Lithology	Depth (mbsf)	Age
IA	Diatom mud	0-6.15	late Miocene to Quaternary
IB	Nannofossil-diatom ooze	6.15-21.1	late Miocene
IIA	Nannofossil ooze	21.1-32.8	middle Miocene to late Miocene
IIB	Nannofossil chalk	32.8-202.45	early Eocene to late Eocene
IIC	Indurated nannofossil chalk	202.45-294.3	late Paleocene to early Eocene

Unit I: Section 114-702A-1H through Sample 114-702A-3H-6, 55 cm; Depth: 0-22.15 mbsf; Section 114-702B-1H through Sample 114-702B-3H-4, 80 cm; Depth: 0-21.1 mbsf; Age: late Miocene to Quaternary.

Unit I consists of diatom mud to muddy diatom ooze overlying alternating nannofossil-diatom ooze and diatom nannofossil ooze. Dropstones, manganese nodules, and volcanic ash admixtures are characteristic of this interval.

Subunit IA: Section 114-702A-1H through Sample 114-702A-2H-2, 55 cm; Depth: 0-6.65 mbsf. Section 114-702B-1H through Sample 114-702B-1H-5, 15 cm; Depth: 0-6.15 mbsf; Age: late Miocene-Quaternary.

Mixtures of diatom ooze and mud in various proportions comprise this subunit. In both Holes 702A and 702B, terrigenous components predominate in Sections 114-702B-1H-1 and 114-702B-1H-2, which overlie biogenic oozes in deeper sections. Colors are pale olive (5Y 6/3) to olive (5Y 5/3 to 5Y 6/3). Diatom oozes occur in Sample 114-702A-1H, 3 cm, Section 114-702A-1H, CC, and Section 114-702B-1H-3 to Sample 114-702B-1H-5, 15 cm. Dropstones, Mn nodules, and stains are common throughout this subunit, which contains the bulk of the ice-rafted detritus for both holes. Pebbles in lower portions of the sedimentary sequence are considered to be largely downhole contamination.

Subunit IB: Samples 114-702A-2H-2, 55 cm, through 114-702A-3H-6, 55 cm; Depth: 6.65-22.15 mbsf. Samples 114-702B-1H-5, 15 cm, through 114-702B-3H-4, 80 cm; Depth: 6.15-21.1 mbsf; Age: late Miocene.

The nannofossil-diatom oozes that comprise this subunit contain biogenic components that vary from section to section. Colors range from white (10Y 8/2 and 2.5Y 8/2) to olive gray (5Y 5/2) to pale yellow (5Y 7/3) and yellowish brown (2.5Y 6/4). Minor lithologies are gray (5G 7/1) nannofossil-bearing

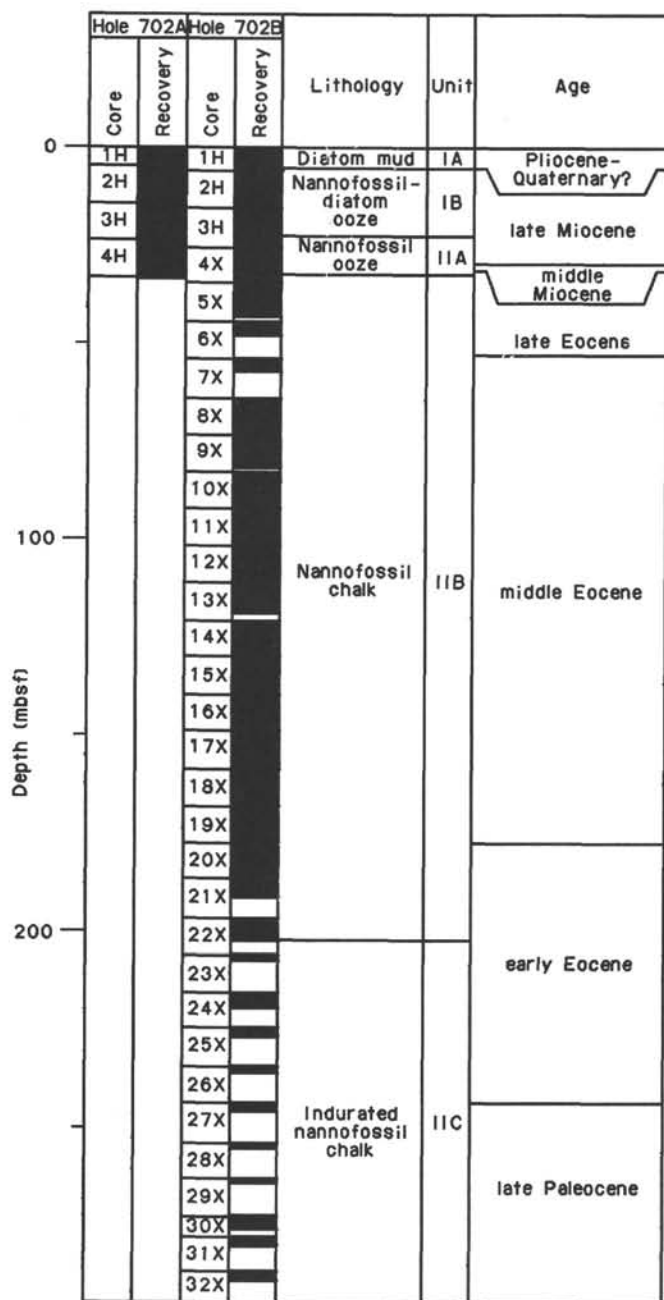


Figure 6. Recovery and lithostratigraphic units, Site 702.

and (ash-bearing) diatom ooze at 52 cm in Section 114-702A-3H-6 and from 0 to 22 cm in Section 114-702B-3H-4. Diatom-bearing nannofossil ooze is a minor lithology in Section 114-702B-3H-3. Volcanic-ash layers and admixtures occur at 125–150 cm in Section 114-702B-2H-1, 7–8 and 69–87 cm in Section 114-702B-2H-2, and 40–50 cm in Section 114-702B-2H-5. Bioturbation is minor to moderate. Burrows cause mottling and apparently some redistribution of volcanic ash. The ichnofacies consists mainly of *Planolites* and some *Zoophycos* traces, particularly in Sections 2 through 5 of Core 114-702A-2H.

The combined sedimentary sequence of Subunits IA and IB represents a much thinner sequence than that observed at other Leg 114 sites. For instance, it seems as if the combined 142-m thickness of Unit I and Subunit IIA in Hole 699A has been telescoped into a total thickness of 21 to 22 m at Site 702. Major episodes of erosion and/or nondeposition are clearly indicated,

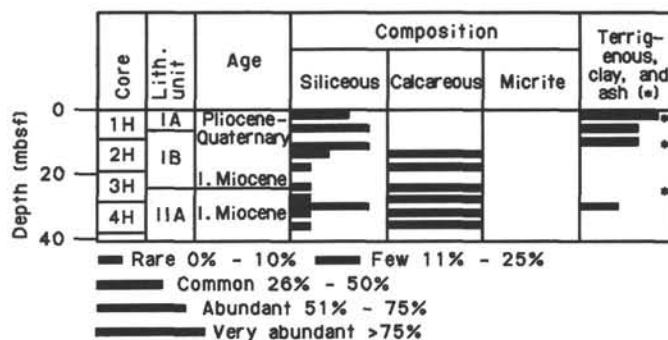


Figure 7. Smear slide summary, Hole 702A.

and indeed, a major (~29–33-m.y.) hiatus (spanning the upper Eocene–lower upper Miocene) separates Units I and II.

Unit II: Sample 114-702A-3H-6, 55 cm, through Section 114-702A-4H, CC; Depth: 22.15–33.1 mbsf. Sample 114-702B-3H-4, 81 cm, through Section 114-702B-32X, CC; Depth: 21.1–294.3 mbsf; Age: late Paleocene to late Miocene.

Unit II is a sequence of nannofossil oozes, chalks, and indurated chalks with intercalated cherts, particularly in the lower part of the section. Ash occurs in the top part of the unit but is not a major component of the sediment. Planktonic and benthic foraminifers are present but comprise less than 10% of the sediment.

Unit II is 273.2 m thick and has been subdivided into three subunits based on the degree of lithification. The three subunits are dominated by ooze, chalk, and indurated chalk, respectively. This subdivision is somewhat subjective, but it provides an indication of the degree of lithification. The overall conditions of sedimentation, namely the quiet, sustained accumulation of nannofossils, remained the same during the time represented by this unit.

Subunit IIA: Sample 114-702A-3H-6, 55 cm, to the bottom of the hole at Section 114-702A-4H, CC; Depth: 22.15–33.1 mbsf. Sample 114-702B-3H-4, 81 cm, through Section 114-702B-4X-3; Depth: 21.1–32.8 mbsf; Age: late Miocene.

Subunit IIA consists almost exclusively of nannofossil ooze (11.7 m thick), with minor admixtures of foraminifers and diatoms. The color differences at the subunit boundary are pronounced (darker colors above, lighter colors below). In addition to the color change, rolled intraclasts occur at the top. In Sample 114-702A-3H-6, 55 cm, the top of this subunit is just below a layer of ash- and nannofossil-bearing diatom ooze. Colors in the subunit are pure white (no color code) or white (5Y 8/2), pale yellow (5Y 7/3), light greenish gray (5G 7/1), and greenish gray (5GY 5/1). Lithic fragments occur throughout Section 114-702B-3H-1. Mn micronodules occur in Section 114-702B-3H-2 at 120 and 132 cm. Both the lithic fragments and Mn nodules may represent downhole contaminations. Ash-bearing horizons or spots occur in Section 114-702B-3H-2 at 15, 20, 41, and 75–81 cm.

Bioturbation occurs in both holes. *Zoophycos* traces are observed in Section 114-702A-4H-1 at 64 and 68 cm.

Subunit IIB: Section 114-702B-4X-4 through Sample 114-702B-22X-5, 15 cm; Depth: 32.8–202.45 mbsf; Age: early Eocene to late Eocene.

This subunit contains a large part (169.85 m) of the drilled sedimentary sequence and consists mainly of nannofossil chalk. The predominant color is white (no color code); subordinate colors are white (2.5Y 8/1, 10YR 8/1), gray (N5 NL), light gray (5Y 7/2), and pale greenish gray (5GY 7/1). Only one horizon

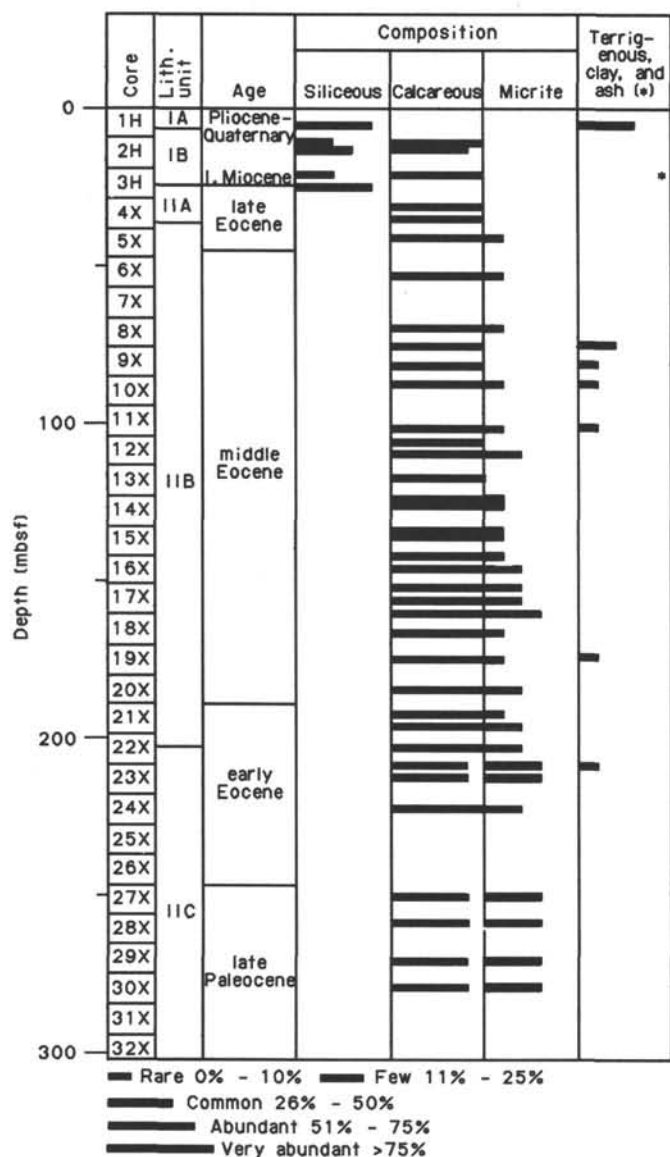


Figure 8. Smear slide summary, Hole 702B.

with a clay content >10% is reported, from 128 to 138 cm in Section 114-702B-8X-6. Foraminifers are a relatively small proportion of the carbonate fraction. Foraminifer-bearing lithologies (>10%) are restricted to Core 114-702B-17X.

Bioturbation is commonly present, but because of the white color of the material, traces do not seem to be as well represented as at other sites.

Planolites and *Zoophycos* traces were identified in Cores 114-702B-9X through 114-702B-11X and together with *Thalassinoides* in Core 114-702B-21X. Only *Planolites* is identified in Cores 114-702B-19X, 114-702B-20X, and 114-702B-22X.

"Pebble contamination" is common in the subunit and is mainly restricted to first sections of cores, particularly near the top of the subunit. No occurrences of pebbles were observed below Core 114-702B-8X.

Faint Mn staining occurs from 42 to 57 cm in Section 114-702B-19X-3. This is the only described occurrence of Mn oxide below Core 114-702B-5X. Micritization begins with a slight enlargement (calcareous overgrowths) of nannofossil fragments and tests in Core 114-702B-16X (148.8 mbsf) and increases progressively toward the bottom of the subunit, albeit not in a uniform fashion. Micritization is an indicator of increasing lithification and density of the sediment (see "Physical Properties" section,

this chapter). The first occurrence of chert, as broken pieces, occurs at 145–150 cm in Sample 114-702B-20X-3 (Table 4).

Subunit IIC: Sample 114-702B-22X-5, 15 cm, through Core 114-702B-28X; Depth: 202.45–294.3 mbsf; Age: late Paleocene to early Eocene.

Subunit IIC extends from Sample 114-702B-22X-5, 15 cm, (202.45 mbsf) to the bottom of the hole at 294.3 mbsf. It is essentially a lithologic continuation of Subunit IIB, except that micrite is pervasive. As a consequence, induration is very conspicuous, rendering some of this material borderline chalk-limestone. Another indicator of lithification is the occurrence of chert, which appears in Section 114-702B-24X-1. The chert occurrences probably led to the poor recovery (Fig. 6).

Colors are white (no color code, 5Y 8/1) and light gray (5Y 7/1) to greenish gray (5GY 6/1).

Clay occurs from 0 to 24 cm in Section 114-702B-32X, CC, and pebbles (as contaminants) are present in Sections 114-702B-29X-1 and 114-702B-32X-1, both of which are "short." Foraminifers are a small percentage of the composition, but reach more than 10% in Sample 114-702B-30X-1, 100 cm (smear slide). Because smear slides are biased against large particles, the actual percentage of foraminifers may be higher than indicated.

Bioturbation is evident in most sections. Faint traces of *Planolites*(?), *Zoophycos*, and composite *Planolites* traces are described in Section 114-702B-30X-1.

Poor recovery in these cores results from the presence of chert (and limestone), as reported from 82 to 88 cm in Section 114-702B-31X-1 and 24 to 36 cm in Section 114-702B-32X, CC. The presence of these hard lithologies probably resulted in the drilling difficulties that ultimately caused us to abandon the hole.

Paleoenvironmental Interpretation

The overall impression given by the bulk of the sediments (Unit II) is one of apparent environmental uniformity. No significant tectonic or climatic events are reflected in the lithologies below the upper Eocene–middle Miocene hiatus.

There is always the question of nondeposition vs. erosion as a mechanism for the formation of a hiatus. Three possible mechanisms for the origin of the upper Eocene–middle Miocene hiatus at Site 702 are (1) mass wasting caused by local faulting (see "Seismic Stratigraphy" section, this chapter), (2) erosion by intense ACC flow that was established by late middle to late Miocene (see Ciesielski et al., 1982, for discussion of antarctic glaciation and current flow), and (3) erosion by a localized current regime, caused by the local topography (see Barker and Burrell, 1982). Present information, mainly micropaleontological, favors the second mechanism. However, detailed shore-based analyses are needed to answer this question. In any case, a change (cooling) to conditions favorable for the deposition of diatoms is indicated by the lithologies of the upper Miocene Subunit IB. The mud-ooze-gravel of ice-rafted detritus and Mn-nodule mixtures of Subunit IA signal the final establishment of a modern sedimentation mode (late Miocene to Quaternary), with deposition

Table 4. Chert nodules, Hole 702B.

Interval	Description
20X-3, 145–150 cm	Broken chert pieces
24X-1, 25–35, 66–74, and 90–96 cm	Chert nodules, dark brown (7.5YR 4/4), with chalk inclusions
25X-1, 0–9 cm	Chert nodules, white (10R 4/3)
31X-1, 82–88 cm	Chert nodule, gray (5Y 5/1)
32X, CC (24–36 cm)	Chert nodules in porcellanite, gray (5Y 6/1)

of some diatom ooze and terrigenous material (plus the growth of Mn nodules) under the influence of a strong, winnowing, current regime.

BIOSTRATIGRAPHY

Site 702 was drilled using the APC and XCB systems in a water depth of 3083.4 m on the Islas Orcadas Rise. Hole 702A penetrated a 34.2-m-thick sequence of diatomaceous mud (0–6.65 m) and nannofossil-diatom ooze (6.65–22.1 m) of Quaternary to late Miocene age, overlying nannofossil ooze (22.1–33.1 m) of late Eocene age. Hole 702B penetrated a 294.3-m-thick sequence of diatom mud (0–6.15 m) and nannofossil-diatom oozes (6.15–21.1 m), spanning a Quaternary to late Miocene age, and an underlying nannofossil ooze and chalk unit (272.2 m thick) of late Eocene to late Paleocene age. In both holes an unconformity is evident because sediments from the uppermost Eocene to middle Miocene are missing.

The results based on the analyses of different fossil groups are summarized in Figure 9, and the age vs. depth relationships and sedimentation rates are given in Table 5 and Figure 10.

Biostratigraphy

The age assignments for Hole 702A are as follows:

Quaternary	114-702A-1H-1, 48 cm
late Pliocene	114-702A-1H-2, 90 cm, to 114-702A-1H-2, 105 cm
early Pliocene	114-702A-1H-3, 60 cm
late Miocene	114-702A-1H, CC, to 114-702A-3H-6, 51 cm

The age assignments for Hole 702B are as follows:

late Pliocene	114-702B-1H-2, 40 cm
late Miocene	114-702B-1H-3, 145 cm, to 114-702B-3H-4, 80 cm
late Eocene	114-702B-4X-3, 7 cm, to 114-702B-5X, CC
middle Eocene	114-702B-6X-2, 70 cm, to 114-702B-20X-1, 100 cm
early Eocene	114-702B-20X-2, 110 cm, to 114-702B-26X, CC
late Paleocene	114-702B-27X-1, 7 cm, to 114-702B-32X, CC

A list of microfossil datums identified is given in Table 5.

Paleocene and Eocene ages are based on nannofossils and planktonic foraminifers, Miocene ages are based on diatoms and nannofossils, and Pliocene and Quaternary ages are based on diatoms.

The youngest nannofossil and planktonic foraminifer zones of the upper Eocene are missing in the upper part of the Paleogene section, below the upper middle Miocene stratigraphic interval.

Siliceous microfossils are abundant in the Quaternary-Miocene section of the hole. Radiolarians are common and moderate to well preserved in the middle to upper Eocene and in the lower part of the Paleocene, whereas diatoms are rare and poorly preserved. Benthic foraminifers are common through the whole section, except for Sections 114-702A-1H, CC, and 114-702B-1H, CC, where they are absent. They are generally well preserved with a high species diversity; in the upper Eocene they are abundant but with a low diversity. The nannofossil floras of the upper to middle sections of the two holes are moderately well preserved but exhibit low diversity. The Paleogene nannofossil floras are in general poorly preserved, with much secondary calcite overgrowth, and are of low diversity.

Planktonic foraminifers are absent in the Quaternary and Pliocene and are rare, with a low diversity, in the Miocene of Hole 702B. They are abundant and moderately preserved through the Paleogene. The species are generally easily recognized, although their tests are recrystallized and show signs of dissolution.

The correlation between calcareous planktonic fossils and paleomagnetic data allows us to calibrate the first appearance datum (FAD) of *Globigerinatheka index* approximately with the boundary between Subchrons C20R and C20N, which is just below the lower boundary of the P12 Zone of the standard zonation.

Besides the long hiatus (29–33 m.y. duration) separating the lower upper Miocene from the upper Eocene (Core 114-702B-3H), another hiatus may be present.

Paleoenvironment

The Neogene siliceous microfossils are characteristic of the high-latitude southern province, whereas in the Paleogene the siliceous and calcareous microfossils reflect warmer surface waters.

The Paleogene sediments were deposited above the planktonic foraminifer lysocline, as evidenced by the abundance, preservation, and continuous presence of this microfossil group. The benthic foraminifers suggest a paleodepth of 1000–2000 m in the late Paleocene through early Eocene. The abundance of radiolarians in the earliest stratigraphic interval of the upper Paleocene may be related to higher productivity and better preservation rather than to a relative increase resulting from planktonic foraminifer dissolution.

As at Sites 699 and 701, the planktonic foraminifers show that a cooling trend occurred during the late middle Eocene and late Eocene. However, the presence of *Morozovella spinulosa* in the lower middle Eocene (P11) may indicate a period of warm influence. The warm-water affinity discoasters are rarely present, and they do not show the marked decline through time as they do at Site 699. This trend may be obscured by poor preservation in the lower part of the section.

Within the upper part of the middle Eocene and the upper Eocene, the low diversity of benthic and planktonic foraminifers and the increase in number and size of *Chiloguembelina cubensis*, a low-productivity indicator species, may indicate a decrease in productivity.

Calcareous Nannofossils

Hole 702A

Samples from four cores and all of the core catchers were examined for nannofossils. The Eocene samples are assigned to Martini's (1971) zonation, as described in the "Explanatory Notes" chapter, this volume.

Biostratigraphy

The samples between Samples 114-702A-1H-2, 32–33 cm, and 114-702A-2H-2, 36–37 cm, are either barren or contain rare, reworked Paleogene nannofossils. The interval between Samples 114-702A-2H-5, 36–37 cm, and 114-702A-3H-6, 4–5 cm, is tentatively assigned to the middle to upper Miocene. They contain nannofossil floras of low diversity, dominated by *Reticulofenestra perplexa*.

A stratigraphic break occurs between Sample 114-702A-3H-6, 4–5 cm, and Section 114-702A-3H, CC, with some Miocene, Oligocene, and upper Eocene strata missing. Sections 114-702A-3H, CC, and 114-702A-4H, CC, are assigned to NP18. They contain rich nannofossil flora assemblages that include *Neococcolithes dubius*, *Chiasmolithus oamaruensis*, and, in the lowermost core-catcher sample, *Discoaster saipanensis*.

Core	Recovery	Age	Calcareous nannofossils	Planktonic foraminifers	Diatoms	Silicoflagellates	Radiolarians
0							
1H		Quaternary			<i>Coscinodiscus lentiginosus</i>	<i>Distephanus boliviensis</i>	<i>Helotholus vema</i>
2H		late Miocene	late-middle Miocene		<i>Coscinodiscus vulnificus</i>	Unzoned	Unzoned
3H		middle Miocene			<i>Denticulopsis hustedtii</i> - <i>Denticulopsis lauta</i>		
4X		late Eocene	NP18	late Eocene P15	<i>Nitzschia denticuloides</i>	Unzoned	(1)
5X					?		(2)
6X							
7X			NP16	late middle Pliocene P14			?
8X					Eocene	Unzoned	(3)
9X							
10X				late middle Eocene P11-13			
100							
11X						Unzoned	
12X		middle Eocene	NP16-15				
13X							
14X							
15X						4	
16X				early middle Eocene P10-11			
17X						Barren	
18X			NP15-16				
19X							
200							
20X						Barren	
21X				early Eocene P9			
22X			NP16 NP13			Barren	
23X		early Eocene		early Eocene P8			
24X			NP12-10				
25X				early Eocene		Barren	
26X							
27X			NP9		late Paleocene P5	Barren	
28X							
29X		late Paleocene	NP8		late Paleocene P4		
30X							
31X			NP7-6			Barren	
32X			NP7-5		late Paleocene P3b		
300					Paleocene		

Figure 9. Summary of paleontological results, Site 702.

Hole 702B

Samples from eight cores and all of the core catchers were examined for nannofossils. All of the examined samples are fossiliferous. The nannofossil floras are assigned to the Martini (1971) zones ("Explanatory Notes" chapter).

Biostratigraphy

The nannofossil floras of Sections 114-702B-1H, CC, to 114-702B-2H, CC, are dominated by *R. perplexa*, with lesser num-

bers of *Coccolithus pelagicus*. This assemblage indicates the presence of middle to upper Miocene strata.

The same stratigraphic break recognized in Hole 702A, with some Miocene, Oligocene, and upper Eocene strata absent, lies between Sections 114-702B-2H, CC, and 114-702B-3H, CC. Sections 114-702B-3H, CC, to 114-702B-5X, CC, are assigned to NP18 (upper Eocene); they contain *C. oamaruensis* and *N. dubius* and lack *Isthmolithus recurvus*. No samples that could be assigned to NP17 were examined. The absence of this zone in

Table 5. Microfossil and magnetostratigraphic datums at Site 702. Multiple disconformities exist in the Neogene portion of the sequence of Hole 702A and 702B. Datums 9–31 are from Hole 702B, and younger datums are from both Holes 702A and 702B. Precise determination of the number and extent of the hiatuses in the condensed section will be presented in the *Scientific Results*.

Microfossil and paleomagnetic datums ^a	Age (Ma)	Reference ^{a,b}	Interval	Depth range ^c (msbf)	Mean position (msbf)
1. *Base <i>Coscinodiscus lentiginosus</i> Zone (D)	+0.62	10	701A-1H-1, 48 cm, to 1H-2, 90 cm	0.48–2.40	(1.44)
2. *LAD <i>Coscinodiscus insignis</i> (D)	+2.49	10	1H-2, 90 cm, to 1H-2, 105 cm	2.40–2.55	(2.48)
3. FAD <i>Nitzschia interfrigidaria</i> (D)	+4.02	10	1H-3, 60 cm, to 1H, CC	3.60–4.60	(4.10)
4. LAD <i>Denticulopsis hustedtii</i> (D)	+4.48	10	1H-3, 60 cm, to 1H, CC	3.60–4.60	(4.10)
	+4.48	10	1H-2, 40 cm, to 701B-1H-3, 145 cm	3.40–4.45	(3.93)
5. LAD <i>Denticulopsis lauta</i> (D)	#8.70	10	1H, CC, to 701A-2H-2, 46 cm	4.60–6.56	(5.58)
	#8.70	10	1H-3, 145 cm, to 701B-1H-4, 50 cm	4.45–5.00	(4.73)
6. L common <i>Nitzschia denticuloides</i> (D)	+8.7–9.1	10	3H-5, 70 cm, to 701A-3H-6, 51 cm	20.80–22.11	(21.46)
	+8.7–9.1	10	3H-4, 14 cm, to 701B-3H-4, 80 cm	20.44–21.10	(20.77)
Hiatus maximum duration = 33 m.y. minimum duration = 29 m.y.			701A-3H-6, 51 cm, to 3H, CC	22.11–23.60	(22.86)
			701B-3H-4, 80 cm, to 3H-4, 85 cm	21.10–21.15	(21.13)
7. *Top NP18 Zone (N)	37.80	4	3H-6, 5 cm, to 701A-3H, CC	21.65–23.60	(22.63)
8. *Top P15 Zone (F)	38.10	4	2H, CC, to 701B-3H, CC	15.80–25.30	(20.55)
9. Top NP16 Zone (N)	42.30	4	5X, CC, to 6X-2, 69 cm	44.30–46.49	(45.40)
10. Base P15 Zone (F)	41.30	7	6X-2, 25 cm, to 6X, CC	46.05–53.80	(49.93)
11. Base P14 Zone (F)	42.70	8	8X-5, 62 cm, to 8X-6, 60 cm	69.92–71.40	(70.66)
12. Base chron C18	42.70	4	8X-6, 104 cm, to 8X-6, 116 cm	71.84–71.96	(71.90)
13. Top chron C19	43.60	4	10X-2, 45 cm, to 10X-2, 46 cm	84.25–84.26	(84.26)
14. Base chron C19	44.00	4	10X-3, 115 cm, to 10X-3, 125 cm	86.45–86.55	(86.50)
15. Top chron C20	44.60	4	11X-5, 85 cm, to 11X-5, 95 cm	98.65–98.75	(98.70)
16. Base P12 Zone (F)	46.00	7	13X-1, 142 cm, to 13X-2, 140 cm	112.22–113.70	(112.96)
17. Base chron C20	46.20	4	13X-2, 104 cm, to 13X-2, 115 cm	113.34–113.45	(113.40)
18. Base? NP15 Zone (N)	50.00	4	14X, CC, to 15X-2, 60 cm	129.80–131.90	(130.85)
19. Top chron C21	48.80	4	17X-6, 95 cm, to 17X-6, 105 cm	157.25–157.35	(157.30)
20. Base P10 Zone (F)	52.00	7	20X-1, 110 cm, to 20X-2, 110 cm	178.40–179.90	(178.65)
21. Base NP14 Zone (N)	52.60	4	21X, CC, to 22X-2, 20 cm	196.30–198.00	(197.15)
22. Top NP12 Zone (N)	53.70	4	22X-2, 21 cm, to 22X, CC	198.01–205.80	(201.91)
23. Base P9 Zone (F)	53.40	6	22X-3, 102 cm, to 22X-4, 100 cm	200.32–201.80	(201.06)
24. Base P8 Zone (F)	55.20	4	24X-3, 10 cm, to 24X, CC	218.40–224.80	(221.60)
25. LAD <i>Fasciculithus</i> (N)	57.60	4	26X, CC, to 27X-1, 6 cm	243.80–243.86	(243.83)
26. Base P6 Zone (F)	57.80	4	26X, CC, to 27X-1, 77 cm	243.80–244.57	(244.19)
27. Base NP9 Zone (N)	59.20	4	27X, CC, to 28X, CC	253.30–262.80	(258.05)
28. Base P5 Zone (F)	58.70	4	27X, CC, to 28X, CC	253.30–262.80	(258.05)
29. Base P4 Zone (F)	61.00	4	30X, CC, to 31X-1, 53 cm	277.30–277.83	(277.57)
30. Base NP8 Zone (N)	59.90	4	30X, CC, to 31X, CC	277.30–286.80	(282.05)
31. Base 3Pb Zone (F)	62.00	4	32X, CC	>294.30	

^a + = direct correlation to paleomagnetic stratigraphy; # = absolute age date; * = probable truncation of datum by hiatus; D = diatom; N = calcareous nannofossil; F = planktonic foraminifers.

^b 1. Wise (1983); 2. Martini and Müller (1986); 3. Perch-Nielsen (1985); 4. Berggren et al. (1985); 5. Kent and Gradstein (1985); 6. Jenkins (1985); 7. McGowan (1986); 8. Paleomagnetic correlation at Hole 702B; 9. Burckle et al. (1978); 10. Ciesielski (1983); 11. Chen (1975); 12. Weaver (1983); 13. L. H. Burckle (Pers. comm, 1980) to Barron (1985); 14. Barron et al. (1985), Ciesielski (1985); 15. Ciesielski (1985); 16. Gombos (1984); 17. Fenner (1984); 18. Weaver and Gombos (1981); 19. Hays and Shackleton (1976); 20. Barron (1985).

^c Core-catcher depths in this table were calculated by assuming the core-catcher sample was obtained from the bottom of the cored interval.

the area of Site 702 possibly results from the extended ranges of *C. oamaruensis* and/or *Chiasmolithus solitus*.

The interval between Sample 114-702B-6X-2, 69–70 cm, and Section 114-702B-9X, CC, is assigned to NP16 (middle Eocene), the top of which is defined by the last appearance datum (LAD) of *C. solitus*. In this study, the base of definite NP16 is taken at the FAD of *Reticulofenestra bisecta*, because of the absence of *Rhabdosphaera gladius* in this area.

The interval between Sample 114-702B-10X-5, 20–21 cm, and Section 114-702B-14X, CC, is assigned to NP16–15 (middle Eocene). This assignment is based on the presence of the overlying definite NP16 strata and the occurrence of *Nannotetrina fulgens* in the lowermost two samples. Supporting evidence for this assignment comes from the presence of *Sphenolithus furcatolithoides* in Section 114-702B-11X, CC, and *Chiasmolithus gigas* in Sample 114-702B-12X-2, 20–21 cm, and Section 114-702B-12X, CC.

Sample 114-702B-15X-2, 60–61 cm, to Section 114-702B-20X, CC, are assigned to NP15–14 (middle to lower Eocene) because of their stratigraphic position between NP16–15 and NP14 strata. Strictly speaking, the whole of the interval from Sample

114-702B-15X-2, 60–61 cm, to Section 114-702B-20X, CC, could be assigned to NP14, but the rarity of *N. fulgens* may mean that its true FAD is not recognized in this hole, and thus, the base of NP15 cannot be accurately defined. Section 114-702B-21X, CC, is assigned to definite NP14 (middle to lower Eocene), based on the co-occurrence of *Discoaster lodoensis* and *Discoaster sublo-doensis*.

Sample 114-702B-22X-2, 20–21 cm, is assigned to NP13 (lower Eocene). The LAD of *Tribrachiatulus orthostylus*, which defines the top of NP12, occurs in Section 114-702B-22X, CC. Thus, the interval from Sections 114-702B-22X, CC, to 114-702B-26X, CC, is assigned to NP12–10 (lower Eocene); these zones are grouped together because the species used to define the bases of NP12 and NP11 are absent from Hole 702B.

The co-occurrence of *Fasciculithus tympaniformis* and *Discoaster multiradiatus* in Sample 114-702B-27X-1, 6–7 cm, to Section 114-702B-27X, CC, is taken here to indicate the presence of NP9 (upper Paleocene). The top of this zone is defined by the FAD of *Tribrachiatulus bramlettei*, but this species is not present in Hole 702B. The base of NP9 is defined by the FAD of *D. multiradiatus*. The absence of *D. multiradiatus* and the pres-

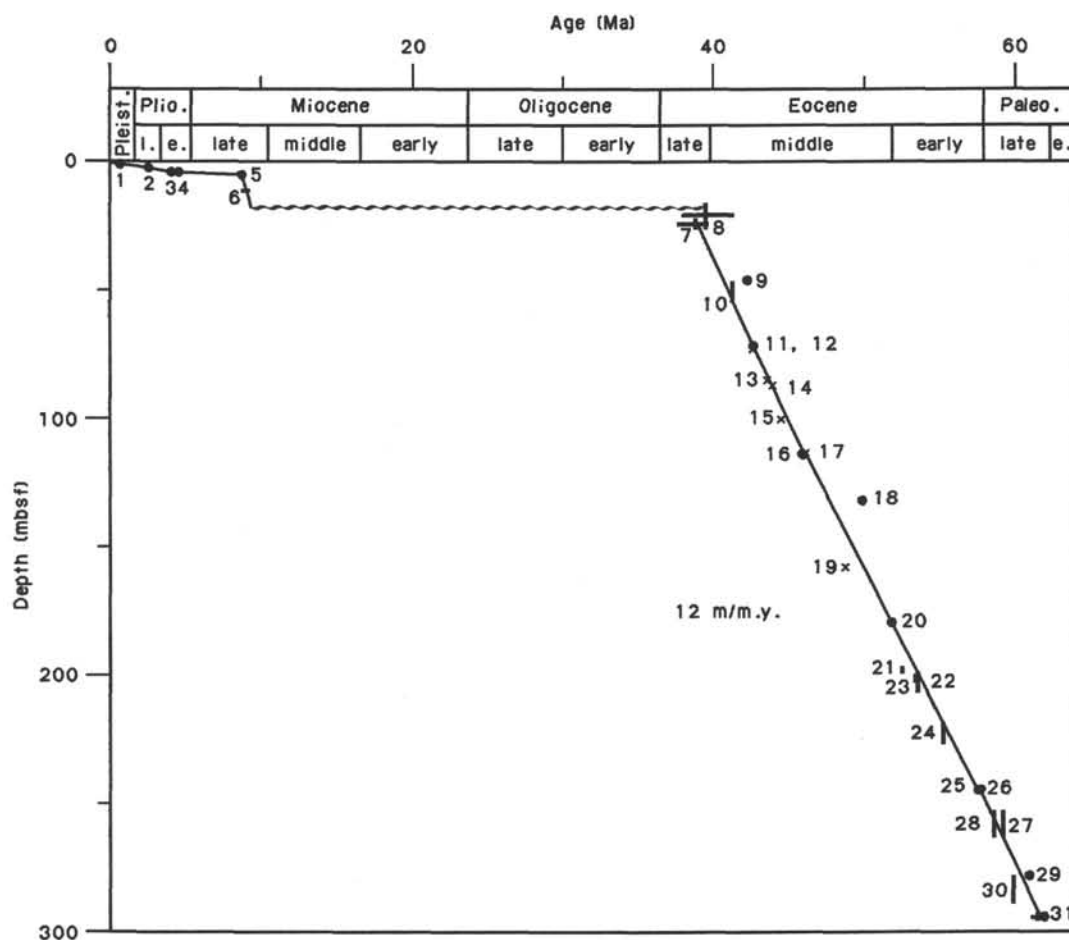


Figure 10. Age-depth relationship of biostratigraphic and magnetostratigraphic datums listed in Table 5.

ence of *Heliolithus riedelii* in Section 114-702B-30X, CC, indicates the presence of NP8 (upper Paleocene) for the interval from Sections 114-702B-28X, CC, to 114-702B-30X, CC.

Section 114-702B-31X, CC, contains *Heliolithus kleinpellii*, the FAD of which defines the base of NP6; thus, this sample is assigned to NP7-6 (upper Paleocene). *Discoaster mohleri* is absent in Hole 702B; its FAD defines the boundary between these two zones.

Section 114-702B-32X, CC, contains *F. tympaniformis* and is thus assigned to NP7-5 (upper Paleocene). It may be restricted to NP5, but the abundance of *H. kleinpellii* is very low, so its FAD in this hole may not be its true FAD.

Paleoenvironment

The assemblages dominated by *R. perplexa* in the upper Miocene sections of both Holes 702A and 702B are similar to those recorded at Site 701. These assemblages are typical of cold surface waters (Haq, 1980).

Calcareous nannofossils are present throughout the upper Eocene to upper Paleocene; this indicates deposition above the CCD. The presence of *Zygrhablithus bijugatus* throughout this section is notable. At Site 699, this species was not recorded above the lower Eocene. This presence may indicate that the depth of Site 702 was less than that of Site 699 through the middle to upper Eocene because this species, a holococcolith, has known shallow-water (less than 1000 m) affinities.

Preservation

Samples above Section 114-702B-6X, CC, contain slightly etched nannofossil floras, and those below the section are over-

grown with secondary calcite. This overgrowth increases down-hole.

Planktonic Foraminifers

Two holes were drilled at Site 702. Four core-catcher samples were examined from Hole 702A; Sections 114-702A-1H, CC, and 114-702A-2H, CC, are late Eocene in age.

Hole 702B penetrated a 294.3-m-thick pelagic sequence of diatom and nannofossil ooze (21.1 m thick) overlying a nannofossil ooze and chalk. The carbonate sequence is from late Paleocene (P3) to late Eocene in age (older than the uppermost zone of upper Eocene, P17). Within it, planktonic foraminifers are abundant and continuously present, whereas radiolarians are rare to common from Sections 114-702B-3H, CC, to 114-702B-13X, CC, and are as abundant as planktonic foraminifers in Sections 114-702B-31X, CC, and 114-702B-32X, CC. These latter two core-catcher samples contain a few Cretaceous foraminifers (*Globigerinelloides* and *Whiteinella* taxa) and shallow-water organisms such as bivalves, stout echinoid spines and plaques, and heavily ornamented ostracodes.

Biostratigraphy

Section 114-702B-1H, CC, is barren. The age of Section 114-702B-2H, CC, is Miocene. The interval from Section 114-702B-3H, CC, to Sample 114-702B-6X-2, 25-27 cm, can be assigned to the P15 Zone. The boundary between late Eocene and middle Eocene is placed at the *Acarinina primitiva* extinction.

Section 114-702B-6X, CC, to Sample 114-702B-13X-3, 140-142 cm, belong to upper middle Eocene *Globigerinatheka index* Zone, P14-11 (upper part), whereas Samples 114-702B-13X-4,

140–142 cm, to 114-702B-17X-3, 30–32 cm, are lower middle Eocene *A. primitiva* Zone, P11. The interval between Samples 114-702B-17X-4, 30–32 cm, and 114-702B-20X-1, 110–112 cm, is assigned to lower middle Eocene *A. primitiva* Zone, P11–10 (lower part).

The interval from Samples 114-702B-20X-2, 110–112 cm, to 114-702B-22X-3, 100–102 cm, is assigned to upper lower Eocene *Morozovella crater* Zone, P9. The interval from Sample 114-702B-22X-4, 100–102 cm, to Section 114-702B-23X, CC, belongs to the lower Eocene *Pseudohastigerina wilcoxensis* Zone, P8.

Globigerinatheka senni is associated with the marker species *Acarinina pentacamerata* in Section 114-702B-23X, CC. The occurrence of *P. wilcoxensis*, *Morozovella marginodentata*, and *Morozovella aequa* between Sample 114-702B-24X-2, 10–12 cm, and Section 114-702B-26X, CC, permits assignment of this interval to lower Eocene *P. wilcoxensis* Zone, P7–6b.

The early Eocene/late Paleocene boundary is not easily recognized, but the interval from Sample 114-702B-27X-1, 7–9 cm, to Section 114-702B-27X, CC, is upper Paleocene on the basis of the absence of *P. wilcoxensis* and *Subbotina pseudobulloides*. The P4 Zone can be identified between Section 114-702B-28X, CC, and Sample 114-702B-31X-1, 53–55 cm. The *Morozovella angulata* zone was recognized from Sections 114-702B-31X, CC, to 114-702B-32X, CC, and therefore, this interval belongs to the upper Paleocene P3b.

The continuity of the planktonic foraminifer assemblages allows the identification of other marker species of the Paleocene standard zonation, such as *Planorotalites pusilla pusilla* (rare), *M. angulata* (common), and the marker species of the lower Eocene, such as *A. pentacamerata*, *Morozovella lensiformis*, and *M. crater*. The FAD of *G. senni* is significant for recognizing the upper part of lower Eocene where morozovellids are lacking. In fact, its FAD occurs within Zone P8 in the low to middle latitudes.

The early Eocene/middle Eocene boundary is placed at the LAD of *M. crater*. The *M. crater* acme Zone is present in this site as well, at 197–198 mbsf, where *M. crater* is very abundant.

The correlation between planktonic foraminifer events and paleomagnetic data allows the calibration of the LAD of *Planorotalites* to the lower part of P11. The FAD of *G. index* falls approximately within the boundary of Subchrons C20R and C20N, which is just below the lower boundary of P12 Zone. This event, consequently, can be assigned to the upper part of P11, in agreement with Bolli (1972). Thus, the upper boundary of the *A. primitiva* Zone falls within the upper part of the P11 Zone. The LAD of *A. primitiva* probably occurs within P14. The *Catapsydrax africanus* horizon falls just below the boundary P13/14.

Within the upper Eocene is the almost co-occurrence of two important events: LAD of *Acarinina rugosoaculeata* or *Acarinina collectea* and FAD of *Globorotalia opima nana*. The former event is considered to fall within P15 Zone (McGowan, 1986).

Paleoenvironment

The presence of other standard marker species in the lower part of upper Paleocene confirms an affinity between low- to midlatitude and high-latitude assemblages. In the uppermost part of the Paleocene the warmest water, strong-keeled morozovellids are absent; on the contrary, subbotinids (*Subbotina patagonica* and *Subbotina eocaenica*) become dominant. A rounded acarininid (*Acarinina nitida*) is very abundant in the lower Eocene (Section 114-702B-24X, CC). Throughout the lower Eocene, angular acarininids are common and *Morozovella* are sometimes common as well, indicating a warm influence. Within the middle Eocene, acarininids become more and more monospecific, and only small, rounded acarininids remain, with the exception of *A. primitiva*. The continuity of the planktonic as-

semblage and its discrete preservation in Hole 702B, however, allow the identification of the presence of a few *Morozovella spinulosa* just below the FAD of *G. index* in P11–12 Zones of middle Eocene, which could be related to a warm episode during the cooling trend that is evident in the upper part of *G. index* Zone, where acarininids disappear around the middle Eocene/late Eocene boundary.

The upper Eocene assemblages are represented mainly by cold-water forms, such as *Catapsydrax*, *Globigerina angiporoides*, *Subbotina linaperta*, *Globorotaloides suteri*, and *G. opima nana*, which are characteristic within the Oligocene. Only *G. index* and a few *Globigerinatheka rubrififormis* persist. The great abundance of large specimens of *Chiloguembelina cubensis* can be related to a period of low productivity in the late Eocene. Bioprovincial indices are species that dominate a region, such as *A. primitiva* earlier and *G. index* later on, but have distributions that are not limited to that region. These species can be used to correlate with faraway areas. In fact, the preceding two species are present at low to middle latitudes as well. The presence of bioprovincial indices is a characteristic of high-latitude regions.

Preservation

Planktonic foraminifers are moderately to poorly preserved within the intervals where siliceous organisms are abundant. Their tests are always recrystallized.

Benthic Foraminifers

Core-catcher samples from Site 702 yielded generally well-preserved, diverse benthic foraminifer assemblages. Four cores were recovered from Hole 702A. The first core contains no benthic foraminifers. Section 114-702A-2H, CC, contains a Neogene assemblage including *Cibicidoides bradyi*, *Epistominella exigua*, *Laticarinia pauperata*, *Pullenia bulloides*, *Sphaeroidina bulloides*, *Anomalinoidea* spp., *Cibicidoides* spp., *Dentalina* spp., *Fissurina* spp., *Gyroidinoidea* spp., *Martinottiella* spp., and *Oridorsalis* spp. Sections 114-702A-3H, CC, and 114-702A-4H, CC, include common to frequent specimens of an Eocene assemblage: *Nuttallides truempyi*, *Cibicidoides praemundulus*, *C. bradyi*, *Cibicidoides eocaena*, *Cibicidoides praemundulus*, *Anomalinoidea capitatus*, *Nonion havanensis*, *P. bulloides*, *Pullenia eocaenica*, *Pullenia quinqueloba*, and *Uvigerina rippensis*.

Thirty-two cores were recovered from Hole 702B. Section 114-702B-1H, CC, contains no benthic foraminifers. Section 114-702B-2H, CC, contains an abundant fauna with low diversity, including *Cibicidoides* spp., *Gyroidinoidea* spp., *Oridorsalis* spp., *Pullenia* spp., and several species of miliolid and agglutinated taxa. The entire Eocene section (Sections 114-702B-3H, CC, to 114-702B-26X, CC) is dominated by *N. truempyi* and *Cibicidoides* species; in particular, abundant *C. praemundulus* and *C. eocaena*, along with common to frequent *Cibicidoides dickersoni*, *Cibicidoides grimsdalei*, *Cibicidoides havanensis*, and *Cibicidoides micrus*, are present. Common to frequent taxa include *A. capitatus*, *Hanzawaia ammophilus*, *Osangularia mexicana*, and buliminids. Buliminids are present in the Eocene cores from Sections 114-702B-9X, CC, to 114-702B-26X, CC, and are abundant from Sections 114-702B-15X, CC, to 114-702B-24X, CC. They include abundant *Bulimina semicostata* and *Bulimina jarvisi* and common to rare *Bulimina alazanensis*, *Bulimina macilenta*, *Bulimina trinitatensis*, *Bulimina tuxpomensis*, and *Buliminella grata*. Other common species are *P. bulloides*, *P. eocaenica*, *P. quinqueloba*, *N. havanensis*, and undifferentiated taxa *Anomalinoidea*, *Gyroidinoidea*, *Lenticulina*, and *Oridorsalis*. *U. rippensis* is abundant from Sections 114-702B-3H, CC, to 114-702B-5X, CC. Deep-water species with isolated occurrences in the Eocene section at this hole are *Abys-*

samina quadrata, *Aragonia aragonensis*, and *Quadriformina profunda*. Agglutinated taxa are rare to common and include *Karriella subglabra*, *Spiroplectamina spectabilis*, *Textularia* sp., and *Vulvulina spinosa*.

The Paleocene section (Sections 114-702B-27X, CC, to 114-702B-32X, CC) is dominated by *Gavelinella beccariiiformis*, with frequent to common occurrences of *Cibicidoides pseudoperlucida*, *Cibicidoides hyphalus*, *Anomalinoidea danica*, *N. truempyi*, and *Osangularia velascoensis*. Other rare to common taxa include *Aragonia velascoensis*, *Bolivinoidea delicatula*, *Gyroidinoidea globosus*, *Gyroidinoidea quadratus*, *Neoponides hillebrandti*, *Neoponides lunata*, *Neoflabellina semireticulata*, *P. bulloides*, and buliminids (*Bulimina midwayensis*, *B. trinitatensis*, and *Bulimina velascoensis*). Common undifferentiated taxa are *Gyroidinoidea*, *Lenticulina*, *Nonion*, *Oridorsalis*, and pleurostomellids. Agglutinated taxa include *Dorothia trochoides*, *Gaudryina pyramidata*, *K. subglabra*, *S. spectabilis*, *Tritaxia havanensis*, *Tritaxia paleocenica*, and *V. spinosa*.

Paleodepth estimates are based on Tjalsma and Lohmann (1983) and van Morkhoven et al. (1986). The upper Paleocene fauna at Hole 702B contains lower bathyal to abyssal assemblages. The dominance of *Stensioina beccariiiformis* over *N. truempyi*, along with moderate to high abundances of *C. hyphalus*, *Lenticulina* spp., and buliminids, suggest that the paleodepth was upper bathyal (1000–2000 m). The Eocene assemblage at Hole 702B is also characteristic of a lower bathyal paleodepth, supported by high abundances of *C. eocaena*, *Lenticulina* spp., and buliminids (especially *Bulimina callahani* and *B. semicostata*) and very low abundances of primarily deeper water species, such as *Abyssamina* spp., *Alabama dissonata*, and *Clinapertina* spp.

Diatoms

Diatoms are abundant to common and well preserved in the Neogene sediments but are rare and very poorly preserved in the upper and upper middle Eocene at Site 702. The tests are so poorly preserved that no zonal assignment or more accurate age determination is possible than “probably Eocene”; below Section 114-702B-7H, CC, the determination of “probably middle Eocene” is possible. Diatoms are completely dissolved, and clinoptilolite is found in the silt fraction below Section 114-702B-13H, CC. Only the bottom two cores (Cores 114-702B-31X and 114-702B-32X) contain a poorly preserved diatom assemblage of Paleocene age. For abundance fluctuations of diatoms and clinoptilolite through Hole 702B see Figure 13 (“Geochemistry” section, this chapter). For the Neogene the subantarctic diatom zonation as given in Ciesielski (1983) was applied.

The identified zones are listed below:

Sample	Depth (mbsf)	Zone	Age
Hole 702A:			
1H-1, 40 cm, to 1H-1, 48 cm	0.4–0.48	<i>Coscinodiscus lentiginosus</i>	Quaternary
1H-2, 90 cm, to 1H-2, 105 cm	2.4–2.55	<i>Coscinodiscus insignis</i>	late Pliocene
1H-3, 60 cm	3.6	<i>Nitzschia praeinterfrigidaria</i>	early Pliocene
1H, CC	4.6	<i>Denticulopsis hustedtii</i>	late Miocene
2H-2, 46 cm, to 3H-5, 70 cm	6.6–20.8	<i>D. hustedtii-Denticulopsis lauta</i>	late Miocene
3H-6, 51 cm	22.11	<i>Nitzschia denticuloides</i>	middle Miocene
3H, CC, to 4H, CC	23.6–33.1		Miocene + late Eocene

Sample	Depth (mbsf)	Zone	Age
Hole 702B:			
1H-2, 40 cm	1.9	<i>Coscinodiscus vulnificus</i>	late Pliocene
1H-3, 145 cm	4.45	<i>D. hustedtii</i>	late Miocene
1H-4, 50 cm, to 3H-4, 14 cm	5.0–20.4	<i>D. hustedtii-D. lauta</i>	late Miocene
3H-4, 80 cm	21.1	<i>N. denticuloides</i>	middle Miocene
3H-4, 85 cm, to 13H, CC	21.2–120.3		Eocene
14H, CC, to 30X, CC	129.8–277.3	Barren	
31X, CC, to 32X, CC	286.8–294.3		Paleocene

A large hiatus spanning approximately 29–33 m.y. separates lower upper Miocene and Eocene sediments in both Cores 114-702A-3H and 114-702B-3H. The smear slides examined in the first three cores from Holes 702A and 702B revealed the presence of many of the established diatom zones. Much closer sample spacing is required to decide whether they are separated by a number of small hiatuses or represent a complete section with slow sediment accumulation.

The Neogene diatom assemblages are characteristic of the subantarctic open-ocean environment. The few Paleocene species found are cosmopolitan.

Radiolarians

Radiolarians were generally well preserved and few to abundant in sediments from Site 702. Based solely on examination of core-catcher samples, radiolarian-bearing sediments were assigned to Hays and Opdyke's (1967) and Chen's (1975) zonal schemes as follows:

114-702A-1H, CC	<i>Helotholus vema</i> (early Pliocene, 2.43–5.10 Ma; γ and τ zones; Gauss-Gilbert Chrons)
114-702A-3H, CC, to 114-702A-4H, CC	unzoned (late middle Miocene–late Eocene)
114-702B-1H, CC	<i>H. vema</i> (early Pliocene, 2.43–5.10 Ma; γ and τ zones; Gauss-Gilbert Chrons)
114-702B-3H, CC, to 114-702B-18X, CC	unzoned (late Eocene–middle Eocene)
114-702B-31X, CC, to 114-702B-32X, CC	unzoned (late Paleocene)

Within the “unzoned” interval of late Eocene–middle Eocene age, specimens of *Lychnocanoma amphirite* and two apparently new species of genus *Thyrsocyrtis* are distinct in their morphology and are much larger than the remaining faunal components (>200 vs. ~100 μ m). Therefore, the following subdivision for the interval seems possible:

114-702B-3H, CC–114-702B-7H, CC: common to abundant occurrence of a *Thyrsocyrtis* species that is closely related to *Thyrsocyrtis bromia* of the low latitudes. The upper part of this interval may be correlative with Section 114-701B-45X, the deepest radiolarian-bearing sample of the previous site. In addition, this interval is probably coeval to the “*Thyrsocyrtis bromia* zonal equivalent” section indicated by Weaver (1983; also in Shaw and Ciesielski, 1983).

114-702B-8X, CC–114-702B-9X, CC: the upper local range of *L. amphirite* and the occurrence of another large new *Thyrsocyrtis* species.

114-702B-10X, CC-114-702B-12X, CC: the lower part of the local range of *L. amphitrite* and the joint occurrence of *Lophoconus titanothericeraos* and *Lophocyrtis biaurita*.

114-702B-13X, CC-114-702B-19X, CC: similar to the preceding, but *L. amphitrite* is absent.

As for the "unzoned" interval of late Paleocene age, both Sections 114-702B-31X, CC, and 114-702B-32X, CC, contain *Buryella tetradica*, *Buryella pentadica*, and *Stylosphera goruna*. The occurrence of the two *Buryella* species is limited to *Bekoma bidartensis* and the underlying, and yet unzoned, interval in the low-latitude zonation (Sanfilippo et al., 1985). The presence of *S. goruna* was reported previously from Paleocene sediments of Site 208 in the Pacific sector of the antarctic region (Dumitrica, 1973).

Silicoflagellates

Core-catcher samples from Site 702 yielded common to abundant and moderate to well-preserved silicoflagellates that can be assigned to the biostratigraphic zonation proposed by Shaw and Ciesielski (1983).

114-702A-1H, CC	<i>Distephanus boliviensis</i>	early Pliocene
114-702A-2H, CC	unzoned	early to middle Miocene
114-702A-3H, CC- 114-702A-4H, CC	<i>Mesocena occidentalis</i>	late Eocene
114-701B-1H, CC	<i>D. boliviensis</i>	early Pliocene
114-702B-2H, CC	unzoned	early to middle Miocene
114-702B-3H, CC- 114-702B-4X, CC	<i>M. occidentalis</i>	late Eocene
114-702B-5X, CC- 114-702B-10X, CC	<i>Dictyocha grandis</i>	middle Eocene
114-702B-31X, CC- 114-702B-32X, CC	<i>Corbisema disymmet- rica disymmetrica</i>	late Paleocene

For the unzoned interval of early to middle Miocene age, both Sections 114-702A-2H, CC, and 114-702B-2H, CC, are characterized by the predominance of *Distephanus crux* and *Distephanus quinquangellus*. No similar assemblage was encountered in shipboard Leg 114 investigations.

Assignment of the upper Eocene *M. occidentalis* Zone here is tentative for Sections 114-702A-3H, CC, 114-702A-4H, CC, and 114-702B-3H, CC, because some of the selected species that would assist in identifying the zone (Shaw and Ciesielski, 1983) are missing (e.g., *Naviculopsis trispinosa*, *Corbisema hastata*, and *Corbisema triacantha*).

Within the *D. grandis* zone, Sections 114-702B-5X, CC, to 114-702B-10X, CC, which is defined by the range of the named species, only the oldest *Dictyocha stelliformis* Subzone can be recognized from Sections 114-702B-9X, CC, to 114-702B-10X, CC. This is because *Mesocena apiculata*, which would define the overlying two subzones, is absent in the examined samples.

According to Site 512 data, the minimum range of the *D. grandis* Zone is from slightly above Chron C20N (44.7 Ma) to the top of Chron C18N (41.3 Ma), and the top of *D. stelliformis* Subzone is placed slightly below Chron C19 (~44.1 Ma) (Shaw and Ciesielski, 1983).

The upper Paleocene samples from Sections 114-702B-31X, CC, and 114-702B-32X, CC, are characterized by the abundant occurrence of *C. disymmetrica disymmetrica*, as observed in Section 114-700B-30R, CC.

Ebridians

As for the previous sites investigated during Leg 114, ebridians were observed in numerous core-catcher samples but were rare to few in abundance.

In addition to *Ammodoichium rectanulare*, which occurs in most of Miocene and Eocene sediments, both *Ammodoichium ampulla* and *Micromarsupium anceps* were observed in lower to middle Eocene Sections 114-702B-3H, CC-114-702B-7X, CC, and *Ebriopsis crenulata* was observed in middle Eocene Sections 114-702B-9X, CC, and 114-702B-10X, CC. We noticed that some of the *E. crenulata* possess lorica or are in the podamphora stage in their ontogeny.

Paleoenvironment

Analysis of core-catcher samples from Site 702 revealed that upper Miocene sediments, Sections 114-702A-2H, CC, and 114-702B-2H, CC, contain warm-water species of the radiolarian genera *Euchitonia* and *Hymeniastrum* and silicoflagellate genus *Dictyocha*, which suggests a relatively warm, surface-water environment. On the other hand, both of the lower Pliocene sediment Sections 114-702A-1H, CC, and 114-702B-1H, CC, consist of typical antarctic assemblages, with the complete absence of the pre-Matuyama and Pliocene subantarctic species listed by Weaver (1983), thus indicating deposition south of the polar front.

GEOCHEMISTRY

Pore waters were squeezed from twelve 5- or 10-cm-long whole-round samples at about 30-m intervals from Holes 702A and 702B. In contrast to the procedures at previous sites, squeezers were maintained in a refrigerator at a temperature near to that of the bottom water (0°–3°C) to provide for an attempted characterization of potential temperature-of-squeezing artifacts for silica and, perhaps, fluoride. Samples to be squeezed were immediately placed in these refrigerated squeezers and the water expressed through 0.4- μ m filters directly into syringes. The squeezers have sufficient thermal inertia that during squeezing, temperatures in the sediment cake are thought not to have increased more than 2°C during the 15-min period of pore-water expression. The water was then post-filtered again from the syringe into sample vials.

The results of the pore-water chemistry are reported in Table 6 and Figures 11 through 13.

Volatile hydrocarbon gases (methane and ethane) were analyzed in all cores (Table 7). Sedimentary organic carbon and calcium carbonate were determined on most core sections (Table 8).

The major lithostratigraphic intervals affecting pore-fluid composition comprise two main units. Unit I (0–21.1 mbsf) consists of a Neogene muddy diatom ooze underlain by a nanofossil-diatom ooze. This upper unit contains ice-rafted debris and sparse volcanic ash shards. Unit II (22.1–294.3 mbsf) is an upper Paleocene to upper Eocene nanofossil ooze that grades downward into nanofossil chalk (32.8–202.5 mbsf) and below that to indurated nanofossil micritic chalk (202.5–294.3 mbsf). Nanofossils show evidence of intense recrystallization and reprecipitation in the lowermost unit. Chert stringers are observed in the basal 100 m of the section, and zeolites (clinoptilolite) are abundant between 170 and 270 mbsf.

Interstitial-Water Chemistry

Pore-water chemistry at Site 702 reflects alteration reactions with basalt basement approximately 100 m below the recovered section, a trace of silicic volcanic ash alteration within the upper sediment column (magnesium and calcium), plus carbonate recrystallization reactions deep in the section (alkalinity). There is some evidence for *in-situ* chert formation near the bottom of the hole (dissolved silica).

Salinity and Chloride

Salinity values at the top of the sediment column reflect the salinity of the overlying bottom water. Salinities and chloride

Table 6. Interstitial-water chemistry data from Holes 702A and 702B.

Sample (cm)	Depth (mbsf)	Volume (mL)	pH	Alkalinity (mmol/L)	Salinity (g/kg)	Magnesium (mmol/L)	Calcium (mmol/L)	Chloride (mmol/L)	Sulfate (mmol/L)	Fluoride ($\mu\text{mol/L}$)	Silica ($\mu\text{mol/L}$)	Mg/Ca
Hole 702A:												
1H-2, 145-150	2.95	46	7.70	2.92	34.2	53.29	10.88	552.00	29.14	67.00	793	4.90
3H-5, 145-150	21.55	64	7.65	2.93	35.0	53.40	11.57	561.00	28.28	65.00	819	4.62
Hole 702B:												
1H-3, 145-150	4.45	60	7.57	3.00	34.7	53.59	10.90	556.00	28.63	67.50	802	4.92
3H-5, 145-150	23.25	43	7.58	2.96	34.5	53.15	11.66	564.00	27.79	70.30	762	4.56
6X-1, 145-150	45.75	47	7.62	3.02	34.8	52.01	13.12	563.00	27.30	68.10	787	3.96
9X-4, 145-150	78.75	40	7.54	2.85	34.4	50.91	14.61	560.00	27.10	71.70	749	3.48
12X-5, 145-150	108.75	34	7.61	2.92	34.5	48.57	16.95	559.00	26.38	68.90	787	2.87
15X-5, 145-150	137.25	37	7.57	2.74	34.6	47.30	18.94	564.00	25.91	70.30	730	2.50
18X-5, 140-150	165.70	36	7.38	2.94	34.6	45.63	21.00	566.00	25.36	76.70	798	2.17
21X-2, 140-150	189.70	32	7.38	2.82	34.9	45.13	22.23	564.00	25.46	81.70	560	2.03
24X-2, 140-150	218.20	25	7.47	2.68	35.0	43.34	24.42	564.00	25.61	92.80	500	1.77
30X-1, 140-150	273.70	17	7.42	2.47	35.2	41.15	28.68	565.00	25.15	99.70	619	1.43

values increase slightly in the uppermost 20 mbsf, decrease to a minimum at about 100 mbsf, and increase again below this depth to constant values. This cyclic, small amplitude, downward-dampened salinity signal is fairly typical of pelagic sediments and reflects the last glacial-interglacial salinity variations in seawater imparted by extraction of water from the oceans into glacial ice during the latest Pleistocene (McDuff, 1985).

Calcium and Magnesium

Calcium concentrations increase fairly linearly downhole from a bottom-water concentration of 10 to about 29 mmol/L, whereas magnesium decreases from a bottom-water concentration of 55 to about 41 mmol/L at the bottom of the hole. There is slight nonlinearity in these vertical profiles in the upper 50 m, which is probably a result of alteration of trace concentrations of silicic ash in the uppermost section. The magnesium to calcium ratio decreases downhole from seawater values of 5.2 to about 1.4.

A plot of calcium vs. magnesium demonstrates that the relative changes in their concentrations are nearly linear with a $\Delta\text{Mg}/\Delta\text{Ca}$ covariation of about -0.74 (Fig. 12). Magnesium and calcium thus display nearly conservative behavior within the sediment column that is indicative of diffusive exchange with basement via alteration of basalts (McDuff, 1981; Gieskes and Lawrence, 1981; Gieskes, 1983). The $\Delta\text{Mg}/\Delta\text{Ca}$ ratio at this site is slightly lower than that observed at Sites 699 and 700 (-0.50), but is much nearer that expected for basalt alteration than for silicic volcanic ash alteration (Baker, 1986). Ash alteration reactions at this site must therefore be minor, as reflected in the trace occurrences of volcanic ash in the uppermost part of the section (see "Lithostratigraphy" section, this chapter).

Alkalinity

Alkalinity at the top of the hole is about 3.0 mmol/L, significantly above bottom-water concentrations (about 2.6 mmol/L). Alkalinity remains fairly constant downhole at values between 2.9 and 3.0 mmol/L to a depth of about 166 mbsf, but it decreases below this to a minimum of 2.5 mmol/L at the bottom of the hole (274 mbsf). Values of pH decrease erratically downhole from about 7.6 to about 7.4 in the base of the section.

These profiles are consistent with little or no organic carbon regeneration or carbonate dissolution reactions in the upper 100 m. The most intense carbonate dissolution/recrystallization is probably occurring near the steepest inflection in the alkalinity gradient, between 130 and 160 mbsf. The downward decrease in alkalinity in the lower part of the section results from contemporaneous carbonate recrystallization and perhaps by calcite

precipitation reactions below the recovered section. These carbonate reactions are too small to affect the vertical calcium profile.

Fluoride, Silica, and Sulfate

Fluoride concentrations are fairly constant at bottom-water concentrations ($70 \mu\text{mol/L}$) down to 137 mbsf, from which they increase downhole to a maximum concentration of $100 \mu\text{mol/L}$ at the bottom of the recovered section (274 mbsf). This profile is very different from that observed in all previous sites on Leg 114. At Sites 698 through 701, fluoride concentrations were slightly less than bottom-water values at the tops of the holes (generally about $60 \mu\text{mol/L}$) and decreased downhole. If the profile in Hole 702B represents *in-situ* conditions, then there is a deep source of fluoride (below the recovered section), with upward diffusion with concomitant consumption of pore-water fluoride into a fluoride-containing solid phase at the depth of the gradient inflection (about 140 mbsf). The lithology at this depth provides no clues as to the fluoride sink.

Because these pore waters were obtained by squeezing at temperatures near that of bottom-water, it is possible that these fluoride data reflect *in-situ* concentrations more closely than the previous profiles (which were squeezed at room temperature, albeit immediately after core retrieval). Previous work on pore-water fluoride extracted from surficial deep-sea sediments suggests an apparent hydrostatic pressure artifact (about $-10 \mu\text{mol/L}/5000 \text{ m water depth}$) and a temperature effect (about $+10 \mu\text{mol/L}/10^\circ\text{C}$) (Froelich et al., 1983). The temperature effect is apparently reversible if the cores are recooled within 24 hr after retrieval to bottom-water temperatures before squeezing. If the temperature gradient in Hole 702B is as high as $20^\circ\text{--}40^\circ\text{C}/\text{km}$, then the *in-situ* temperatures at the depth of the deepest pore-water sample (274 mbsf) could be as high as $5^\circ\text{--}10^\circ\text{C}$ above bottom-water temperatures. Thus, our squeezing temperatures could be progressively colder than *in-situ* temperatures. This effect should cause the values observed at Site 702 to be lower than *in-situ* values, particularly at the bottom of the hole, and the values observed at all previous sites to be at or higher than *in-situ* ones. The sense of this temperature artifact is thus exactly opposite our observations. In the absence of additional evidence, we conclude that neither the fluoride data from Hole 702B nor from previous sites are affected seriously by squeezing artifacts and that the profiles recovered reflect *in-situ* conditions closely. Thus, the reactions affecting the fluoride gradient at Site 702 are apparently different from those observed at other sites, but the reasons for this difference are not apparent and will require additional work.

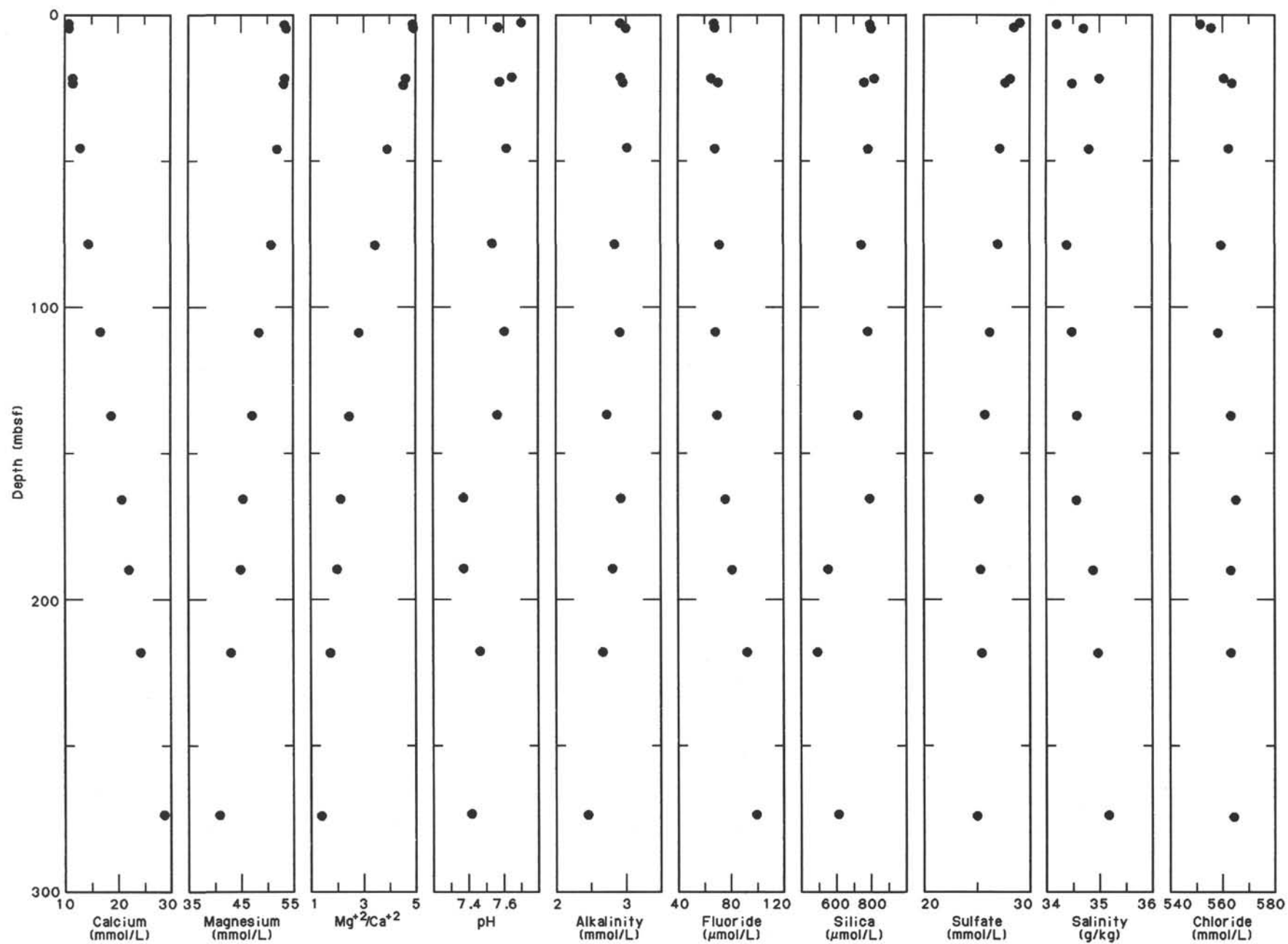


Figure 11. Pore-water calcium, magnesium, Mg/Ca ratio, pH, titration alkalinity, fluoride, dissolved silica, sulfate, salinity, and chloride profiles, Site 702.

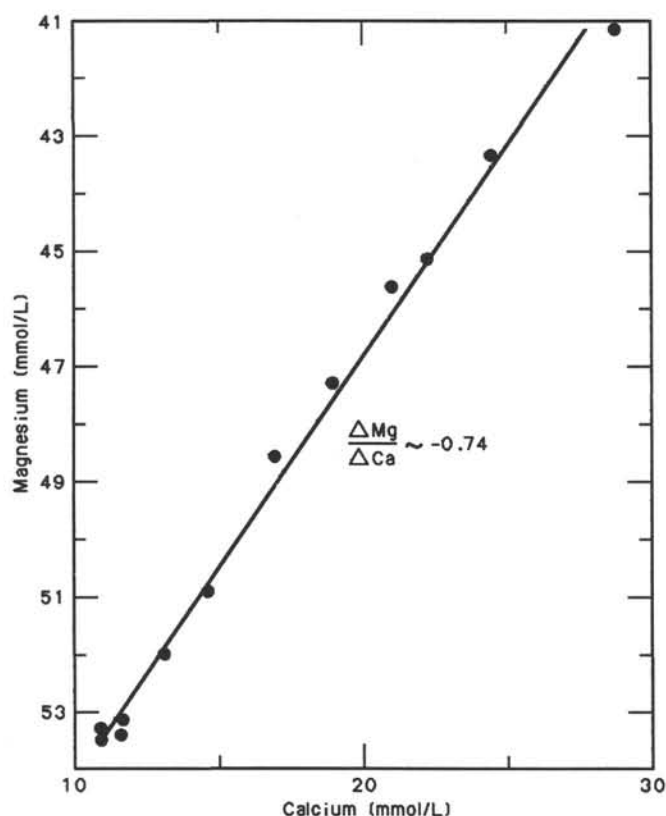


Figure 12. Pore-water calcium vs. magnesium in Holes 702A and 702B. The line through the data is a linear least-squares fit of all the data. The $\Delta\text{Mg}/\Delta\text{Ca}$ covariation at Site 702 is about -0.74 . However, the trend is not perfectly linear, suggesting some nonconservative behavior of calcium and/or magnesium in the sediment column, perhaps as a result of alteration of traces of silicic volcanic ash.

Dissolved silica concentrations at the top of the hole are about $800 \mu\text{mol/L}$, far above bottom-water concentrations (about $100 \mu\text{mol/L}$). The silica concentrations remain remarkably constant at $780 \pm 30 \mu\text{mol/L}$ from the top of the hole to about 180 mbsf, below which concentrations fall to about $500\text{--}600 \mu\text{mol/L}$. The shape of this profile suggests dissolution of biosiliceous opal above 180 mbsf, with diffusion downward into the interval between about 180 mbsf and the bottom of the hole, 294 mbsf. Chert stringers are common in this interval (Table 4 and Fig. 13), suggesting that dissolution of diatomaceous opal has provided the silica for chert precipitation by diffusion from higher up in the section.

Dissolved silica is also known to be susceptible to temperature-of-squeezing artifacts. The concentrations of dissolved silica in Hole 702B are significantly lower in diatom-rich intervals than as observed at the previous sites. The higher and more erratic values ($1000\text{--}1400 \mu\text{mol/L}$) in previous "warm-squeezed" samples are undoubtedly a result of this temperature effect. However, the relative concentration levels accurately reflect the lithology of siliceous constituents.

Sulfate decreases slightly from bottom-water concentrations of 28.9 mmol/L to a low of about 25.2 mmol/L at the bottom of the hole and thus, is never completely depleted in the recovered section. Most of the curvature in this gradient is confined to the upper 150 m. Pore-water sulfate is almost constant below 150 mbsf ($25.4 \pm 0.2 \text{ mmol/L}$), implying the existence of very slight microbial sulfate reduction throughout only the upper 150 m or so of the sediment column. Organic carbon values (Fig. 14) exceed 0.25% only in the interval between about 30

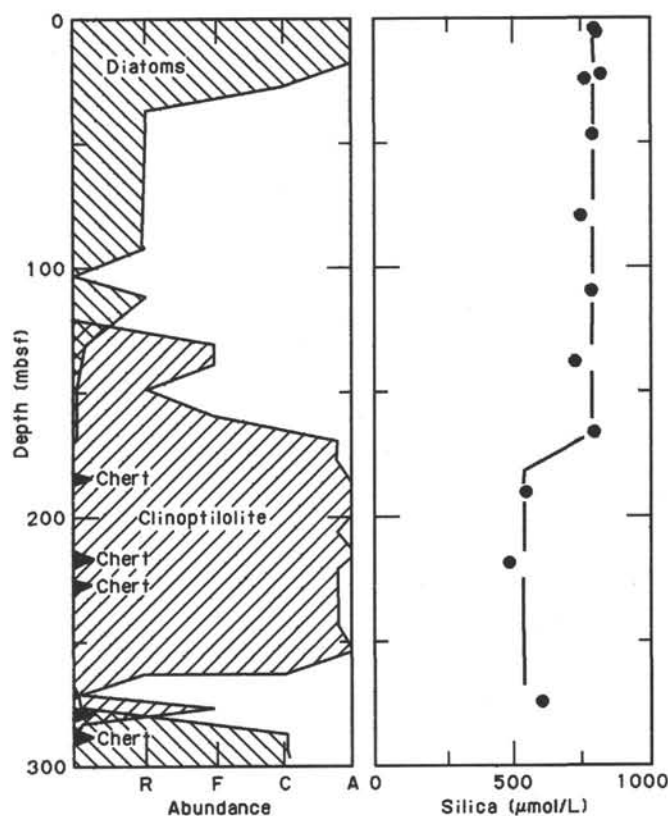


Figure 13. Relative abundances of diatoms, zeolites (clinoptilolite), and chert in the sediments and dissolved silica concentrations in the pore waters of Holes 702A and 702B.

and 150 mbsf, consistent with the sulfate profile. Organic carbon values below about 160 mbsf are effectively zero. Negative values reflect uncertainty in the analytical technique and are statistically indistinguishable from zero organic carbon.

Volatile Hydrocarbon Gases

Methane and ethane levels are very low, at detection levels. Thus, methanogenesis in the presence of pore-water sulfate is not occurring at this site.

Sedimentary Organic and Inorganic Carbon

The organic carbon data are discussed in conjunction with sulfate diagenesis (see the preceding). The calcium carbonate data are presented in the "Lithostratigraphy" and "Physical Properties" sections.

PALEOMAGNETICS

Shipboard paleomagnetic analyses concentrated on the Paleocene-Eocene section recovered from Hole 702B because of the poor prospects of obtaining an age-diagnostic polarity reversal sequence from the short Miocene section recovered at this site. The Paleocene-Eocene section was rotary cored with the XCB system, resulting in random core azimuths. Thus, the paleomagnetic declination values could not be used for polarity determinations, and polarity assignments were made on the basis of inclination values alone.

Paleomagnetic Determinations

The magnetic intensity of these calcareous sediments is extremely weak, typically in the range 10^{-1} to 10^{-2} mA/m (10^{-7} to 10^{-8} emu/cm^3). Consequently the majority of measurements

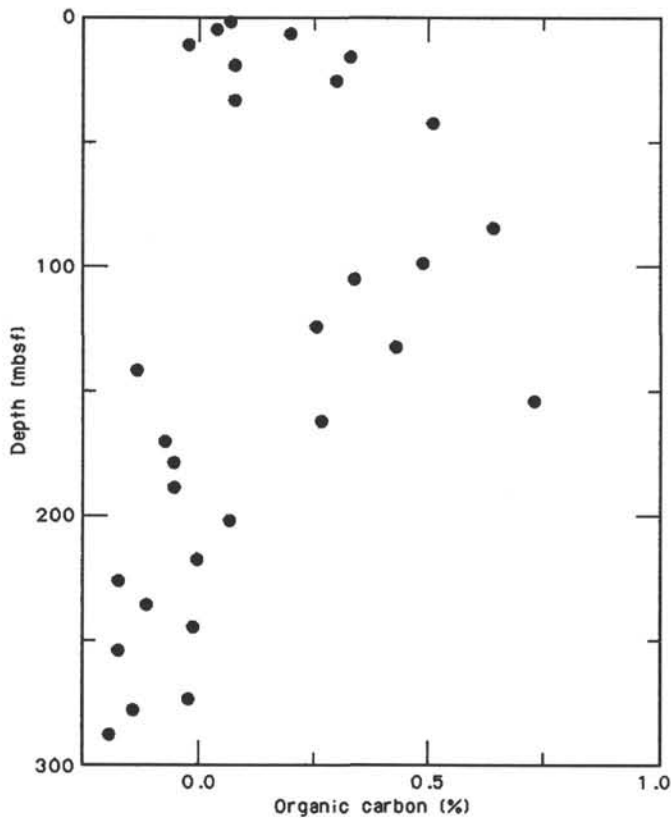


Figure 14. Percent organic carbon profile in Holes 702A and 702B. The plotted values reflect an absolute accuracy of about $\pm 0.2\%$ in these calcium carbonate-rich sediments. Values less than zero are due to the statistical difficulty in determining organic carbon by the difference of two large numbers (total carbon minus carbonate carbon) and are effectively equal to zero organic carbon.

on the pass-through cryogenic magnetometer were made using the most sensitive range. Relatively calm seas during drilling at this site helped to minimize instrument noise, so reliable paleomagnetic determinations were achieved from the majority of cores despite their very weak intensity of magnetization and the common occurrence of biscuiting. At previous sites on Leg 114, we observed that the drilling slurry that occupies the space between and around core biscuits commonly carries a remanent magnetization, which is probably acquired by mechanical alignment of ferromagnetic mineral grains during flow of the slurry in the core. This effect, however, does not appear to be prevalent in the more weakly magnetic carbonates at Site 702, and the paleomagnetic signal from the core biscuits in Hole 702B was not significantly degraded by the presence of the drilling slurry.

Magnetic Polarity

The sequence of magnetic polarity zones identified in Hole 702B is shown in Figure 15. The magnetostratigraphic record in Cores 114-702B-8X to 114-702B-13X is well defined. Preliminary nannofossil data indicate a probable age range of NP16 to NP15 for the interval from Sample 114-702B-15X-2, 60 cm, to Section 114-702B-21X, CC, and foraminifer data indicate a late middle Eocene age. Consequently, a correlation of this set of magnetozones can be made with Chrons C18N to C20R, which span this age interval. The relative durations of these chron match the relative thicknesses of the successive magnetozones in this interval particularly well (Fig. 10), suggesting a fairly uniform sedimentation rate of about 12 m/m.y. during this period.

Correlation of the long reverse magnetozones in Cores 114-702B-13X to 114-702B-17X and the dominantly normal magne-

Table 7. Volatile hydrocarbon gases (methane and ethane) from Site 702 headspace samples.

Sample (cm)	Depth (mbsf)	C ₁ (ppm)	C ₂ (ppm)
Hole 702A:			
1H-2, 140-145	2.90	3.3	0.8
2H-5, 145-150	10.81	2.5	0.0
3H-6, 0-5	21.60	3.3	0.0
4H-6, 0-5	31.10	5.7	0.0
Hole 702B:			
1H-4, 0-5	4.50	7.1	0.5
2H-5, 0-5	12.30	3.2	0.0
3H-6, 0-5	23.30	3.8	0.1
4H-5, 0-5	31.30	3.9	0.0
5X-5, 0-5	40.80	3.7	0.1
6X-2, 0-5	45.80	2.8	0.0
7X-2, 0-5	55.30	3.3	0.0
8X-6, 0-5	70.80	3.7	0.9
9X-3, 145-150	77.25	2.7	0.8
10X-3, 0-5	85.30	4.6	1.6
11X-3, 0-5	94.80	1.9	0.0
12X-3, 0-5	104.30	4.3	0.0
13X-3, 0-5	113.80	1.7	2.9
14X-4, 0-5	124.80	1.7	0.0
15X-3, 0-5	132.80	2.2	0.0
17X-6, 0-5	156.30	1.7	0.0
18X-3, 0-5	161.30	2.5	0.0
19X-3, 0-5	170.80	1.7	0.0
20X-3, 0-5	180.30	2.0	0.0
21X-3, 0-5	189.80	1.6	0.0
22X-4, 0-5	200.80	3.7	1.3
24X-3, 0-5	218.30	5.1	0.0
26X-1, 0-5	234.30	0.8	0.0
29X-1, 0-5	262.80	0.0	0.0
30X-2, 0-5	274.29	3.8	0.3

tozone in Cores 114-702B-17X to 114-702B-21X with the polarity time scale is less straightforward. The most simple interpretation is that the reverse magnetozones in Cores 114-702B-13X to 114-702B-17X represents Chron C20R and that at least the upper part of the underlying normal magnetozones represents Chron C21N (Fig. 15). This interpretation is consistent with the available nannofossil data, which indicate an age in the range of NP16 to NP15 for this interval.

The short reverse polarity magnetozones in Core 114-702B-20X provisionally can be interpreted as representing part of Chron C21R, and the normal magnetozones that extends from the lower part of this core to the upper part of Core 114-702B-21X can be interpreted as Chron C22N. This interpretation requires the existence of a stratigraphic hiatus within Core 114-702B-20X at a depth of about 183 mbsf in order to explain the very short length of the reverse polarity magnetozones. The absence or attenuation of this magnetozones would support the suggested occurrence of a hiatus within Core 114-702B-20X. There is evidence from physical-property data for a hiatus at this level (see "Physical Properties" section).

PHYSICAL PROPERTIES

Physical-property measurements in carbonate-rich pelagic sediments at Site 702 serve two main purposes: (1) to investigate the variability of physical properties and the relationship to the occurrence of seismic reflectors in a homogeneous nannofossil ooze and (2) to investigate whether hiatuses (see "Biostratigraphy" section, this chapter) are associated with changes in the physical properties.

The methods of physical-property measurements were described in the "Explanatory Notes" chapter. Four sets of measurements were obtained on selected samples of undisturbed

Table 8. Sedimentary organic carbon and calcium carbonate data, Site 702.

Sample (cm)	Depth (mbsf)	C _{org} (%)	CaCO ₃ (%)
Hole 702A:			
1H-1, 100-102	1.00	0.07	0.08
1H-2, 109-111	2.59		0.08
1H-3, 91-93	3.91		0.17
2H-2, 98-100	5.84	0.20	0.17
2H-3, 98-100	7.34		40.78
2H-4, 99-101	8.85		39.28
2H-5, 99-101	10.35		55.04
2H-6, 99-101	11.85		70.06
2H-7, 99-101	13.35		41.20
3H-1, 100-102	15.10	0.33	63.63
3H-2, 100-102	16.60		65.39
3H-3, 100-102	18.10		56.38
3H-4, 100-102	19.60		50.21
3H-5, 99-101	21.09		44.62
3H-6, 48-50	22.08		2.92
3H-6, 99-101	22.59		78.73
4H-1, 99-101	24.59	0.30	86.24
4H-2, 99-101	26.09		84.57
4H-3, 99-101	27.59		84.57
4H-4, 99-101	29.09		80.40
4H-5, 99-101	30.59		86.99
4H-6, 99-101	32.09		88.57
Hole 702B:			
1H-3, 100-102	4.00	0.04	0.08
2H-3, 100-102	10.30	-0.02	52.38
3H-2, 100-102	18.30	0.08	59.13
3H-3, 100-102	19.80		51.62
3H-5, 100-102	22.80		85.23
4H-5, 105-107	32.35	0.08	83.48
5H-5, 100-102	41.80	0.51	82.65
8X-2, 100-102	65.80	0.01	89.07
8X-4, 113-115	68.93		91.91
9X-3, 59-61	76.39	-0.02	88.99
10X-2, 34-36	84.14	0.64	83.98
10X-4, 74-76	87.54		85.57
11X-5, 48-50	98.28	0.49	79.65
12X-3, 50-52	104.80	0.34	89.07
12X-5, 69-71	107.99		86.99
13X-3, 25-27	114.05	0.88	89.82
13X-5, 124-126	118.04		89.24
14X-3, 39-41	123.69	0.26	90.32
15X-2, 70-72	132.00	0.43	87.90
15X-5, 111-113	136.91		94.99
16X-2, 50-52	141.30	-0.13	92.99
16X-6, 41-43	147.21		94.99
16X-6, 86-88	147.66		92.57
17X-4, 50-52	153.80	0.73	87.34
17X-5, 28-30	155.08		89.49
18X-3, 42-44	161.72	0.27	91.07
18X-5, 50-52	164.80		93.41
19X-2, 60-62	169.90	-0.07	95.24
19X-5, 40-42	174.20		95.08
19X-6, 110-112	176.40		92.41
20X-1, 123-125	178.53	-0.05	94.58
20X-2, 120-122	180.00		92.57
20X-4, 88-90	182.68		92.91
21X-2, 37-39	188.67	-0.05	95.49
22X-4, 109-111	201.89	0.07	90.91
22X-5, 38-40	205.61		88.74
24X-2, 69-71	217.49	0.00	94.83
25X-1, 108-110	225.88	-0.17	93.99
26X, CC (14-16)	235.54	-0.11	91.66
27X-1, 70-72	244.50	-0.01	91.24
28X, CC (35-37)	253.97	-0.17	92.24
30X-1, 111-113	273.41	-0.02	93.07
30X-2, 54-56	274.34		93.49
31X-1, 48-50	277.78	-0.14	88.07
32X, CC (4-5)	287.58	-0.19	75.81
32X, CC (29-31)	287.83		63.30

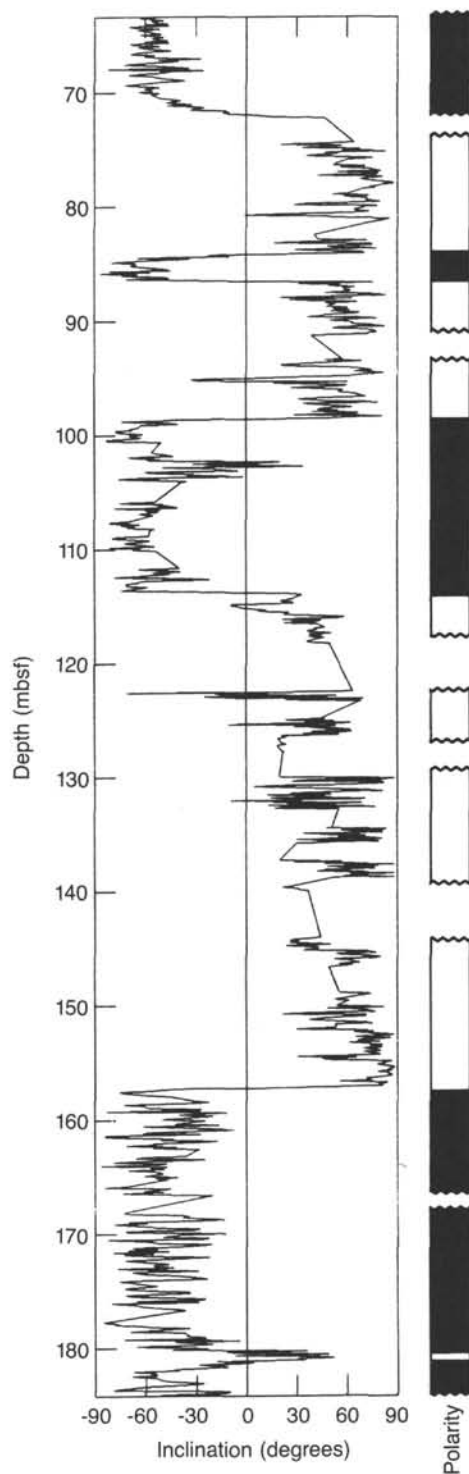


Figure 15. Variation of the inclination of remanent magnetization with depth in Hole 702B. Lines indicate data from pass-through magnetometer measurements of half cores, after alternating field demagnetization at 5 or 9 mT. The polarity zonation based on the inclination record is also shown. See Table 5 for correlation of polarity zonation with the GPTS.

sediment sections cored with the APC (Holes 702A and 702B) and XCB (Cores 114-702B-4X to 114-702B-32X) systems: (1) index properties (wet-bulk density, dry-bulk density, porosity, water content, and grain density), (2) compressional-wave (*P*-wave) velocity, (3) vane shear strength, and (4) thermal conductivity. The carbonate content (see "Geochemistry" section, this chap-

Table 9. Index properties, Site 702.

Sample (cm)	Depth (mbsf)	Water content (%)	Porosity (%)	Densities		
				Wet bulk (g/cm ³)	Dry bulk (g/cm ³)	Grain (g/cm ³)
Hole 702A:						
1H-1, 100-102	1.00	25.38	48.46	2.00	1.49	2.80
1H-2, 109-111	2.59	40.07	64.36	1.66	1.00	2.73
1H-3, 91-93	3.91	36.41	60.49	1.72	1.09	2.71
2H-2, 98-100	5.84	65.64	82.78	1.33	0.46	2.52
2H-3, 98-100	7.34	57.52	77.89	1.41	0.60	2.62
2H-4, 99-101	8.85	55.73	78.25	1.45	0.64	2.88
2H-5, 99-101	10.35	48.38	71.25	1.53	0.79	2.67
2H-6, 99-101	11.85	42.76	67.64	1.66	0.95	2.83
2H-7, 99-101	13.35	52.23	74.16	1.49	0.71	2.65
3H-1, 100-102	15.10	46.07	69.84	1.60	0.86	2.74
3H-2, 100-102	16.60	45.22	68.24	1.57	0.86	2.63
3H-3, 100-102	18.10	47.11	70.74	1.56	0.82	2.74
3H-4, 100-102	19.60	49.57	73.11	1.57	0.79	2.80
3H-5, 99-101	21.09	54.74	75.17	1.47	0.66	2.52
3H-6, 48-50	22.08	53.23	75.20	1.48	0.69	2.69
3H-6, 99-101	22.59	30.11	54.22	1.86	1.30	2.79
4H-1, 99-101	24.59	29.51	53.13	1.96	1.38	2.75
4H-2, 99-101	26.09	33.78	57.32	1.85	1.23	2.67
4H-3, 99-101	27.59	32.82	59.03	1.93	1.30	2.99
4H-4, 99-101	29.09	35.07	59.12	1.80	1.17	2.71
4H-5, 99-101	30.59	35.14	59.92	1.78	1.15	2.80
4H-6, 99-101	32.09	33.23	57.15	1.91	1.28	2.72
Hole 702B:						
1H-3, 100-102	4.00	40.95	65.24	1.67	0.99	2.74
2H-3, 100-102	10.30	49.26	72.73	1.55	0.79	2.77
3H-2, 100-102	18.30	48.62	71.97	1.56	0.80	2.74
3H-3, 100-102	19.80	49.46	72.94	1.54	0.78	2.78
3H-5, 100-102	22.80	34.23	58.46	1.78	1.17	2.74
4X-5, 105-107	32.35	35.35	60.55	1.88	1.21	2.84
5X-5, 100-102	41.80	34.13	61.69	2.34	1.54	3.15
8X-2, 100-102	65.80	35.09	58.67	1.82	1.18	2.66
8X-4, 113-115	68.93	32.58	56.52	1.85	1.25	2.73
9X-3, 59-61	76.39	28.59	52.55	1.95	1.40	2.81
10X-2, 34-36	84.14	30.66	54.98	1.90	1.31	2.80
10X-4, 74-76	87.54	30.96	55.03	1.88	1.30	2.77
11X-5, 48-50	98.28	32.04	56.56	1.87	1.27	2.80
12X-3, 50-52	104.80	33.04	57.89	1.93	1.29	2.83
12X-5, 69-71	107.99	30.00	53.88	1.91	1.34	2.76
13X-3, 25-27	114.05	31.03	56.06	1.89	1.30	2.88
13X-5, 124-126	118.04	29.98	55.20	1.93	1.35	2.92
14X-3, 39-41	123.69	28.32	54.11	2.12	1.52	3.03
15X-2, 70-72	132.00	28.12	52.18	1.97	1.42	2.83
15X-5, 111-113	136.91	28.05	53.04	1.94	1.40	2.94
16X-2, 50-52	141.30	30.13	54.98	1.96	1.37	2.87
16X-4, 86-88	144.66	31.86	57.45	1.87	1.28	2.93
16X-6, 41-43	147.21	30.64	55.72	1.90	1.32	2.89
17X-4, 50-52	153.80	29.02	52.39	1.91	1.36	2.73
17X-5, 28-30	155.08	29.06	53.73	1.98	1.40	2.88
18X-3, 3-44	161.72	29.82	52.85	2.10	1.48	2.67
18X-5, 50-52	164.80	28.21	52.70	1.80	1.30	2.88
19X-2, 60-62	169.90	28.35	51.44	1.93	1.38	2.72
19X-5, 40-42	174.20	28.20	52.00	1.93	1.38	2.80
19X-6, 110-112	176.40	24.32	47.15	2.03	1.54	2.82
20X-1, 123-125	178.53	25.77	48.21	2.05	1.52	2.72
20X-2, 120-122	180.00	25.79	49.42	2.01	1.49	2.85
20X-4, 88-90	182.68	27.35	51.33	1.99	1.44	2.84
21X-2, 37-39	188.67	28.21	52.60	1.98	1.42	2.86
22X-4, 109-111	201.89	32.41	66.21	2.45	1.65	4.15
22X-6, 38-40	205.61	19.48	40.23	2.27	1.83	2.83
24X-2, 69-71	217.49	26.53	50.63	2.03	1.49	2.88
25X-1, 108-110	225.88	23.33	46.68	2.24	1.72	2.92
26X, CC (14-16)	235.54	20.85	41.86	2.19	1.73	2.78
27X-1, 70-72	244.50	22.88	45.44	2.14	1.65	2.85
28X, CC (35-37)	253.97	17.59	36.82	2.30	1.89	2.77
30X-1, 111-113	273.41	20.87	41.74	2.19	1.73	2.76
30X-2, 54-56	274.34	23.08	45.47	2.08	1.60	2.82
31X-1, 48-50	277.78	18.07	38.19	2.21	1.81	2.85
32X, CC (4-5)	287.58	26.38	48.52	1.99	1.46	2.67
32X, CC (29-31)	287.83	5.99	13.34	2.54	2.39	2.45

ter) is shown for comparison with the physical-property data. All the data presented are unfiltered for any bad data points.

Physical-Property Summary and Lithostratigraphic Correlation

Index properties, carbonate content, *P*-wave velocity, thermal conductivity, and shear strength data from Holes 702A and

Table 10. Calcium carbonate, Site 702.

Sample (cm)	Depth (mbsf)	CaCO ₃ (%)
Hole 702A:		
1H-1, 100-102	1.00	0.08
1H-2, 109-111	2.59	0.08
1H-3, 91-93	3.91	0.17
2H-2, 98-100	5.84	0.17
2H-3, 98-100	7.34	40.78
2H-4, 99-101	8.85	39.28
2H-5, 99-101	10.35	55.04
2H-6, 99-101	11.85	70.06
2H-7, 99-101	13.35	41.20
3H-1, 100-102	15.10	63.63
3H-2, 100-102	16.60	65.39
3H-3, 100-102	18.10	56.38
3H-4, 100-102	19.60	50.21
3H-5, 99-101	21.09	44.62
3H-6, 48-50	22.08	2.92
3H-6, 99-101	22.59	78.73
4H-1, 99-101	24.59	86.24
4H-2, 99-101	26.09	84.57
4H-3, 99-101	27.59	84.57
4H-4, 99-101	29.09	80.40
4H-5, 99-101	30.59	86.99
4H-6, 99-101	32.09	88.57
Hole 702B:		
1H-3, 100-102	4.00	0.08
2H-3, 100-102	10.30	52.38
3H-2, 100-102	18.30	59.13
3H-3, 100-102	19.80	51.62
3H-5, 100-102	22.80	85.23
4X-5, 105-107	32.35	83.48
5X-5, 100-102	41.80	82.65
8X-2, 100-102	65.80	89.07
8X-4, 113-115	68.93	91.91
9X-3, 59-61	76.39	88.99
10X-2, 34-36	84.14	83.98
10X-4, 74-76	87.54	85.57
11X-5, 48-50	98.28	79.65
12X-3, 50-52	104.80	89.07
12X-5, 69-71	107.99	86.99
13X-3, 25-27	114.05	89.82
13X-5, 124-126	118.04	89.24
14X-3, 39-41	123.69	90.32
15X-2, 70-72	132.00	87.90
15X-5, 111-113	136.91	94.99
16X-2, 50-52	141.30	92.99
16X-6, 41-43	147.21	94.99
16X-6, 86-88	147.66	92.57
17X-4, 50-52	153.80	87.34
17X-5, 28-30	155.08	89.49
18X-3, 42-44	161.72	91.07
18X-5, 50-52	164.80	93.41
19X-2, 60-62	169.90	95.24
19X-5, 40-42	174.20	95.08
19X-6, 110-112	176.40	92.41
20X-1, 123-125	178.53	94.58
20X-2, 120-122	180.00	92.57
20X-4, 88-90	182.68	92.91
21X-2, 37-39	188.67	95.49
22X-4, 109-111	201.89	90.91
22X-5, 38-40	205.61	88.74
24X-2, 69-71	217.49	94.83
25X-1, 108-110	225.88	93.99
26X, CC (14-16)	235.54	91.66
27X-1, 70-72	244.50	91.24
28X, CC (35-37)	253.97	92.24
30X-1, 111-113	273.41	93.07
30X-2, 54-56	274.34	93.49
31X-1, 48-50	277.78	88.07
32X, CC (4-5)	287.58	75.81
32X, CC (29-31)	287.83	63.30

Table 11. *P*-wave velocity, Site 702.

Sample (cm)	Depth (mbsf)	Direction ^a	Velocity (m/s)
Hole 702A:			
1H-2, 110-112	2.60	C	1681.8
1H-3, 90-92	3.90	C	1677.7
2H-2, 98-100	5.84	C	1559.6
2H-4, 100-102	8.86	C	1547.2
2H-6, 100-102	11.86	C	1544.7
3H-2, 100-102	16.60	C	1563.6
3H-4, 100-102	19.60	C	1547.9
3H-6, 100-102	22.60	C	1631.9
3H-6, 47-49	22.07	C	1581.8
4H-2, 100-102	26.10	C	1596.9
4H-2, 100-102	26.10	C	1614.6
4H-6, 100-102	32.10	C	1640.9
Hole 702B:			
1H-3, 100-102	4.00	C	1664.3
2H-3, 100-102	10.30	C	1556.0
8X-3, 100-102	67.30	C	1693.5
9X-3, 60-62	76.40	C	1753.5
10X-2, 33-35	84.13	C	1698.8
10X-4, 73-75	87.53	C	1795.2
11X-5, 48-50	98.28	A	1924.1
11X-5, 48-50	98.28	B	1940.8
11X-5, 48-50	98.28	C	1921.3
12X-3, 50-52	104.80	A	1743.0
12X-3, 50-52	104.80	B	1652.0
12X-5, 69-71	107.99	A	1921.8
12X-5, 69-71	107.99	B	1926.6
12X-5, 69-71	107.99	C	1900.8
13X-2, 25-27	112.55	A	1921.1
13X-2, 25-27	112.55	B	1797.4
13X-2, 25-27	112.55	C	1781.7
13X-5, 124-126	118.04	A	1971.0
13X-5, 124-126	118.04	B	1976.4
13X-5, 124-126	118.04	C	1921.6
14X-3, 39-41	123.69	C	1931.7
15X-2, 70-72	132.00	A	1798.3
15X-2, 70-72	132.00	C	1770.6
15X-2, 111-113	132.41	C	1812.6
16X-4, 86-88	144.66	A	1888.5
16X-4, 41-43	144.21	C	1876.6
16X-4, 86-88	144.66	C	1876.6
16X-6, 41-43	147.21	A	1849.6
16X-6, 41-43	147.21	C	1867.6
17X-4, 50-52	153.80	A	1957.0
17X-4, 50-52	153.80	C	1987.7
17X-5, 28-30	155.08	A	2130.3
17X-5, 28-30	155.08	C	2043.1
18X-3, 42-44	161.72	C	1857.4
18X-5, 50-52	164.80	C	1820.9
19X-2, 60-62	169.90	C	1830.8
19X-6, 110-112	176.40	C	2006.9
20X-1, 123-125	178.53	C	1956.5
20X-2, 120-122	180.00	C	1857.1
20X-4, 88-90	182.68	C	1841.2
21X-2, 37-39	188.67	C	1942.3
26X, CC (14-16)	235.54	C	2061.0
26X, CC (14-16)	235.54	C	2082.5
28X, CC (0)	253.62	C	2346.2
30X-1, 111-113	273.41	A	2445.3
30X-1, 111-113	273.41	C	2328.7
30X-2, 54-56	274.34	A	2358.4
30X-2, 54-56	274.34	B	2326.7
30X-2, 54-56	274.34	C	2244.1
31X-1, 48-50	277.78	C	2157.4
32X, CC (4-5)	287.58	C	2023.1
32X, CC (29-31)	287.83	C	4460.7

^a A = perpendicular to split-core surface; B = parallel to split-core surface; C = axial.

Table 12. Thermal conductivity, Site 702.

Sample (cm)	Depth (mbsf)	Thermal conductivity (W/m/K)
Hole 702A:		
1H-1, 100-100	1.00	0.9630
1H-2, 100-100	2.50	1.8020
1H-3, 100-100	4.00	1.9900
2H-2, 100-100	5.86	0.8590
2H-3, 100-100	7.36	0.9270
2H-5, 100-100	10.36	1.1170
2H-6, 100-100	11.86	1.3810
3H-2, 100-100	16.60	1.1270
3H-4, 100-100	19.60	1.0310
3H-6, 100-100	22.60	1.5640
4H-2, 100-100	26.10	1.3720
4H-4, 100-100	29.10	1.3680
4H-6, 100-100	32.10	1.6170
Hole 702B:		
1H-2, 100-100	2.50	0.8960
1H-4, 100-100	5.50	1.1810
2H-3, 100-100	10.30	1.1370
2H-5, 100-100	13.30	1.0980
4X-2, 100-100	27.80	1.3470
4X-3, 100-100	29.30	1.3960
5X-3, 100-100	38.80	1.4860
5X-4, 100-100	40.30	1.3430

Table 13. Shear strength, Site 702.

Sample (cm)	Depth (mbsf)	Shear strength (kPa)
Hole 702A:		
1H-2, 110-112	2.60	7.0
1H-2, 110-112	2.60	7.0
2H-2, 98-100	5.84	46.5
2H-4, 100-102	8.86	55.9
2H-6, 100-102	11.86	48.9
3H-2, 100-102	16.60	14.4
3H-4, 100-102	19.60	14.0
3H-6, 100-102	22.60	55.9
4H-2, 100-102	26.10	146.1
4H-4, 100-102	29.10	132.6
4H-6, 100-102	32.10	165.2
Hole 702B:		
1H-3, 100-102	4.00	46.5
2H-3, 100-102	10.30	65.2

702B are listed in Tables 9 through 13. Downcore profiles of wet-bulk density, porosity, water content, grain density, carbonate content, *P*-wave velocity, thermal conductivity, and shear strength are illustrated in Figure 16, with a window of the upper 35 mbsf profiles of wet-bulk density, water content, carbonate content, and *P*-wave velocity shown in Figure 17. The overall pattern at Site 702 shows an increase in wet-bulk density and *P*-wave velocity and a decrease in porosity and water content with depth (Fig. 16), which parallel the consolidation of sediments of Paleocene to Eocene age (see "Biostratigraphy" section) between approximately 32 and 280 mbsf. High concentrations of carbonate (80% to 90%) prevail throughout this depth interval (Fig. 16) and provide an excellent opportunity to study consolidated calcareous deep-sea sediments in comparison to con-

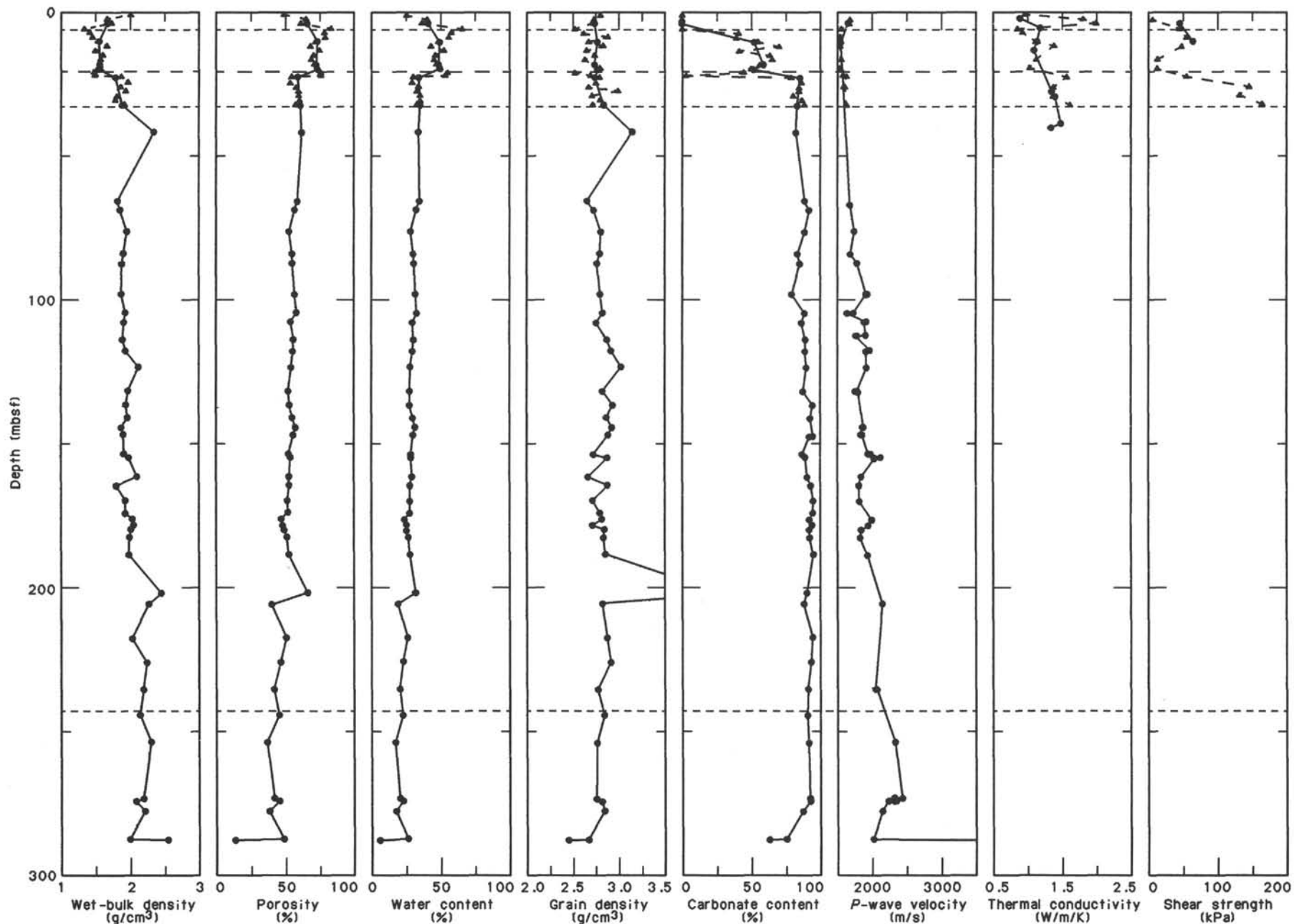


Figure 16. Wet-bulk density, porosity, water content, grain density, carbonate content, *P*-wave velocity, thermal conductivity, and shear strength profiles for Holes 701A (solid triangles) and 701B (dots).

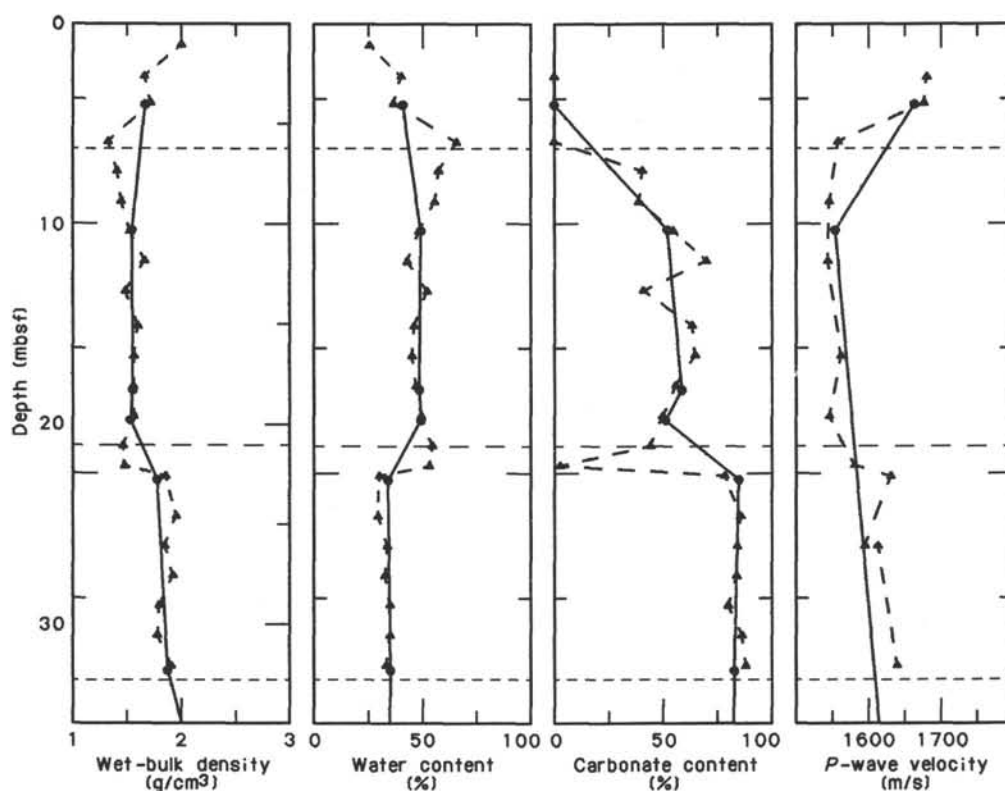


Figure 17. Wet-bulk density, water content, carbonate content, and *P*-wave velocity from 0–35 mbsf for Holes 701A (solid triangles) and 701B (dots).

solidated siliceous deep-sea sediments. Siliceous sediments appear to be less consolidated than calcareous sediments, as was seen at Site 701, where diatomaceous clay-bearing oozes show neither a distinct increase in wet-bulk density nor a distinct increase in velocity with depth (see “Physical Properties” section, “Site 701” chapter, this volume). To illustrate the changes in physical properties of calcareous deep-sea sediments, we summarize the physical properties of the two lithological units (see “Lithostratigraphy” section) in the following.

Lithostratigraphic Unit I (0–22.1 mbsf), the only unit with siliceous sediments at Site 702, is subdivided into two subunits of diatomaceous ooze (Subunit IA; 0–6.65 mbsf) and nannofossil diatomaceous ooze (Subunit IB; 6.65–22.1 mbsf). High fluctuations in carbonate content (2%–70%) dominate throughout Subunit IB (Figs. 16 and 17). In contrast, Subunit IA has no carbonate and surprisingly high, but constant, velocities of about 1680 m/s at 5 mbsf (Figs. 16 and 17). Throughout Subunit IB velocities are considerably lower and vary between 1500 and 1600 m/s. The low velocities might have been caused by the low wet-bulk density (Fig. 17) and possibly by low rigidity values of the nannofossil diatomaceous ooze.

Subunit IA (0–6.65 mbsf, upper Miocene to Quaternary)

	Mean	Minimum	Maximum
Wet-bulk density (g/cm ³)	1.68	1.33	2.00
Dry-bulk density (g/cm ³)	1.01	0.46	1.49
Grain density (g/cm ³)	2.69	2.52	2.80
Porosity (%)	64.06	48.46	82.78
Water content (%)	41.88	25.38	65.64
Carbonate content (%)	0.13	0.08	0.17
Thermal conductivity (W/m/K)	1.236	0.859	1.990
Shear strength (kPa)	26.75	7.00	46.50
<i>P</i> -wave velocity (m/s)	1645	1560	1682

Subunit IB (6.65–22.1 mbsf, upper Miocene)

	Mean	Minimum	Maximum
Wet-bulk density (g/cm ³)	1.53	1.41	1.66
Dry-bulk density (g/cm ³)	0.77	0.60	0.95
Grain density (g/cm ³)	2.72	2.52	2.88
Porosity (%)	72.61	67.64	78.25
Water content (%)	49.74	42.76	57.52
Carbonate content (%)	52.66	39.28	70.06
Thermal conductivity (W/m/K)	1.116	0.927	1.381
Shear strength (kPa)	33.30	14.00	55.90
<i>P</i> -wave velocity (m/s)	1551	1544	1564

Lithostratigraphic Unit II (22.1–294.3 mbsf) is subdivided into three subunits. The top of Unit II (22.1 mbsf) is marked by a distinct change in physical properties (Fig. 16), which presumably corresponds to an unconformity (see “Biostratigraphy” section), and an extremely low carbonate content of 2.92% (22.08 mbsf), caused by high concentrations of clay and volcanic ash (see “Lithostratigraphy” section). In contrast, high carbonate values of 80% to 90% prevail throughout the remainder of Subunit IIA (nannofossil ooze; 22.1–32.8 mbsf), Subunit IIB (nannofossil chalk; 32.8–202.45 mbsf), and the upper part of Subunit IIC (indurated nannofossil chalk; 202.45–294.3 mbsf). Only in the lower part of Subunit IIC does carbonate concentration decrease (from 93% to 63%; Fig. 16), causing an abrupt decrease in water content (from 23% to 6%), porosity (from 46% to 13%), and grain density (from 2.82 to 2.45 g/cm³) and an increase in wet-bulk density (from 2.08 to 2.54 g/cm³). Contrary to the almost homogeneous carbonate content throughout the subunits, wet-bulk density, grain density, and *P*-wave velocity (Fig. 16) illustrate changes in the downcore record that might generate reflectors in the seismic record. For example, at the transition from nannofossil chalk to indurated nannofossil chalk

between 182 and 202 mbsf, wet-bulk density, grain density, and porosity increase markedly (Fig. 16). An extremely high grain density of 4.15 g/cm³ is observed at a depth of 201.89 mbsf. This value may be explained by the presence of stained sediments and iron-manganese particles in an interval where a hiatus is likely (see "Biostratigraphy" section). Another abrupt increase in wet-bulk density and in *P*-wave velocity, which also may give rise to a distinct reflector, occurs at the bottom of the downcore record in Subunit IIC. This change corresponds to the first occurrence of porcellanite and chert. These sediments were too indurated to allow measurements of shear strength and thermal conductivity.

Subunit IIA (22.1–32.8 mbsf, upper Eocene)

		Mean	Minimum	Maximum
Wet-bulk density	(g/cm ³)	1.85	1.48	1.96
Dry-bulk density	(g/cm ³)	1.18	0.69	1.38
Grain density	(g/cm ³)	2.77	2.52	2.99
Porosity	(%)	59.41	53.13	75.20
Water content	(%)	35.25	29.51	54.74
Carbonate content	(%)	76.17	2.92	88.57
Thermal conductivity	(W/m/K)	1.480	1.368	1.617
Shear strength	(kPa)	124.95	55.09	165.20
<i>P</i> -wave velocity	(m/s)	1597	1548	1641

Subunit IIB (32.8–202.45 mbsf, lowermost Eocene to upper Eocene)

		Mean	Minimum	Maximum
Wet-bulk density	(g/cm ³)	1.99	1.80	2.45
Dry-bulk density	(g/cm ³)	1.42	1.18	1.65
Grain density	(g/cm ³)	2.88	2.66	4.15
Porosity	(%)	53.21	47.15	61.69
Water content	(%)	28.84	24.32	35.09
Carbonate content	(%)	90.62	82.65	95.24
Thermal conductivity	(W/m/K)	1.415	1.343	1.486
<i>P</i> -wave velocity	(m/s)	1880	1652	2130

Subunit IIC (202.45–294.3 mbsf, upper Paleocene to lower Eocene)

		Mean	Minimum	Maximum
Wet-bulk density	(g/cm ³)	2.21	1.99	2.54
Dry-bulk density	(g/cm ³)	1.79	1.46	2.39
Grain density	(g/cm ³)	2.75	2.45	2.85
Porosity	(%)	38.50	13.34	48.52
Water content	(%)	19.26	5.99	26.38
Carbonate content	(%)	87.86	63.30	93.49
<i>P</i> -wave velocity	(m/s)	2439	2023	4461

Hiatuses and Physical Properties

Wet-bulk density, porosity, and water content (Fig. 16) show two distinct breaks in the downcore record that correspond to hiatuses observed in the combined record of biostratigraphic and magnetostratigraphic data (see "Biostratigraphy" and "Paleomagnetism" sections). Within the uncertainty of the stratigraphy and the average physical-properties sample interval (one sample per 1.5-m section), the position of hiatus I is between 20.80 and 22.11 mbsf, and a possible second hiatus is between 182 and 202 mbsf. Both hiatuses are within the range of changes in lithology. Hiatus I occurs in an interval of extremely low carbonate content within the transition from nannofossil diatomaceous ooze to nannofossil ooze. Hiatus II probably occurs within the transition from nannofossil chalk to indurated nannofossil chalk. Increased wet-bulk densities and decreased porosities in the underlying sediment sections mark the hiatuses. This is indicative of sediment removal by erosion (see "Physical Properties" section, "Site 699" chapter, this volume). However, changes in the sediment facies have to be considered, as they will impose a strong overprint on changes in the physical prop-

erties caused by hiatuses. In the case of hiatus II, its position in a sequence of nannofossil chalk to indurated nannofossil chalk strongly suggests that sediment diagenesis has taken place after the erosional event.

The uncertainty of the exact duration of hiatus I allows only a rough estimation of the missing sediment section. A conservative value of 10 m/m.y. was used for the sedimentation rate. A missing time interval from approximately 38 to 9 m.y. (26 m.y.) thus represents a minimum removal of 260 m of sediments.

Comparison of Sites 702 and 701

Figure 18 illustrates the composite section for porosity and is based on correlation of the biostratigraphic record (see "Biostratigraphy" section) between Sites 702 and 701:

Core: 114-702B-3H	114-701C-49X
Depth (mbsf): 22.80	455.31
Age: middle/late Eocene (NP18)	middle/late Eocene (NP16/15)

The lack of any distinct consolidation in the sediments of the upper 400 m is most impressive in contrast with a marked gradient in porosity below 400 m, which is obviously an effect of increasing consolidation with depth. This dramatic change occurs in an interval where the sediment facies change from dominantly siliceous material above to calcareous material below 400 m. Because siliceous sediments have much lower grain densities (less than 2.6 g/cm³) than calcareous sediments (greater than 2.6 g/cm³), the effective overburden pressure of siliceous sediments is believed to be much lower than that of calcareous sediments, which in turn is reflected in the history of the sediment consolidation at Sites 702 and 701.

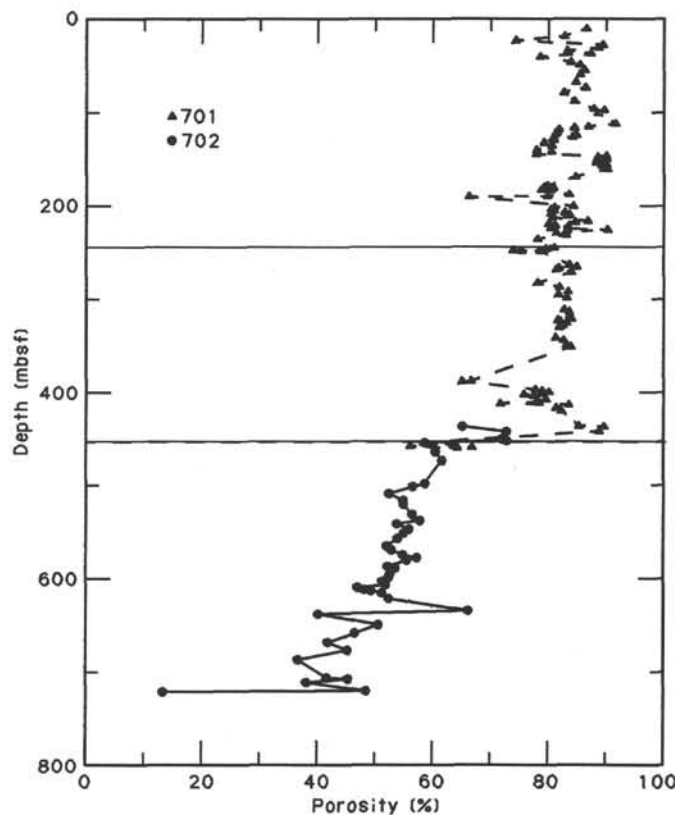


Figure 18. Composite section of porosity from Sites 702 and 701. Lithostratigraphic units are shown by solid lines for Site 701 and by dashed lines for Site 702.

SEISMIC STRATIGRAPHY

We chose to locate Site 702 on a structure considered from the site survey data to be a basement high, flanked by onlapping older strata and covered by about 200 m of sediments (Fig. 4). On approach, *JOIDES Resolution* started recording seismic data on a 270° course about 7 nmi east of the site (Fig. 19). It soon became clear that the apparent basement structure was a horst, bounded and cut by faults, and that the upper seismic unit was strongly attenuated. The expected depth to basement increased from less than 200 to over 350 mbsf. The vessel turned and the beacon was dropped over a fault block about 1 nmi east of the crest of the structural high (Fig. 19).

The sediments at Site 702 are a thin (22.1-m) diatom mud and nanofossil-diatom ooze of middle Miocene and younger age overlying a thick Eocene and older carbonate section (Fig. 20). The carbonates show an increasing degree of lithification with depth, from the upper nanofossil ooze to chalk to indurated chalk. Silicified limestone was encountered at the bottom of the hole.

The seismic *P*-wave velocity shows a linear increase with depth in the carbonate section from about 1560 m/s at 6 mbsf to 2300 m/s at 275 mbsf, where there is an apparent low-velocity zone above the silicified limestone. In addition, the relatively high velocity in the upper diatom mud leads to a shallow velocity inversion in the underlying nanofossil ooze. The wet-bulk density changes by 15% at the Eocene/Miocene unconformity at 21 mbsf, from where it increases linearly with depth toward the bottom of the hole.

The high-resolution (3.5-kHz) seismic data show an eastward-dipping reflector that correlates with the base of the diatom mud at Site 702 (Fig. 21). Thus, the upper Pliocene-Quaternary diatom mud wedges out locally above the anticline formed by the older section in this area (Fig. 22). The nanofossil ooze/chalk transition is not reflected in any significant change in the physical properties and does not appear to be associated with any reflection event. The chalk unit shows weak acoustic stratification throughout, but with different spectral characteristics as a function of depth; the upper part exhibits a relatively low-frequency and the lower part a higher frequency stratification (Fig. 22). This contrasts with the essentially reflection-free appearance of the upper part of the chalk unit at Site 700. Around 202 mbsf the chalk grades into indurated chalk, the only physical-property expression of which is a slight increase in

wet-bulk density. The corresponding change in seismic-reflection character is distinct, as also seen at Site 700. The silicified limestone appearing at the bottom of the hole represents a jump in seismic velocity from about 2 to over 4 km/s and is associated with a very strong seismic-reflection event.

The basal seismic sequence on the Islas Orcadas Rise is a 140-ms-wide band of high-amplitude reflections that is vertically displaced and forms a north-trending horst passing under Site 702. Several faults cut through the structure. The sequence consists of upper Paleocene to lower Eocene indurated chalk overlying older silicified limestone. The younger, overlying sequence of early Eocene to late middle Eocene age forms a faulted anticline. The thickness of sediments above basement is about 200 m for the total depth of Hole 702B, assuming a velocity of 4 km/s. Reworked microfossils of late Turonian to Maestrichtian age suggest that the Islas Orcadas Rise was formed sometime in the Late Cretaceous ("Biostratigraphy" section). Two episodes of faulting have affected the Paleogene sediments on the rise. Displacements of the basal sequence during the oldest episode have been compensated by syntectonics and later deposition. The anticline was formed by a post-late middle Eocene, pre-late Miocene event.

SUMMARY AND CONCLUSIONS

Summary

Site 702 is located on the central part of the Islas Orcadas Rise (50°56.786'S, 26°22.117'W; water depth of 3083.4 m), a north-northwest-trending aseismic ridge more than 500 km long and 50–100 km wide that rises over 1000 m above the adjacent seafloor (Fig. 1). The Islas Orcadas Rise and Meteor Rise were once conjugate features, prior to separation by seafloor spreading in the Eocene (Fig. 2). The major objectives of this site were (1) to determine the age, nature, and subsidence history of the Islas Orcadas Rise and (2) to investigate the influence of the shallow Islas Orcadas and Meteor rises on oceanic water-mass communication between the southern high-latitude region and the South Atlantic.

The central part of Islas Orcadas Rise is relatively smooth, and the seismic data show an up to 0.8-s-thick (TWT) section with a major unconformity at or near the seafloor (Fig. 4). The site location was chosen to be on a structure considered from the site survey data to be a basement high, flanked by onlapping

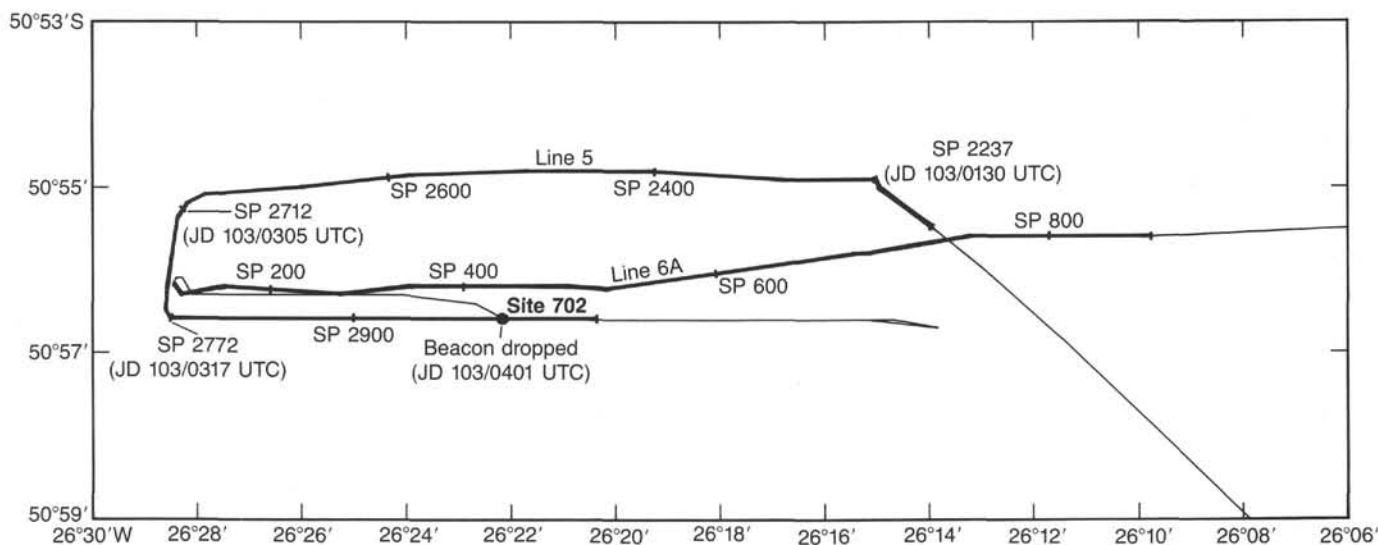


Figure 19. Track of *JOIDES Resolution* on approach and departure from Site 702.

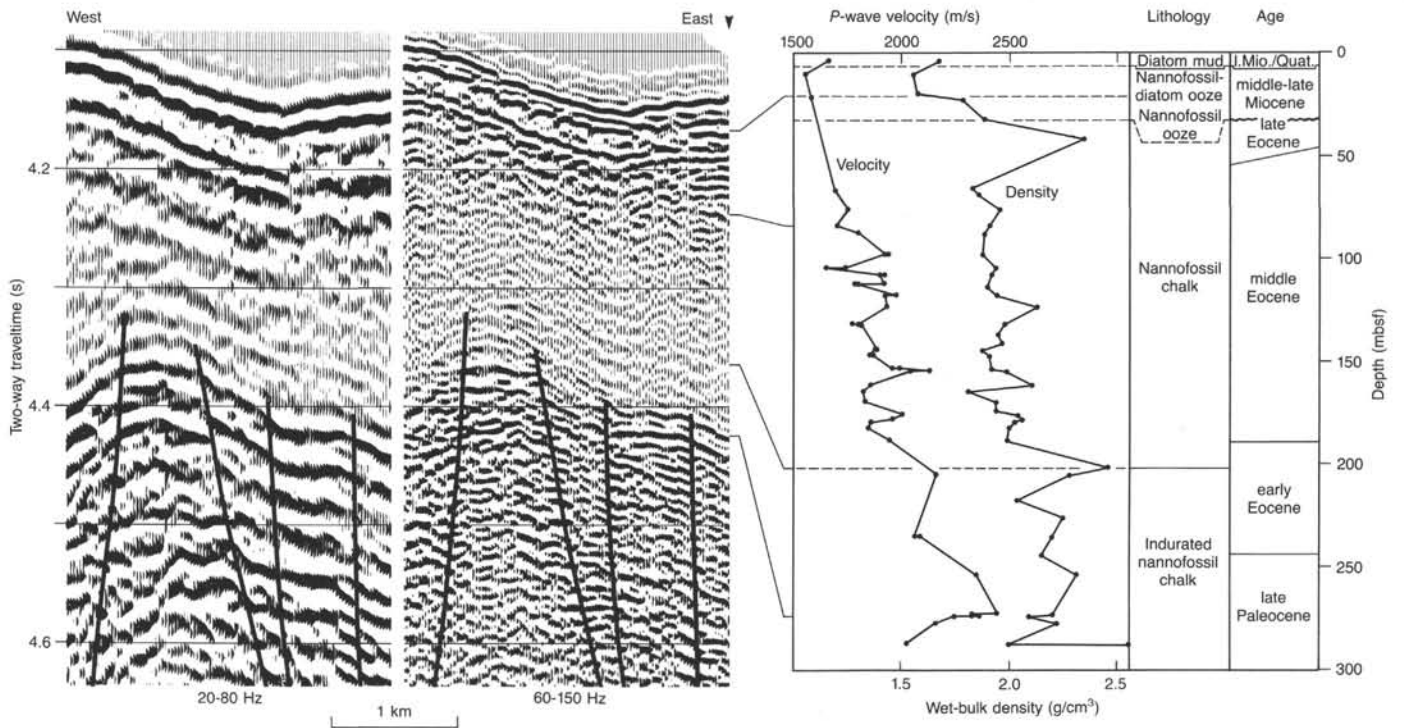


Figure 20. Summary of Site 702 *P*-wave velocity and wet-bulk density (from “Physical Properties” section), lithology (from “Lithostratigraphy” section), and age (from “Biostratigraphy” section) correlated with single-channel seismic-reflection data obtained by *JOIDES Resolution* over the site location.

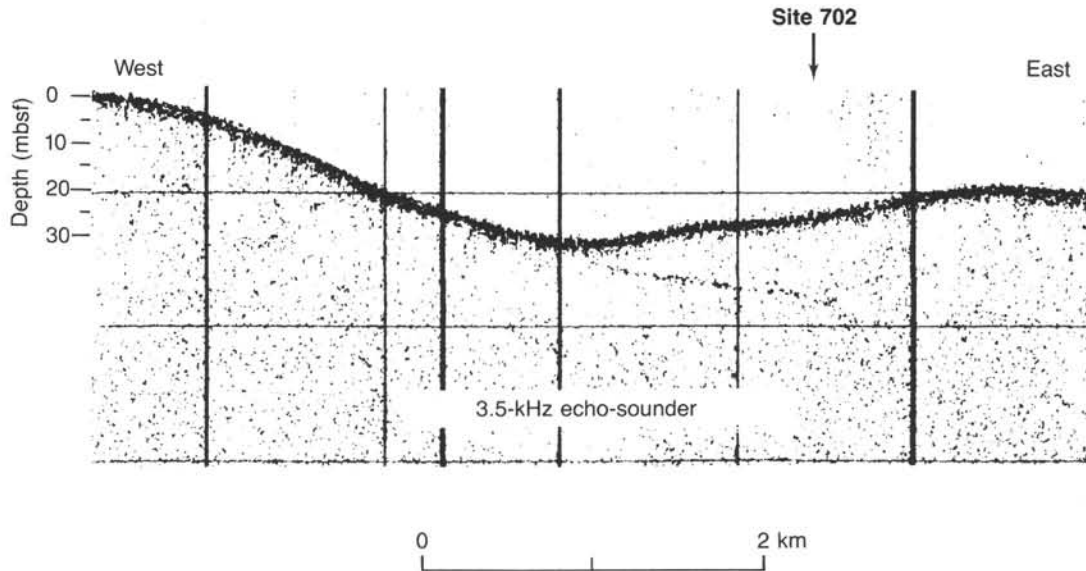


Figure 21. High-resolution (3.5-kHz) seismic-reflection profile acquired by *JOIDES Resolution* over Site 702.

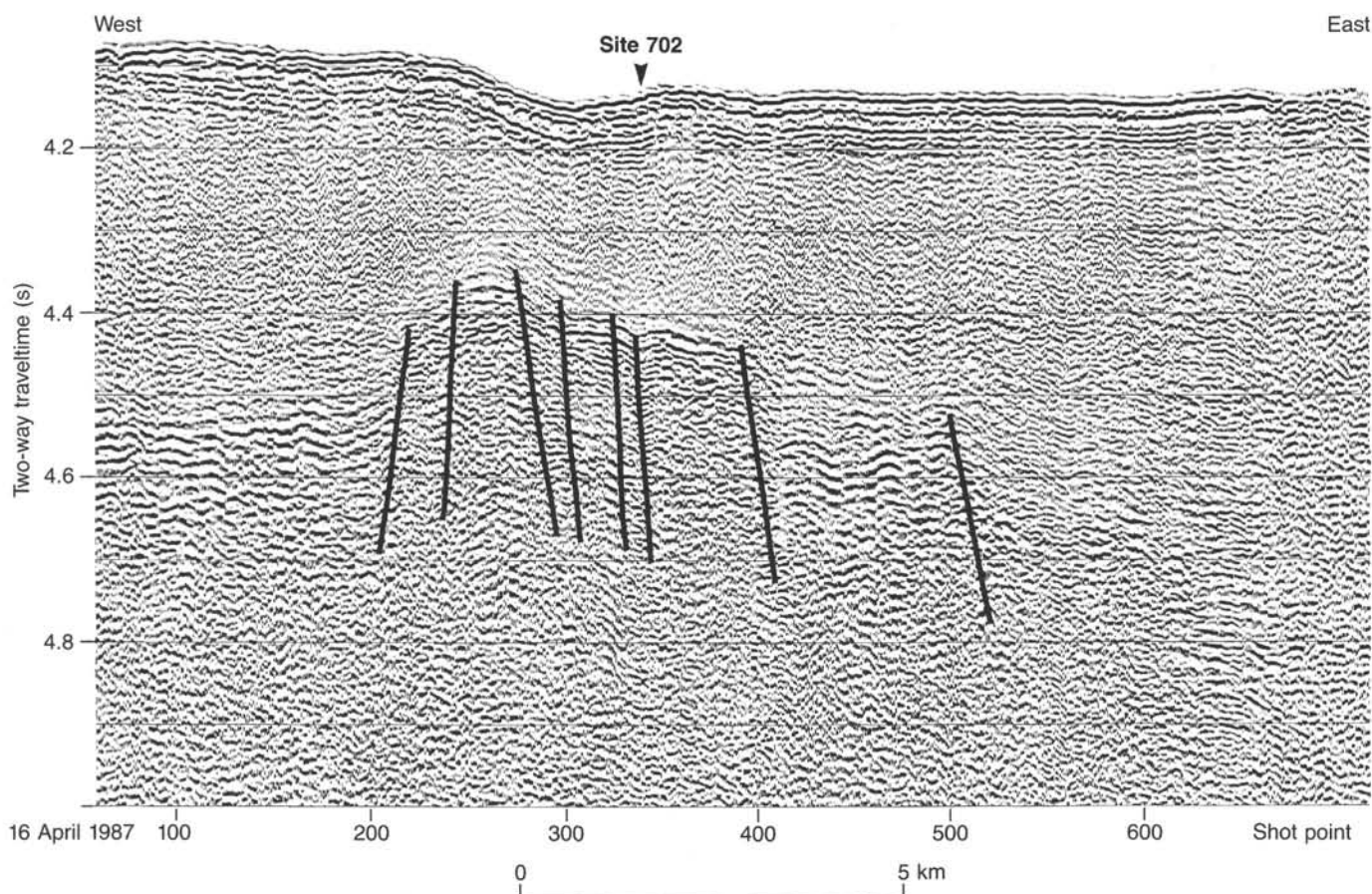


Figure 22. Single-channel seismic-reflection line acquired by *JOIDES Resolution* upon leaving Site 702.

older strata and covered by about 200 m of sediments. Surveying on approach showed it to be a 4.5-km-wide horst bounded and cut by faults, with an attenuated upper part of the section but a greater depth to basement (>350 mbsf) than initially expected (Fig. 22).

Site 702 is about 1 nmi east of the crest of the structural high and consists of two holes: Hole 702A, with 4 cores taken with the APC to a depth of 33.1 mbsf at 100% recovery, and Hole 702B, with 3 cores taken with the APC and 29 cores taken with the XCB system to 294.3 mbsf for a recovery of 195.2 m (66.3%). Sediment recovery for Hole 702B was good (87%) to a depth of 205 mbsf, but dropped sharply below this depth because of the occurrence of frequent chert stringers. The Navidrill core barrel was deployed and tested on a silicified limestone encountered at 294 mbsf, but no material was retrieved, and the site was abandoned.

The stratigraphic section at Hole 702B consists of a thin layer of diatom ooze and nannofossil-diatom ooze above a thick sequence of pelagic carbonates that exhibits increasing down-hole lithification (Fig. 23). The thick pelagic carbonate sequence is remarkably uniform in its appearance, with the percentage of carbonate generally ranging from 95% to 80%. Holes 702A and 702B were divided into two lithologic units and five subunits on the basis of their biosiliceous and carbonate content, in addition to the degree of sediment lithification and diagenesis (Tables 2 and 3; Figs. 5 and 40, "Site 700" chapter, this volume).

Unit I, between the seafloor and 21.1 mbsf in Hole 702A, is divided into two subunits. Subunit IA (0–6.65 mbsf) consists of a diatom mud and diatom ooze of late Miocene to Quaternary age. Subunit IB (6.65–22.1 mbsf) is late Miocene in age and is

predominantly nannofossil-diatom ooze, with some alternations of nannofossil-bearing and ash-bearing diatom ooze. This unit contains the bulk of ice-rafted dropstones and sand found in both holes, has manganese nodules and staining (Subunit IA), and contains a large concentration of volcanic ash.

Unit II is an ~273-m-thick pelagic carbonate sequence (21.1/22.15–294.3 mbsf) of late Paleocene–late Eocene age that is divided into subunits based on the degree of lithification. Unit II is separated from Unit I by a hiatus of ~29–33 m.y. Subunit IIA (22.15–33.1 mbsf) is of late Eocene age and consists of a very homogeneous nannofossil ooze, with only a minor proportion of foraminifers and diatoms. Subunit IIB (32.8–202.45 mbsf) is a nannofossil chalk of early to late Eocene age. This subunit also displays little variation in carbonate content (90%) and microfossil constituents. Micrite becomes apparent below Core 114-702B-16X (148.8 mbsf) in Subunit IIB, and chert was first noted in Core 114-702B-20X (181.8 mbsf) (Table 4). Subunit IIC (202.45–294.3 mbsf), the basal sequence of the site, is an indurated chalk that is similar to the overlying subunits in its homogeneity but differs by the conspicuous presence of micrite. This early late Paleocene to earliest Eocene age subunit has numerous chert layers that caused poor recovery of this interval. Toward the base of Subunit IIC, the chalk becomes increasingly indurated with some zones of silicification. The base of the unit is a very hard, silicified limestone that could not be penetrated significantly by the XCB system, which lead to termination of Hole 702B.

Site 702 was the fifth site on Leg 114 to recover a significant representation of Eocene and Paleocene sediments. More than 1000 m of Paleocene to Eocene sediments were recovered at

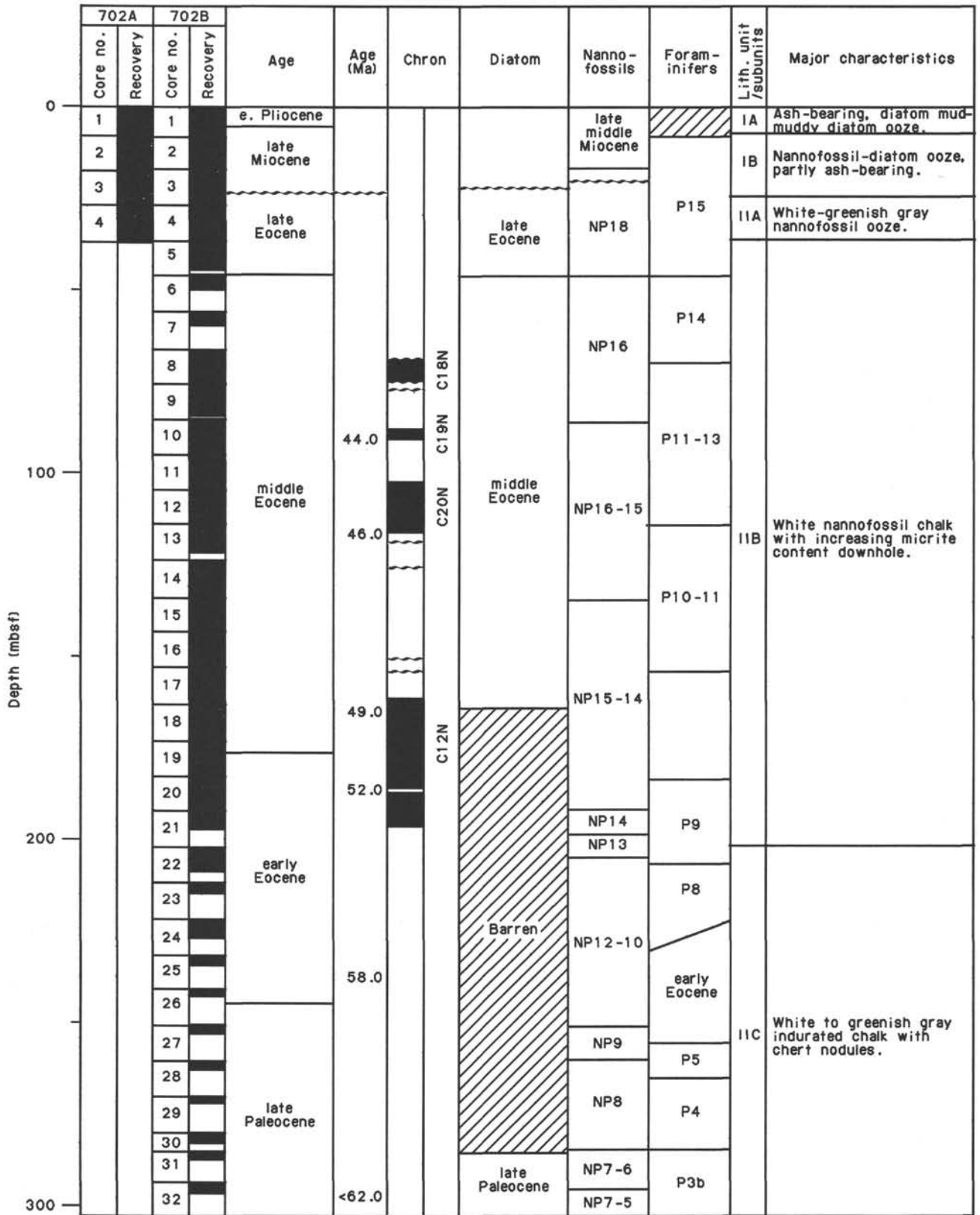


Figure 23. Summary of a variety of data from Site 702, including depth of cores and recovery, age, paleomagnetic data, selected micropaleontologic ages, lithostratigraphic units and a description of their major characteristics, variations in smear slide constituents with depth, percent carbonate, and porosity.

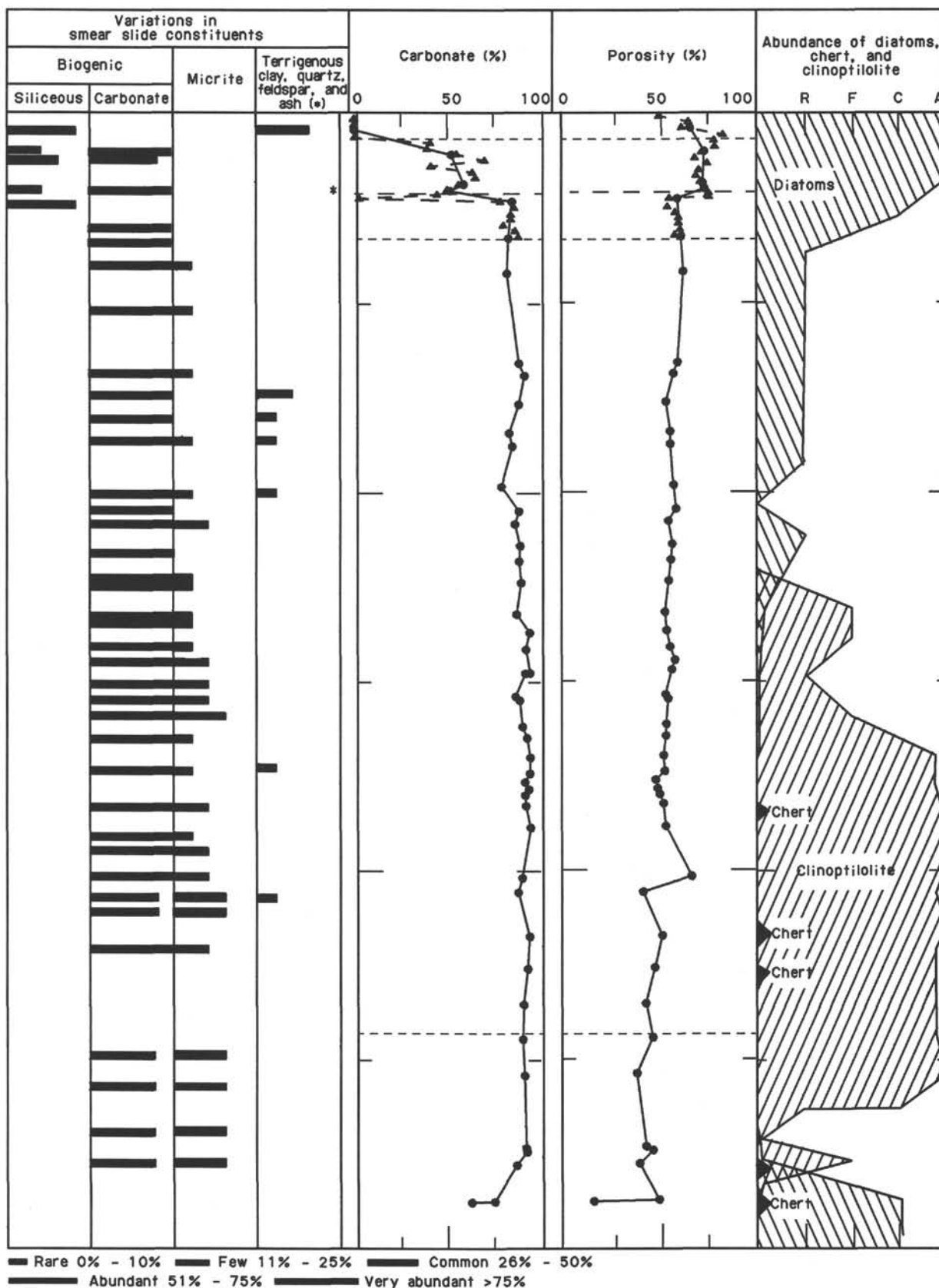


Figure 23 (continued).

Sites 698 to 702, providing the most complete stratigraphic representation of this interval yet obtained from the Southern Ocean.

A relatively complete succession of magnetic polarity zones was identified between approximately 20 and 205 mbsf. Good core recovery (86%) and relatively little core disturbance in this interval resulted in identification of early to late Eocene Chrons C20R through C18N. This magnetostratigraphic framework adds to our previous paleomagnetic representation of the Late Cretaceous–earliest Paleocene, late Oligocene, late Miocene, and Pliocene to Quaternary. These sections will make a significant contribution toward age calibration of high-latitude biozones and paleoenvironmental history.

Sedimentation rates at Site 702 were about 12 m/m.y. during the Paleogene. A major hiatus of ~29–33 m.y. (~22 mbsf) spans the uppermost Eocene to upper Miocene. Additional hiatuses of yet undetermined duration occur in the 24-m upper Miocene to Quaternary section.

Calcareous microfossils are abundant throughout the Eocene section, where the carbonate content is generally 85% to 95%, but are less abundant in the upper Miocene, where the carbonate content declines to no more than 40% to 70%. Benthic foraminifers are abundant, diverse, and well preserved throughout, except in the upper Miocene to Quaternary. Planktonic foraminifers are abundant and moderately well preserved throughout the Paleocene–Eocene, rare with low diversity in the Miocene, and absent from the Pliocene–Quaternary. Calcareous nanofossils are moderately well preserved in the Neogene but are generally poorly preserved in the Paleogene.

Siliceous microfossils are abundant in the Neogene, persist down to the upper lower Eocene, and are absent in the remainder of the sequence, except for the lower upper Paleocene where they are again present. As was the case at the previous sites, Paleogene sequences without biosiliceous microfossils were attributed to the dissolution of biosiliceous opal and the subsequent downward diffusion to form zeolites, chert, or porcellanite (see “Geochemistry” section; Figs. 21 and 23, “Site 700” chapter).

Conclusions

Seismic and Tectonic Interpretation

Most of the older sedimentary sequence of the Islas Orcadas Rise–Meteor Rise aseismic ridge system was obtained at Site 702. This predominantly lower upper Paleocene–upper Eocene section represents an ~23-m.y. history of pelagic carbonate sedimentation during a period that post-dates the rifting of these aseismic ridges. Although basement was not reached, the age of the Islas Orcadas Rise was further constrained to be older than ~62 Ma. A Late Cretaceous age for the rise is suggested by reworked planktonic foraminifers and calcareous nanofossils present in the basal 20 m of the section, about 150 m above the inferred depth of basement. An early Eocene extensional episode generated numerous small half-grabens over much of the rise, and a major post-late Eocene to pre-late Miocene tectonic event formed a north-trending horst through the location of Site 702.

Paleoenvironmental History

Late Paleocene

Benthic foraminifer assemblages of this age are indicative of lower bathyal depths, 1000–2000 m below sea level (mbsl). Elsewhere on the Islas Orcadas Rise, the elevated basement high on the eastern margin would have been between 1000 and 2000 mbsl, and isolated basement peaks were probably near sea level. Transported Cretaceous foraminifers and calcareous nanofos-

sils may have originated from the adjacent elevated fault block to the west of the site.

The uniformity of the upper Paleocene indurated nanofossil chalk is witness to stable environmental conditions at this time. Calcium carbonate percentages are consistently between 95% and 88%, except in the basal core (114-702B-32X), where carbonate declines to 63%–75% in response to a higher biogenic silica content.

The presence of biosiliceous microfossils has been noted at all Leg 114 sites that recovered sediments of late Paleocene age (Sites 698 through 700 and 702). In contrast, Eocene siliceous microfossils are poorly preserved or absent at these same sites. At Site 702 and the previous sites, the poor representation of siliceous microfossils in the Eocene appears to be related to their dissolution and reprecipitation as zeolites and chert (see “Geochemistry” section). The better preservation of Paleocene siliceous microfossils is still an enigma; however, it may be related to a higher overall siliceous microfossil productivity (see “Summary and Conclusions” section, “Site 698” chapter, this volume).

Foraminifer assemblages are similar to those of previous Leg 114 Paleocene sections. The warm-water representatives of the low latitudes are present, including the strong-keeled morozovellids. Calcareous nanofossil assemblages include discoasters but are less diverse than at previous Leg 114 sites as a result of dissolution. A distinct, but short-lived, cooling event occurred near the Paleocene/Eocene boundary, which was also noted in the previous sites. Near the boundary, the strong-keeled morozovellids, warm-water indicators, are absent or extremely rare. At the same time subotinids are dominant, which, in conjunction with the previous observation, suggests surface-water cooling and increased stratification of surface waters.

Early Eocene

Lower Eocene nanofossil oozes and Eocene chalks are remarkably homogeneous, except for minor amounts of chert in lowermost Eocene. Calcium carbonate content shows little variation (95% to 87%), and the sediment is composed dominantly of nanofossils. Overall, the early Eocene appears to have been a time of quiet deposition and sustained accumulation of calcareous microfossils.

Foraminifer assemblages are rich in angular acariniids, indicative of surface waters warm enough to allow this typical lower latitude group to migrate into the subantarctic. Similar assemblages were noted at Sites 698, 699, and 700.

One period of nondeposition or erosion may have occurred during the middle early Eocene. The shipboard foraminifer stratigraphy of this site suggests that Zone P7 and a part of P8 may be missing between Sections 114-702B-21X, CC, and 114-702B-22X, CC. This interval is coincident with a change of physical properties between 182 and 202 mbsf, within the transition from nanofossil chalk to nanofossil ooze (“Physical Properties” section). Post-cruise analyses are inconclusive at this time as to the presence of a minor unconformity within the lower Eocene.

Middle to Early Late Eocene

Middle Eocene to lower upper Eocene sediments of Site 702 are homogeneous nanofossil chalks with little variation in the percent carbonate (generally 95% to 85%) or relative contributions of foraminifers (<10%) and calcareous nanofossils. Foraminifers from this section provide evidence for a middle to late Eocene cooling of surface waters, as recorded in previous sites. The onset of cooling from the warmer early Eocene conditions began during the middle Eocene; the cooling caused a decline in the abundance of acariniids, which became more monospecific, smaller, and rounded. By the late Eocene, foraminifer as-

semblages took on a much cooler water affinity, represented mainly by cold-water forms such as *Catapsydrax* and species that are much more characteristic of cooler Oligocene assemblages.

On the basis of the benthic foraminifer assemblages, Site 702 subsided to near its present water depth (3083 m) after the late Eocene. Assemblages of the Eocene are indicative of the lower bathyal (1000–2000 m). Late Paleocene to Eocene subsidence of Site 702 was only minor and had no effect on the preservation of carbonate, indicating that the site was still well above the CCD. Site 701, to the east of the Islas Orcadas Rise, was at a depth from 2500 to ~3000 m during the Eocene. Carbonate is sparse to absent (<20%) in the upper Eocene of Site 701. The record of carbonate deposition at Sites 701 and 702 suggests a late Eocene lysocline position between 2000 and 3000 mbsl and a CCD position that varied slightly above and below 3800 mbsl.

Early Late Eocene–Late Middle Miocene Hiatus

An abrupt change in lithology, physical properties, and age occurs between 21.2 and 21.1 mbsf, which marks a major hiatus between lower upper Eocene and upper Miocene sediments. Formation of this hiatus may have been in part caused by nondeposition; however, the change in physical properties is also indicative of major erosion. The timing of the erosional event that is responsible for the major hiatus is probably age equivalent at all Leg 114 sites, varying only in the depth of cutting. The hiatus represents a great interval of time in the shallow sites (Site 698: 2128 mbsl, lower middle Eocene–Pliocene; Site 702: 3083 mbsl, lower upper Eocene–upper middle Miocene) than at deeper sites (Site 699: 3705 mbsl, lowermost Miocene–upper Miocene; Site 701: 4636 mbsl, lower Miocene–middle Miocene). We have previously related these hiatuses to the onset of more vigorous circulation caused by the advent of a deep-reaching ACC caused by opening of the Drake Passage (“Summary and Conclusions” section, “Site 699” chapter). Differences in the duration of the hiatuses with depth suggest (1) a current intensity of upper to “mid” CPDW (Sites 698 and 702) that was greater than the lower CPDW and Antarctic Bottom Water (Sites 699 and 701) and (2) a longer period of erosion at shallower depths during the early opening stages of the Drake Passage, when the sill depth was above that of the deeper sites.

Little can be said of the depositional environment between the early Miocene and late middle Miocene, as this age interval is largely missing at all Leg 114 sites. Other, later erosional episodes may have contributed to the depth of cutting at Leg 114 sites. It is clear, however, that there was a significant change in the intensity of ACC circulation during the late middle Miocene to late Miocene, which allowed renewed deposition at all Leg 114 sites.

Late Miocene–Quaternary

The upper middle Miocene to Quaternary sequence of Site 702 is greatly attenuated to a thickness of only 21 to 22 m. The preliminary biostratigraphic examination of this interval reveals the presence of a number of Neogene diatom zones, suggesting that the attenuation of the Neogene may be the consequence of low sedimentation rates as well as multiple erosional/nondepositional events. Because of the condensed nature of this sequence, paleoenvironmental interpretation of the Neogene will require much more detailed study; however, several of its characteristics are worthy of mention here.

Sediments disconformably overlying the upper Eocene are late Miocene in age (22.15–~5.0 mbsf). Most of the interval between 20.8 and 5.0 mbsf appears to be of late Miocene age (~9.0 to 6.5 Ma) and consists primarily of nannofossil diatom

ooze with a surprising amount of carbonate (39% to 70%). The carbonate values of these upper Miocene sediments suggest that the site was positioned to the north of the ACZ during the time of deposition. The presence of carbonate and the scarcity of ice-rafted detritus are consistent with previous studies that have suggested that the major late Miocene northward advance of the polar front occurred after 9.0 Ma (Ciesielski et al., 1983).

During the latest Miocene to Quaternary (between ~9.0 Ma to Holocene), the sediments of Subunit IA were deposited (0–6.65 mbsf). These sediments are distinct from those of Subunit IB by the conspicuous absence of carbonate and the presence of common dropstones and sand-size ice-rafted detritus in the diatomaceous ooze and mud. The assemblage of diatoms includes the typical endemic species of the southern high latitudes. All the characteristics of this subunit are similar to those in similar-age sediments from the subantarctic sector of the Southern Ocean (Ciesielski et al., 1983; Ledbetter and Ciesielski, 1986).

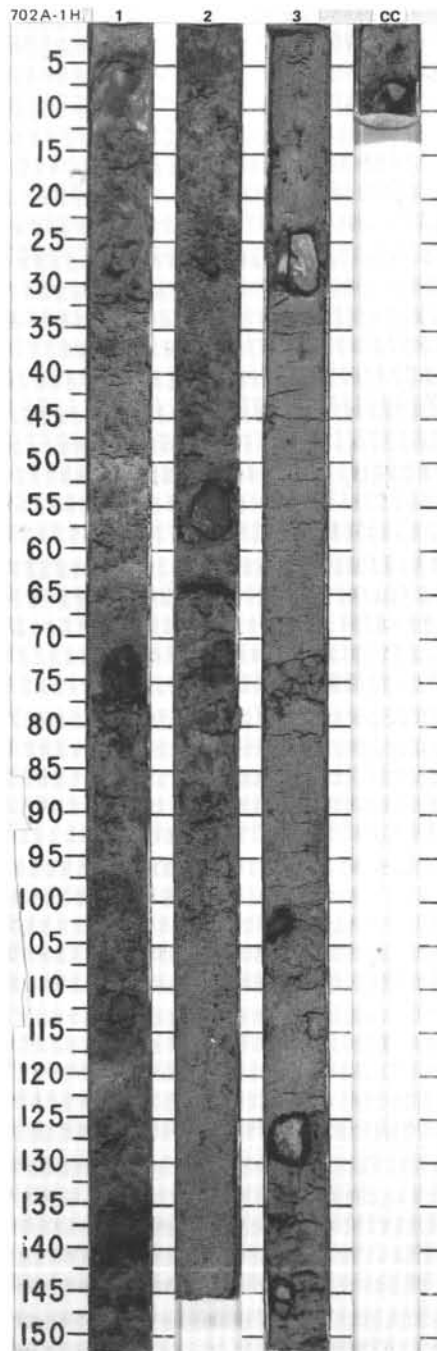
REFERENCES

- Baker, P. A., 1986. Pore water chemistry of carbonate-rich sediments, Lord Howe Rise, Southwest Pacific Ocean. In Kennett, J. P., von der Borch, C. C., et al., *Init. Repts. DSDP*, 90: Washington (U.S. Govt. Printing Office), 1249–1256.
- Barker, P. F., and Burrell, J., 1982. The influence upon Southern Ocean circulation, sedimentation, and climate of the opening of Drake Passage. *Antarct. Geosci. Sump. Antarct. Geol. Geophys.*, 3rd, 1977 (1982), 377–385.
- Barron, J. A., 1985. Miocene to Holocene planktic diatoms. In Bolli, H. M., Saunders, J. B., and Perch-Nielsen, K. (Eds.), *Plankton Stratigraphy*: Cambridge (Cambridge Univ. Press), 763–810.
- Berggren, W. A., Kent, D. V., and Flynn, J. J., 1985. Paleogene geochronology and chronostratigraphy. In Snelling, N. J. (Ed.), *The Chronology of the Geological Record*: Geol. Soc. London Mem., 10:141–195.
- Bolli, H. M., 1972. The genus *Globigerinatheka* Bronnimann. *J. Foraminiferal Res.*, 2:109–136.
- Burckle, L. H., Clarke, D. B., and Shackleton, N. J., 1978. Isochronous last-abundant-appearance datum (LAAD) of the diatom *Hemidiscus karstenii* in the sub-Antarctic. *Geology*, 6:243–246.
- Chen, P. H., 1975. Antarctic radiolaria. In Hayes, D. E., Frakes, L. A., et al., *Init. Repts. DSDP*, 28: Washington (U.S. Govt. Printing Office), 437–513.
- Ciesielski, P. F., 1978. The Maurice Ewing Bank of the Malvinas (Falkland) Plateau: depositional and erosional history and its paleoenvironmental implications [Ph.D. dissert.]. Florida State Univ., Tallahassee.
- , 1983. The Neogene and Quaternary diatom biostratigraphy of subantarctic sediments, Deep Sea Drilling Project Leg 71. In Ludwig, W. J., Krasheninnikov, V. A., et al., *Init. Repts. DSDP*, 71: Washington (U.S. Govt. Printing Office), 635–666.
- , 1985. Middle Miocene to Quaternary diatom biostratigraphy of Deep Sea Drilling Project Site 592, Chatham Rise, Southwest Pacific. In Kennett, J. P., von der Borch, C. C., et al., *Init. Repts. DSDP*, 90: Washington (U.S. Govt. Printing Office), 1249–1256.
- Ciesielski, P. F., Ledbetter, M. T., and Elwood, B. B., 1982. The development of Antarctic glaciation and the Neogene paleoenvironment of the Maurice Ewing Bank. *Mar. Geol.*, 46:1–51.
- Ciesielski, P. F., and Weaver, F. M., 1983. Neogene and Quaternary paleoenvironmental history of the Deep Sea Drilling Project Leg 71 sediments, southwest Atlantic Ocean. In Ludwig, W. J., Krasheninnikov, V. A., et al., *Init. Repts. DSDP*, 71: Washington (U.S. Govt. Printing Office), 461–477.
- Ciesielski, P. F., and Wise, S. W., Jr., 1977. Geologic history of the Maurice Ewing Bank of the Falkland Plateau (southwest Atlantic sector of the Southern Ocean) based upon piston and drill cores. *Mar. Geol.*, 25:175–207.
- Dumitrica, P., 1973. Paleocene, late Oligocene and post-Oligocene silicoflagellates in southwestern Pacific sediments cored on DSDP Leg 21. In Burns, R. E., Andrews, J. E., et al., *Init. Repts. DSDP*, 21: Washington (U.S. Govt. Printing Office), 837–883.

- Fenner, J. M., 1986. Eocene-Oligocene planktic diatom stratigraphy in the low latitudes and the high southern latitudes. *Micropaleontology*, 30:319-342.
- Froelich, P. N., Kim, K. K., Jahnke, R. J., Burnett, W. R., and Deakin, M., 1983. Pore water fluoride in Peru continental margin sediments: uptake from seawater. *Geochim. Cosmochim. Acta*, 47:1605-1612.
- Gieskes, J. M., 1983. The chemistry of interstitial waters of deep-sea sediments: interpretation of deep-sea drilling data. In Riley, J. P., and Chester, R. (Eds.), *Chemical Oceanography* (Vol. 8): London (Academic Press), 222-269.
- Gieskes, J. M., and Lawrence, J. R., 1981. Alteration of volcanic matter in deep-sea sediments: evidence from the chemical composition of interstitial waters from deep-sea drilling cores. *Geochim. Cosmochim. Acta*, 45:1687-1703.
- Gombos, A. M., Jr., 1983. Middle Eocene diatoms from the South Atlantic. In Ludwig, W. J., Krasheninnikov, V. A., et al., *Init. Repts. DSDP*, 71: Washington (U.S. Govt. Printing Office), 583-634.
- Gordon, A. L., Georgi, D. T., and Taylor, H. W., 1977. Antarctic Polar Front Zone in the Western Scotia Sea—Summer 1975. *J. Phys. Oceanogr.*, 7:309-328.
- Haq, B. U., 1980. Biogeographic history of Miocene calcareous nannoplankton and paleoceanography of the Atlantic Ocean. *Micropaleontology*, 26:414-443.
- Hays, J. D., and Opdyke, N. D., 1967. Antarctic radiolaria, magnetic reversals, and climatic change. *Science*, 158:1001-1011.
- Hays, J. D., and Shackleton, N. J., 1976. Globally synchronous extinction of the radiolarian *Stylactrus universus*. *Geology*, 4:649-652.
- Jenkins, D. G., 1985. Southern mid-latitude Paleocene to Holocene planktic foraminifera. In Bolli, H. M., Saunders, J. B., and Perch-Nielsen, K. (Eds.), *Plankton Stratigraphy*: Cambridge (Cambridge Univ. Press), 263-282.
- Kent, D. V., and Gradstein, F., 1985. A Cretaceous and Jurassic geochronology. *Geol. Soc. Am. Bull.*, 96:1419-1427.
- LaBrecque, J. L. (Ed.), 1986. *South Atlantic Ocean and Adjacent Continental Margin Atlas 13*: Ocean Margin Drilling Program Reg. Atlas Ser., 13.
- LaBrecque, J. L., and Hayes, D. E., 1979. Seafloor spreading in the Agulhas Basin. *Earth Planet. Sci. Lett.*, 45:411-428.
- Ledbetter, M. T., and Ciesielski, P. F., 1986. Post-Miocene disconformities and paleoceanography in the Atlantic sector of the Southern Ocean. *Palaeogeogr. Palaeoclimatol. Palaeoecol.*, 52:185-214.
- Martini, E., 1971. Standard Tertiary and Quaternary calcareous nannoplankton zonation. In Farrinacci, A. (Ed.), *Proc. Planktonic Conf. II Rome 1970*: Rome (Technoscienze), 2:739-785.
- Martini, E., and Müller, C., 1986. Current Tertiary and Quaternary calcareous nannoplankton stratigraphy and correlation. *Newsl. Stratigr.*, 16:99-112.
- McDuff, R. E., 1981. Major cation gradients in DSDP interstitial waters: the role of diffusive exchange between seawater and upper oceanic crust. *Geochim. Cosmochim. Acta*, 45:1703-1713.
- , 1985. The chemistry of interstitial waters, Deep Sea Drilling Project Leg 86. In Heath, G. R., Burckle, L. H., et al., *Init. Repts. DSDP*, 86: Washington (U.S. Govt. Printing Office), 675-687.
- McGowran, B., 1986. Cainozoic oceanic and climatic events: the Indo-Pacific foraminiferal biostratigraphic records. *Palaeogr. Palaeoclimatol. Palaeoecol.*, 55:247-265.
- Morkhoven, F.P.C.M. van, Berggren, W. A., and Edwards, A. S., 1986. Cenozoic cosmopolitan deep-water benthic foraminifera. *Cent. Rech. Explor. Prod. Elf Aquitaine Mem.*, 11.
- Perch-Nielsen, K., 1985. Cenozoic calcareous nannofossils. In Bolli, H. M., Saunders, J. B., and Perch-Nielsen, K. (Eds.), *Plankton Stratigraphy*: Cambridge (Cambridge Univ. Press), 427-554.
- Reid, J. R., Nowlin, W. D., Jr., and Patzert, W. C., 1977. On the characteristics and circulation of the Southwestern Atlantic Ocean. *J. Phys. Oceanogr.*, 7:62-91.
- Sanfilippo, A., Westberg-Smith, M. J., and Riedel, W. R., 1985. Cenozoic radiolaria. In Bolli, H. M., Saunders, J. B., and Perch-Nielsen, K. (Eds.), *Plankton Stratigraphy*: Cambridge (Cambridge Univ. Press), 573-630.
- Shaw, C. A., and Ciesielski, P. F., 1983. Silicoflagellate biostratigraphy of middle Eocene to Holocene subantarctic sediments recovered by Deep Sea Drilling Project Leg 71. In Ludwig, W. J., Krasheninnikov, V. A., et al., *Init. Repts. DSDP*, 71: Washington (U.S. Govt. Printing Office), 687-737.
- Tjalsma, R. C., and Lohmann, G. P., 1983. Paleocene-Eocene bathyal and abyssal benthic foraminifera from the Atlantic Ocean. *Micropaleontol. Spec. Publ.*, 4.
- Weaver, F. M., 1983. Cenozoic radiolarians from the southwest Atlantic, Falkland Plateau region, Deep Sea Drilling Project Leg 71. In Ludwig, W. J., Krasheninnikov, V. A., et al., *Init. Repts. DSDP*, 71: Washington (U.S. Govt. Printing Office), 667-686.
- Weaver, F. M., and Gombos, A. M., Jr., 1981. Southern high latitude diatom biostratigraphy. In Warme, J. E., Douglas, R. G., and Winterer, E. L. (Eds.), *The Deep Sea Drilling Project: A Decade of Progress*: Spec. Publ. Soc. Econ. Paleontol. Mineral., 32:445-470.
- Wise, S. W., 1983. Mesozoic and Cenozoic calcareous nannofossils recovered by Deep Sea Drilling Project Leg 71 in the Falkland Plateau region, southwest Atlantic Ocean. In Ludwig, W. J., Krasheninnikov, V. A., et al., *Init. Repts. DSDP*, 71: Washington (U.S. Govt. Printing Office), 481-550.

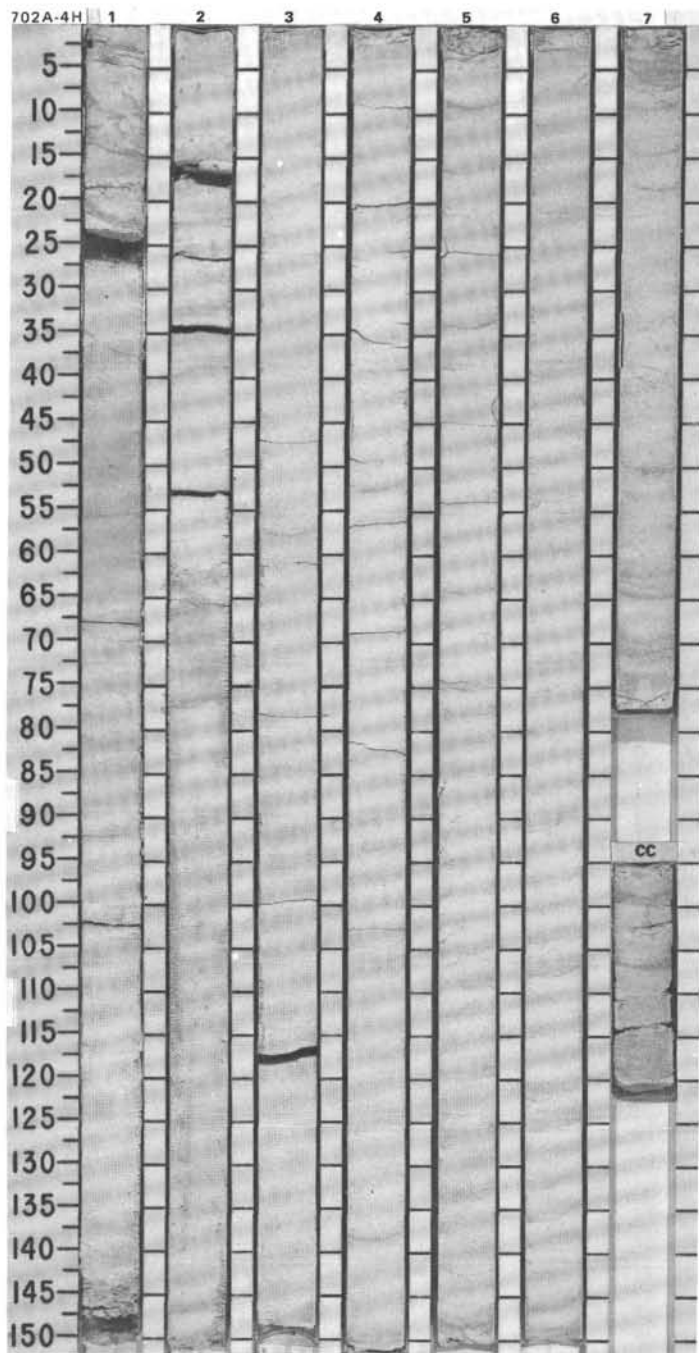
Ms 114A-109

TIME-ROCK UNIT	BIOSTRAT. ZONE/ FOSSIL CHARACTER				PALEOMAGNETICS	PHYS. PROPERTIES	CHEMISTRY	SECTION	METERS	GRAPHIC LITHOLOGY	DRILLING DISTURB.	SED. STRUCTURES	SAMPLES	LITHOLOGIC DESCRIPTION																																	
	FORAMINIFERS	NANNOFOSSILS	RADIOLARIANS	DIATOMS																																											
	Barren	Barren	<i>Heliotholus vema</i>					1	0.5 1.0					DIATOM SILTY MUD to SILTY DIATOM OOZE * Drilling deformation: Moderate in Section 1. Major lithology: Diatom silty mud, pale olive (5Y 6/3), with darker hues (olive, 5Y 4/3) caused by Mn staining; grading to silty diatom ooze, olive (5Y 6/3). Dropstones and Mn-oxide stain throughout. Dropstones conspicuous in Section 1, 7-10, 85-88, 102-103, 125-127, and 145-147 cm; Section 2, 25, 55-57, and 73-95 cm; and Section 3, 25-32, 75-80, 102-104, 123-129, and 143-147 cm. Mn-oxide stain particularly in Section 1, 71-79, 103-117, and 135-145 cm; Section 2, 102-104, 123-129, and 143-147 cm, and CC, 8 cm. SMEAR SLIDE SUMMARY (%): <table style="margin-left: 40px;"> <tr> <td></td> <td>1, 40</td> <td>3, 60</td> </tr> <tr> <td></td> <td>D</td> <td>D</td> </tr> </table> TEXTURE: IW Sand 20 Silt 50 Clay 30 * COMPOSITION: <table style="margin-left: 40px;"> <tr> <td>Quartz/feldspar</td> <td>25</td> <td>15</td> </tr> <tr> <td>Clay</td> <td>30</td> <td>20</td> </tr> <tr> <td>Volcanic glass</td> <td>5</td> <td>—</td> </tr> <tr> <td>Accessory minerals</td> <td>1</td> <td>—</td> </tr> <tr> <td> Opauques</td> <td>1</td> <td>—</td> </tr> <tr> <td>Diatoms</td> <td>37</td> <td>55</td> </tr> <tr> <td>Radiolarians</td> <td>Tr</td> <td>5</td> </tr> <tr> <td>Sponge spicules</td> <td>1</td> <td>—</td> </tr> <tr> <td>Silicoflagellates</td> <td>Tr</td> <td>5</td> </tr> </table>		1, 40	3, 60		D	D	Quartz/feldspar	25	15	Clay	30	20	Volcanic glass	5	—	Accessory minerals	1	—	Opauques	1	—	Diatoms	37	55	Radiolarians	Tr	5	Sponge spicules	1	—	Silicoflagellates	Tr	5
	1, 40	3, 60																																													
	D	D																																													
Quartz/feldspar	25	15																																													
Clay	30	20																																													
Volcanic glass	5	—																																													
Accessory minerals	1	—																																													
Opauques	1	—																																													
Diatoms	37	55																																													
Radiolarians	Tr	5																																													
Sponge spicules	1	—																																													
Silicoflagellates	Tr	5																																													
			<i>Distephanus boliviensis</i>				2																																								
							3																																								
							CC																																								



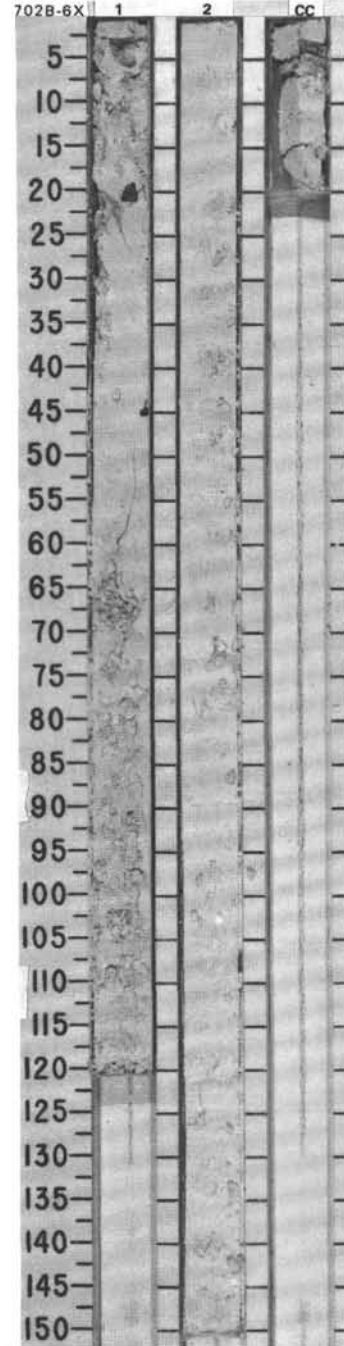
SITE 702 HOLE A CORE 4H CORED INTERVAL 3107.0-3116.5 mbsf: 23.6-33.1 mbsf

TIME-ROCK UNIT	BIOSTRAT. ZONE/ FOSSIL CHARACTER					PHYS. PROPERTIES	CHEMISTRY	SECTION	METERS	GRAPHIC LITHOLOGY	DRILLING DISTURB.	SED. STRUCTURES	SAMPLES	LITHOLOGIC DESCRIPTION																																			
	FORAMINIFERS	NANNOFOSSILS	RADIOLARIANS	DIATOMS	SILICO- FLAGELLATES																																												
UPPER EOCENE						$\phi=57.15$ $\beta_g=2.72$		1	0.5				*	NANNOFOSSIL OOZE and FORAMINIFER-BEARING NANNOFOSSIL OOZE Major lithologies: Nannofossil ooze, pure white (no color code) to white (5Y 8/1), Sections 1 through 6. Foraminifer-bearing nannofossil ooze, pure white (no color code), in Section 7 and CC. <i>Zoophycos</i> traces in Section 1, 64 and 68 cm. SMEAR SLIDE SUMMARY (%): <table style="margin-left: 20px;"> <tr> <td></td> <td>1, 50</td> <td>1, 120</td> <td>4, 50</td> <td>7, 50</td> </tr> <tr> <td></td> <td>D</td> <td>D</td> <td>D</td> <td>D</td> </tr> </table> COMPOSITION: <table style="margin-left: 20px;"> <tr> <td>Foraminifers</td> <td>—</td> <td>4</td> <td>5</td> <td>15</td> </tr> <tr> <td>Nannofossils</td> <td>90</td> <td>92</td> <td>87</td> <td>81</td> </tr> <tr> <td>Diatoms</td> <td>8</td> <td>—</td> <td>—</td> <td>3</td> </tr> <tr> <td>Radiolarians</td> <td>1</td> <td>2</td> <td>3</td> <td>1</td> </tr> <tr> <td>Silicoflagellates</td> <td>1</td> <td>2</td> <td>5</td> <td>—</td> </tr> </table>		1, 50	1, 120	4, 50	7, 50		D	D	D	D	Foraminifers	—	4	5	15	Nannofossils	90	92	87	81	Diatoms	8	—	—	3	Radiolarians	1	2	3	1	Silicoflagellates	1	2	5	—
	1, 50	1, 120	4, 50	7, 50																																													
	D	D	D	D																																													
Foraminifers	—	4	5	15																																													
Nannofossils	90	92	87	81																																													
Diatoms	8	—	—	3																																													
Radiolarians	1	2	3	1																																													
Silicoflagellates	1	2	5	—																																													
UPPER EOCENE	P15					$\phi=57.32$ $\beta_g=2.67$		2	1.0				*																																				
NP 18						$\phi=59.03$ $\beta_g=2.99$		3																																									
unzoned						$\phi=59.12$ $\beta_g=2.71$		4					*																																				
EOCENE						$\phi=59.92$ $\beta_g=2.80$		5																																									
<i>Mesocena occidentalis</i>						$\phi=59.92$ $\beta_g=2.80$		6																																									
						$\phi=57.15$ $\beta_g=2.72$		7					*																																				
								CC																																									



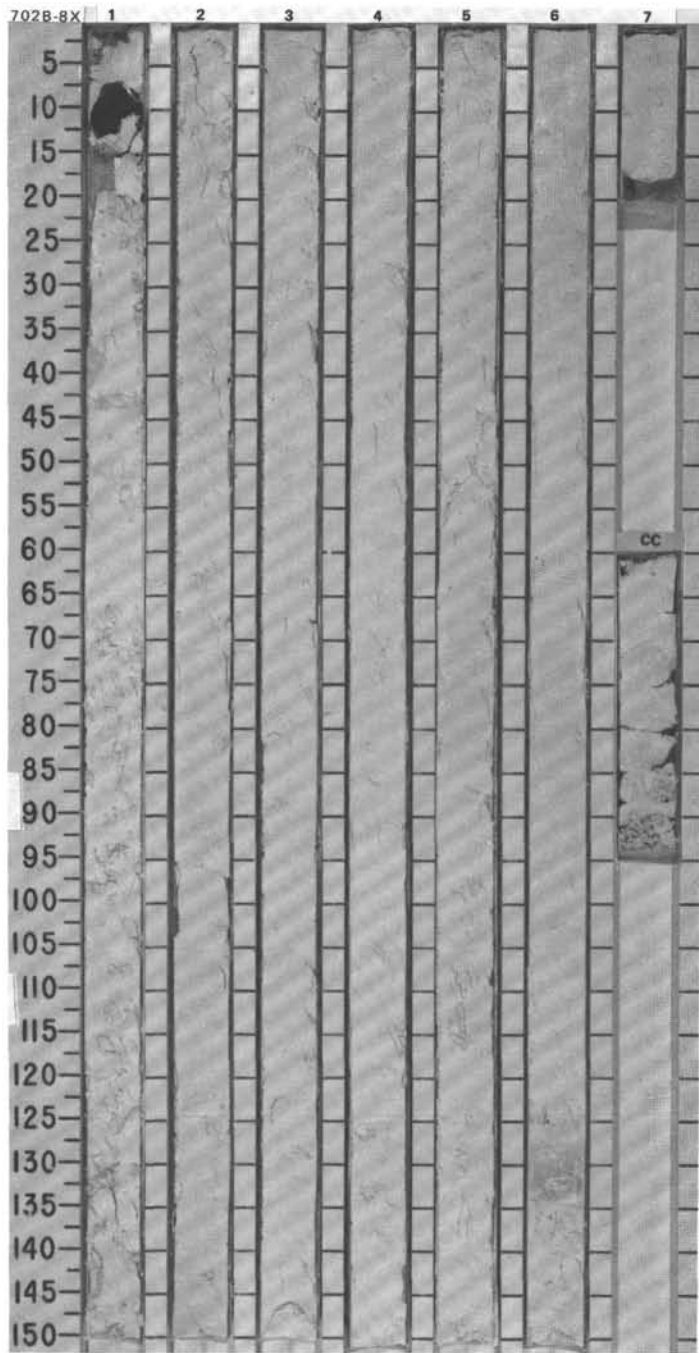
SITE 702 HOLE B CORE 6X CORED INTERVAL 3128.0-3137.5mbsl; 44.3-53.8 mbsf

TIME-ROCK UNIT		BIOSTRAT. ZONE/ FOSSIL CHARACTER		PHYS. PROPERTIES	CHEMISTRY	SECTION	METERS	GRAPHIC LITHOLOGY	DRILLING DISTURB.	SED. STRUCTURES	SAMPLES	LITHOLOGIC DESCRIPTION
FORAMINIFERS	NANNOFOSSILS	RADIOLARIANS	DIA TOMS									
MIDDLE EOCENE	UPPER MIDDLE EOCENE	P14	not examined			1	0.5 1.0					NANNOFOSSIL CHALK Drilling disturbance: Moderately fractured. Major lithology: Nannofossil chalk, white (no color code). Minor lithology: One pebble (quartzite) in Section 1, 19-20 cm (contamination?). SMEAR SLIDE SUMMARY (%): Foraminifers 2 Nannofossils 46 Radiolarians D Sponge spicules Tr Micrite 3
G. index Zone	NP 16		unzoned			2						
			EOCENE			cc						
			<i>Dictyochoa grandis</i>									



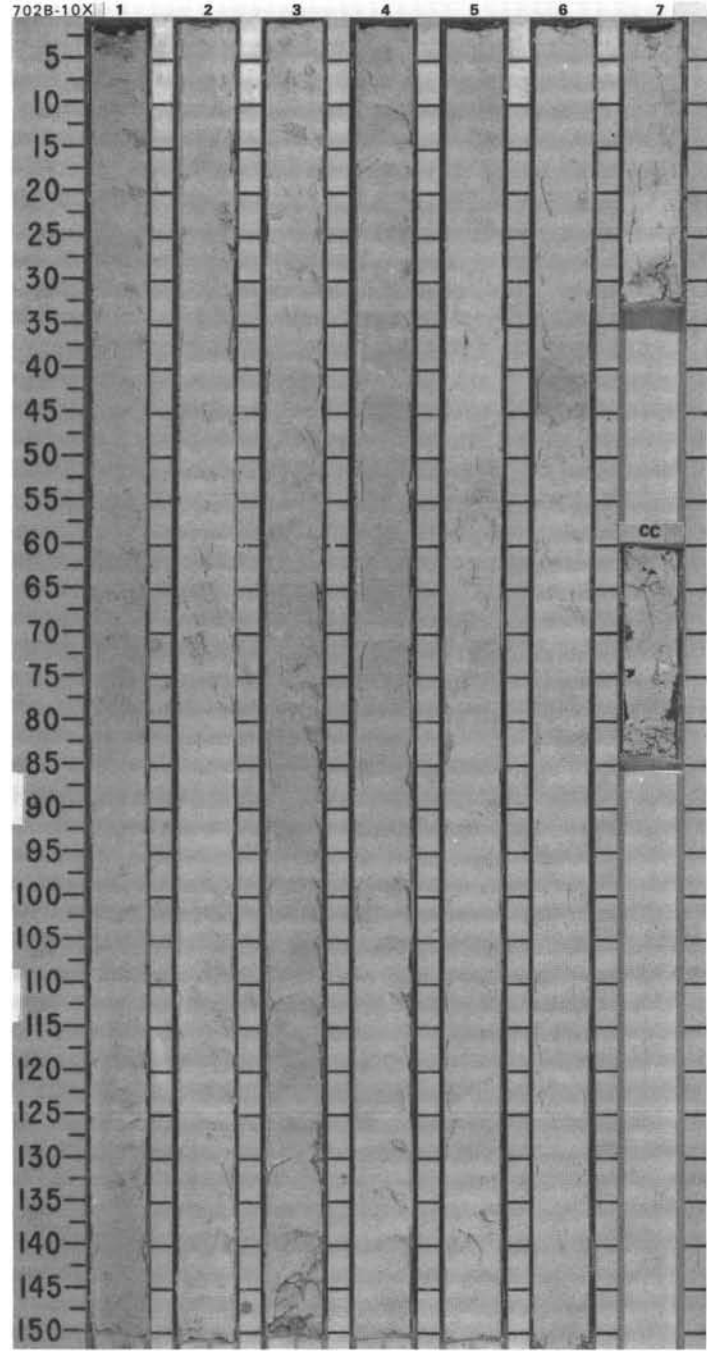
SITE 702 HOLE B CORE 8X CORED INTERVAL 3147.0-3156.5 mbsl; 63.3-72.8 mbsf

TIME-ROCK UNIT	BIOSTRAT. ZONE/ FOSSIL CHARACTER	FORAMINIFERS	NANNOFOSSILS	RADIOLARIANS	DIATOMS	SILICO- FLAGELLATES	PALEOMAGNETICS	PHYS. PROPERTIES	CHEMISTRY	SECTION	METERS	GRAPHIC LITHOLOGY	DRILLING DISTURB.	SED. STRUCTURES	SAMPLES	LITHOLOGIC DESCRIPTION																														
MIDDLE EOCENE										1	0.5 1.0					<p>NANNOFOSSIL CHALK</p> <p>Drilling disturbance: Moderately fractured.</p> <p>Major lithology: Nannofossil chalk, white (no color code). Bioturbation throughout Section 6, particularly at 129-138 cm, where color is light gray (N 7/0).</p> <p>Minor lithology: Clay-bearing nannofossil chalk in Section 6, 128-138 cm. Mudstone(?) pebble in Section 1, 5-12 cm.</p> <p>SMEAR SLIDE SUMMARY (%):</p> <table border="0"> <tr> <td></td> <td>1, 45</td> <td>6, 135</td> </tr> <tr> <td>D</td> <td></td> <td>M</td> </tr> </table> <p>COMPOSITION:</p> <table border="0"> <tr> <td>Clay</td> <td>—</td> <td>10</td> </tr> <tr> <td>Volcanic glass</td> <td>—</td> <td>1</td> </tr> <tr> <td>Foraminifers</td> <td>1</td> <td>—</td> </tr> <tr> <td>Nannofossils</td> <td>94</td> <td>89</td> </tr> <tr> <td>Diatoms</td> <td>Tr</td> <td>—</td> </tr> <tr> <td>Radiolarians</td> <td>Tr</td> <td>Tr</td> </tr> <tr> <td>Sponge spicules</td> <td>Tr</td> <td>—</td> </tr> <tr> <td>Micrite</td> <td>5</td> <td>—</td> </tr> </table>		1, 45	6, 135	D		M	Clay	—	10	Volcanic glass	—	1	Foraminifers	1	—	Nannofossils	94	89	Diatoms	Tr	—	Radiolarians	Tr	Tr	Sponge spicules	Tr	—	Micrite	5	—
	1, 45	6, 135																																												
D		M																																												
Clay	—	10																																												
Volcanic glass	—	1																																												
Foraminifers	1	—																																												
Nannofossils	94	89																																												
Diatoms	Tr	—																																												
Radiolarians	Tr	Tr																																												
Sponge spicules	Tr	—																																												
Micrite	5	—																																												
UPPER MIDDLE EOCENE P14										2																																				
UPPER MIDDLE EOCENE P12 - P13										3																																				
UPPER MIDDLE EOCENE P16										4																																				
unzoned EOCENE										5																																				
<i>Dictyocha grandis</i>										6																																				
										7																																				
										CC																																				



SITE 702 HOLE B CORE 10X CORED INTERVAL 3166.0-3175.5 mbsl; 82.3-91.8 mbsf

TIME-ROCK UNIT	BIOSTRAT. ZONE/ FOSSIL CHARACTER	SECTION	METERS	GRAPHIC LITHOLOGY	DRILLING DISTURB.	SED. STRUCTURES	SAMPLES	LITHOLOGIC DESCRIPTION
MIDDLE EOCENE								<p>NANNOFOSSIL CHALK</p> <p>Drilling disturbance: Moderately fractured.</p> <p>Major lithology: Nannofossil chalk, white (2.5Y 8/0), in Sections 1, 2, and 3; white (10YR 8/1) in Section 4, and white (no color code) in Sections 5, 6, and 7. Light gray (5Y 7/1) where moderately bioturbated (<i>Planolites</i>) in Section 6, 33-61 cm. Minor bioturbation throughout Sections 3 and 4. <i>Zoophycos</i> in Section 4, 45 cm.</p> <p>SMEAR SLIDE SUMMARY (%):</p> <p>1, 65 D</p> <p>COMPOSITION:</p> <p>Clay 5 Nannofossils 90 Radiolarians Tr Micrite 5</p>
UPPER MIDDLE EOCENE P12 - P13		Chronozone C18R	0.5 1.0				*	
not examined		Chronozone C19N						
unzoned		$\phi=54.98$ $\rho_0=2.80$						
EOCENE		Chronozone C19R						
<i>Dictyochoa grandis</i>		$\phi=55.03$ $\rho_0=2.77$						
Chronozone C19R								
CC								

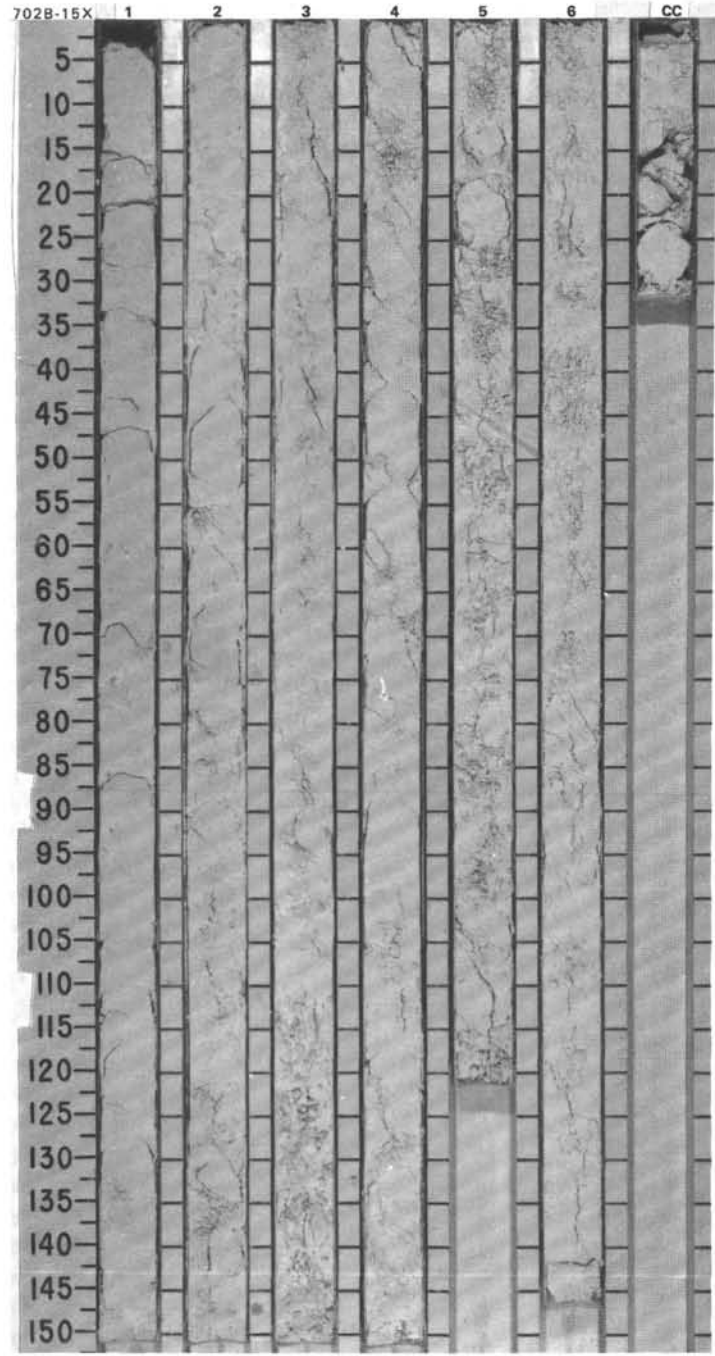


SITE 702 HOLE B CORE 13X CORED INTERVAL 3194.5-3204.0 mbsl; 110.8-120.3 mbsf

TIME-ROCK UNIT		BIOSTRAT. ZONE/ FOSSIL CHARACTER	SECTION	METERS	GRAPHIC LITHOLOGY	DRILLING DISTURB. SED. STRUCTURES	SAMPLES	LITHOLOGIC DESCRIPTION
FORAMINIFERS	NANNOFOSSILS							
MIDDLE EOCENE		UPPER MIDDLE EOCENE	P12	1	0.5 1.0			NANNOFOSSIL CHALK Drilling disturbance: Moderately fractured. Major lithology: Nannofossil chalk. Moderate bioturbation in shades of white (7.5YR 8/1) visible in Section 4, 118-130 cm.
UPPER MIDDLE EOCENE								
LOWER MIDDLE EOCENE		G. <i>index</i> Zone NP 15-16 unzoned	P11	2				* SMEAR SLIDE SUMMARY (%): COMPOSITION: Foraminifers 7 8 Nannofossils 93 82 Diatoms 1 2
MIDDLE EOCENE								
Barren		Chronozone C20R $\phi = 56.06$ $f_0 = 2.88$	3					
Eocene								
A. <i>primitiva</i> Zone		Chronozone C20R $\phi = 55.02$ $f_0 = 2.82$	4					
LOWER MIDDLE EOCENE								
P11		Chronozone C20R $\phi = 55.02$ $f_0 = 2.82$	5					
UPPER MIDDLE EOCENE								
P12		Chronozone C20R $\phi = 56.06$ $f_0 = 2.88$	6					
MIDDLE EOCENE								
P12		Chronozone C20R $\phi = 56.06$ $f_0 = 2.88$	7					
UPPER MIDDLE EOCENE								
P12		Chronozone C20R $\phi = 56.06$ $f_0 = 2.88$	8					
MIDDLE EOCENE								
P12		Chronozone C20R $\phi = 56.06$ $f_0 = 2.88$	9					
UPPER MIDDLE EOCENE								
P12		Chronozone C20R $\phi = 56.06$ $f_0 = 2.88$	10					
MIDDLE EOCENE								
P12		Chronozone C20R $\phi = 56.06$ $f_0 = 2.88$	11					
UPPER MIDDLE EOCENE								
P12		Chronozone C20R $\phi = 56.06$ $f_0 = 2.88$	12					
MIDDLE EOCENE								
P12		Chronozone C20R $\phi = 56.06$ $f_0 = 2.88$	13					
UPPER MIDDLE EOCENE								
P12		Chronozone C20R $\phi = 56.06$ $f_0 = 2.88$	14					
MIDDLE EOCENE								
P12		Chronozone C20R $\phi = 56.06$ $f_0 = 2.88$	15					
UPPER MIDDLE EOCENE								
P12		Chronozone C20R $\phi = 56.06$ $f_0 = 2.88$	16					
MIDDLE EOCENE								
P12		Chronozone C20R $\phi = 56.06$ $f_0 = 2.88$	17					
UPPER MIDDLE EOCENE								
P12		Chronozone C20R $\phi = 56.06$ $f_0 = 2.88$	18					
MIDDLE EOCENE								
P12		Chronozone C20R $\phi = 56.06$ $f_0 = 2.88$	19					
UPPER MIDDLE EOCENE								
P12		Chronozone C20R $\phi = 56.06$ $f_0 = 2.88$	20					
MIDDLE EOCENE								
P12		Chronozone C20R $\phi = 56.06$ $f_0 = 2.88$	21					
UPPER MIDDLE EOCENE								
P12		Chronozone C20R $\phi = 56.06$ $f_0 = 2.88$	22					
MIDDLE EOCENE								
P12		Chronozone C20R $\phi = 56.06$ $f_0 = 2.88$	23					
UPPER MIDDLE EOCENE								
P12		Chronozone C20R $\phi = 56.06$ $f_0 = 2.88$	24					
MIDDLE EOCENE								
P12		Chronozone C20R $\phi = 56.06$ $f_0 = 2.88$	25					
UPPER MIDDLE EOCENE								
P12		Chronozone C20R $\phi = 56.06$ $f_0 = 2.88$	26					
MIDDLE EOCENE								
P12		Chronozone C20R $\phi = 56.06$ $f_0 = 2.88$	27					
UPPER MIDDLE EOCENE								
P12		Chronozone C20R $\phi = 56.06$ $f_0 = 2.88$	28					
MIDDLE EOCENE								
P12		Chronozone C20R $\phi = 56.06$ $f_0 = 2.88$	29					
UPPER MIDDLE EOCENE								
P12		Chronozone C20R $\phi = 56.06$ $f_0 = 2.88$	30					
MIDDLE EOCENE								
P12		Chronozone C20R $\phi = 56.06$ $f_0 = 2.88$	31					
UPPER MIDDLE EOCENE								
P12		Chronozone C20R $\phi = 56.06$ $f_0 = 2.88$	32					
MIDDLE EOCENE								
P12		Chronozone C20R $\phi = 56.06$ $f_0 = 2.88$	33					
UPPER MIDDLE EOCENE								
P12		Chronozone C20R $\phi = 56.06$ $f_0 = 2.88$	34					
MIDDLE EOCENE								
P12		Chronozone C20R $\phi = 56.06$ $f_0 = 2.88$	35					
UPPER MIDDLE EOCENE								
P12		Chronozone C20R $\phi = 56.06$ $f_0 = 2.88$	36					
MIDDLE EOCENE								
P12		Chronozone C20R $\phi = 56.06$ $f_0 = 2.88$	37					
UPPER MIDDLE EOCENE								
P12		Chronozone C20R $\phi = 56.06$ $f_0 = 2.88$	38					
MIDDLE EOCENE								
P12		Chronozone C20R $\phi = 56.06$ $f_0 = 2.88$	39					
UPPER MIDDLE EOCENE								
P12		Chronozone C20R $\phi = 56.06$ $f_0 = 2.88$	40					
MIDDLE EOCENE								
P12		Chronozone C20R $\phi = 56.06$ $f_0 = 2.88$	41					
UPPER MIDDLE EOCENE								
P12		Chronozone C20R $\phi = 56.06$ $f_0 = 2.88$	42					
MIDDLE EOCENE								
P12		Chronozone C20R $\phi = 56.06$ $f_0 = 2.88$	43					
UPPER MIDDLE EOCENE								
P12		Chronozone C20R $\phi = 56.06$ $f_0 = 2.88$	44					
MIDDLE EOCENE								
P12		Chronozone C20R $\phi = 56.06$ $f_0 = 2.88$	45					
UPPER MIDDLE EOCENE								
P12		Chronozone C20R $\phi = 56.06$ $f_0 = 2.88$	46					
MIDDLE EOCENE								
P12		Chronozone C20R $\phi = 56.06$ $f_0 = 2.88$	47					
UPPER MIDDLE EOCENE								
P12		Chronozone C20R $\phi = 56.06$ $f_0 = 2.88$	48					
MIDDLE EOCENE								
P12		Chronozone C20R $\phi = 56.06$ $f_0 = 2.88$	49					
UPPER MIDDLE EOCENE								
P12		Chronozone C20R $\phi = 56.06$ $f_0 = 2.88$	50					
MIDDLE EOCENE								
P12		Chronozone C20R $\phi = 56.06$ $f_0 = 2.88$	51					
UPPER MIDDLE EOCENE								
P12		Chronozone C20R $\phi = 56.06$ $f_0 = 2.88$	52					
MIDDLE EOCENE								
P12		Chronozone C20R $\phi = 56.06$ $f_0 = 2.88$	53					
UPPER MIDDLE EOCENE								
P12		Chronozone C20R $\phi = 56.06$ $f_0 = 2.88$	54					
MIDDLE EOCENE								
P12		Chronozone C20R $\phi = 56.06$ $f_0 = 2.88$	55					
UPPER MIDDLE EOCENE								
P12		Chronozone C20R $\phi = 56.06$ $f_0 = 2.88$	56					
MIDDLE EOCENE								
P12		Chronozone C20R $\phi = 56.06$ $f_0 = 2.88$	57					
UPPER MIDDLE EOCENE								
P12		Chronozone C20R $\phi = 56.06$ $f_0 = 2.88$	58					
MIDDLE EOCENE								
P12		Chronozone C20R $\phi = 56.06$ $f_0 = 2.88$	59					
UPPER MIDDLE EOCENE								
P12		Chronozone C20R $\phi = 56.06$ $f_0 = 2.88$	60					
MIDDLE EOCENE								
P12		Chronozone C20R $\phi = 56.06$ $f_0 = 2.88$	61					
UPPER MIDDLE EOCENE								
P12		Chronozone C20R $\phi = 56.06$ $f_0 = 2.88$	62					
MIDDLE EOCENE								
P12		Chronozone C20R $\phi = 56.06$ $f_0 = 2.88$	63					
UPPER MIDDLE EOCENE								
P12		Chronozone C20R $\phi = 56.06$ $f_0 = 2.88$	64					
MIDDLE EOCENE								
P12		Chronozone C20R $\phi = 56.06$ $f_0 = 2.88$	65					
UPPER MIDDLE EOCENE								
P12		Chronozone C20R $\phi = 56.06$ $f_0 = 2.88$	66					
MIDDLE EOCENE								
P12		Chronozone C20R $\phi = 56.06$ $f_0 = 2.88$	67					
UPPER MIDDLE EOCENE								
P12		Chronozone C20R $\phi = 56.06$ $f_0 = 2.88$	68					
MIDDLE EOCENE								
P12		Chronozone C20R $\phi = 56.06$ $f_0 = 2.88$	69					
UPPER MIDDLE EOCENE								
P12		Chronozone C20R $\phi = 56.06$ $f_0 = 2.88$	70					
MIDDLE EOCENE								
P12		Chronozone C20R $\phi = 56.06$ $f_0 = 2.88$	71					
UPPER MIDDLE EOCENE								
P12		Chronozone C20R $\phi = 56.06$ $f_0 = 2.88$	72					
MIDDLE EOCENE								
P12		Chronozone C20R $\phi = 56.06$ $f_0 = 2.88$	73					
UPPER MIDDLE EOCENE								
P12		Chronozone C20R $\phi = 56.06$ $f_0 = 2.88$	74					
MIDDLE EOCENE								
P12		Chronozone C20R $\phi = 56.06$ $f_0 = 2.88$	75					
UPPER MIDDLE EOCENE								
P12		Chronozone C20R $\phi = 56.06$ $f_0 = 2.88$	76					
MIDDLE EOCENE								
P12		Chronozone C20R $\phi = 56.06$ $f_0 = 2.88$	77					
UPPER MIDDLE EOCENE								
P12		Chronozone C20R $\phi = 56.06$ $f_0 = 2.88$	78					
MIDDLE EOCENE								
P12		Chronozone C20R $\phi = 56.06$ $f_0 = 2.88$	79					
UPPER MIDDLE EOCENE								
P12		Chronozone C20R $\phi = 56.06$ $f_0 = 2.88$	80					
MIDDLE EOCENE								
P12		Chronozone C20R $\phi = 56.06$ $f_0 = 2.88$	81					
UPPER MIDDLE EOCENE								
P12		Chronozone C20R $\phi = 56.06$ $f_0 = 2.88$	82					
MIDDLE EOCENE								
P12		Chronozone C20R $\phi = 56.06$ $f_0 = 2.88$	83					
UPPER MIDDLE EOCENE								
P12		Chronozone C20R $\phi = 56.06$ $f_0 = 2.88$	84					
MIDDLE EOCENE								
P12		Chronozone C20R $\phi = 56.06$ $f_0 = 2.88$	85					
UPPER MIDDLE EOCENE								
P12		Chronozone C20R $\phi = 56.06$ $f_0 = 2.88$	86					
MIDDLE EOCENE								
P12		Chronozone C20R $\phi = 56.06$ $f_0 = 2.88$	87					
UPPER MIDDLE EOCENE								
P12		Chronozone C20R $\phi = 56.06$ $f_0 = 2.88$	88					

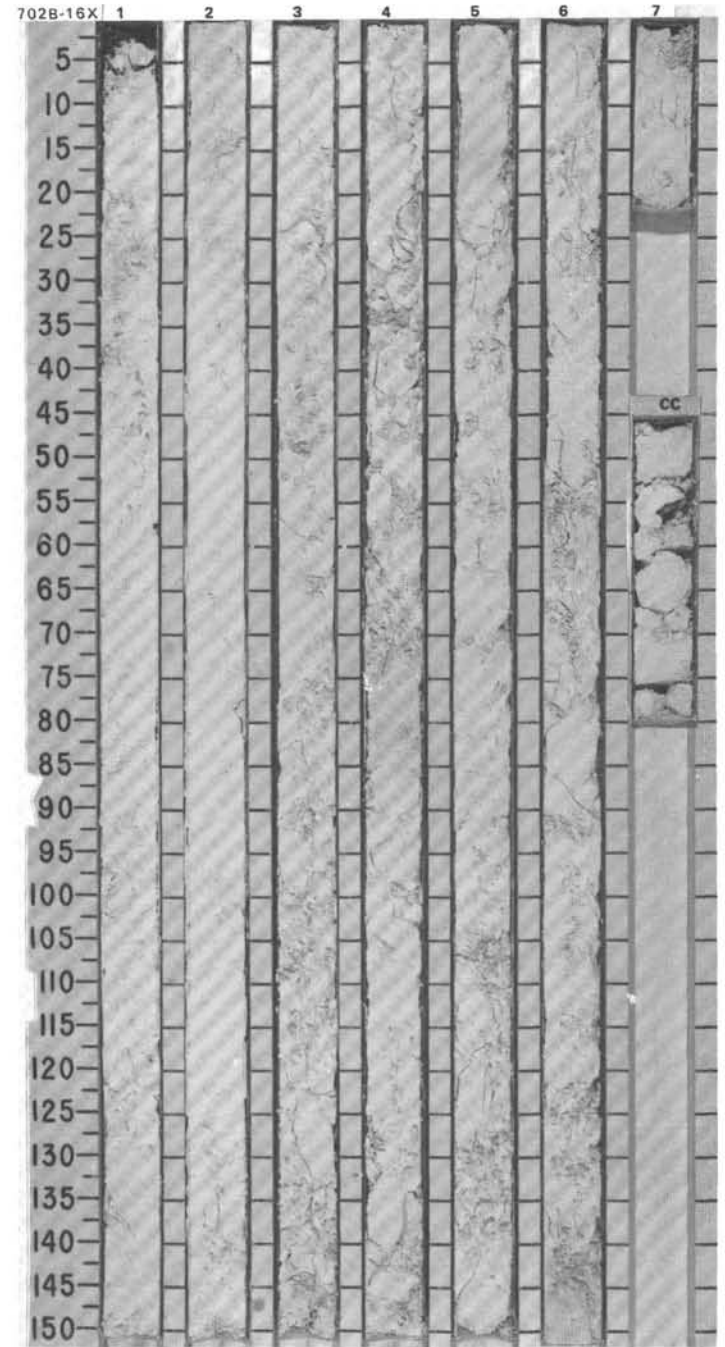
SITE 702 HOLE B CORE 15X CORED INTERVAL 3213.5-3223.0 mbsl; 129.8-139.3 mbsf

TIME-ROCK UNIT	BIOSTRAT. ZONE/ FOSSIL CHARACTER	FORAMINIFERS	NANNOFOSSILS	RADIOLARIANS	DIAZONS	SILICO- FLAGELLATES	PALEOMAGNETICS	PHYS. PROPERTIES	CHEMISTRY	SECTION	METERS	GRAPHIC LITHOLOGY	DRILLING DISTURB.	SED. STRUCTURES	SAMPLES	LITHOLOGIC DESCRIPTION																		
MIDDLE EOCENE	LOWER MIDDLE EOCENE P11		not examined							1	0.5 1.0					<p>NANNOFOSSIL CHALK</p> <p>Drilling disturbance: Moderately to highly fractured.</p> <p>Major lithology: Nannofossil chalk, white (no color code).</p> <p>SMEAR SLIDE SUMMARY (%):</p> <table border="0"> <tr> <td></td> <td>1, 77</td> <td>CC,</td> </tr> <tr> <td></td> <td>D</td> <td>25</td> </tr> <tr> <td></td> <td></td> <td>D</td> </tr> </table> <p>COMPOSITION:</p> <table border="0"> <tr> <td>Foraminifers</td> <td>5</td> <td>5</td> </tr> <tr> <td>Nannofossils</td> <td>87</td> <td>87</td> </tr> <tr> <td>Micrite</td> <td>8</td> <td>8</td> </tr> </table>		1, 77	CC,		D	25			D	Foraminifers	5	5	Nannofossils	87	87	Micrite	8	8
	1, 77	CC,																																
	D	25																																
		D																																
Foraminifers	5	5																																
Nannofossils	87	87																																
Micrite	8	8																																
	NP 14-15									2																								
	unzoned									3																								
	Barren									4																								
	Barren									5																								
	Chronozone C20R									6																								
										CC																								



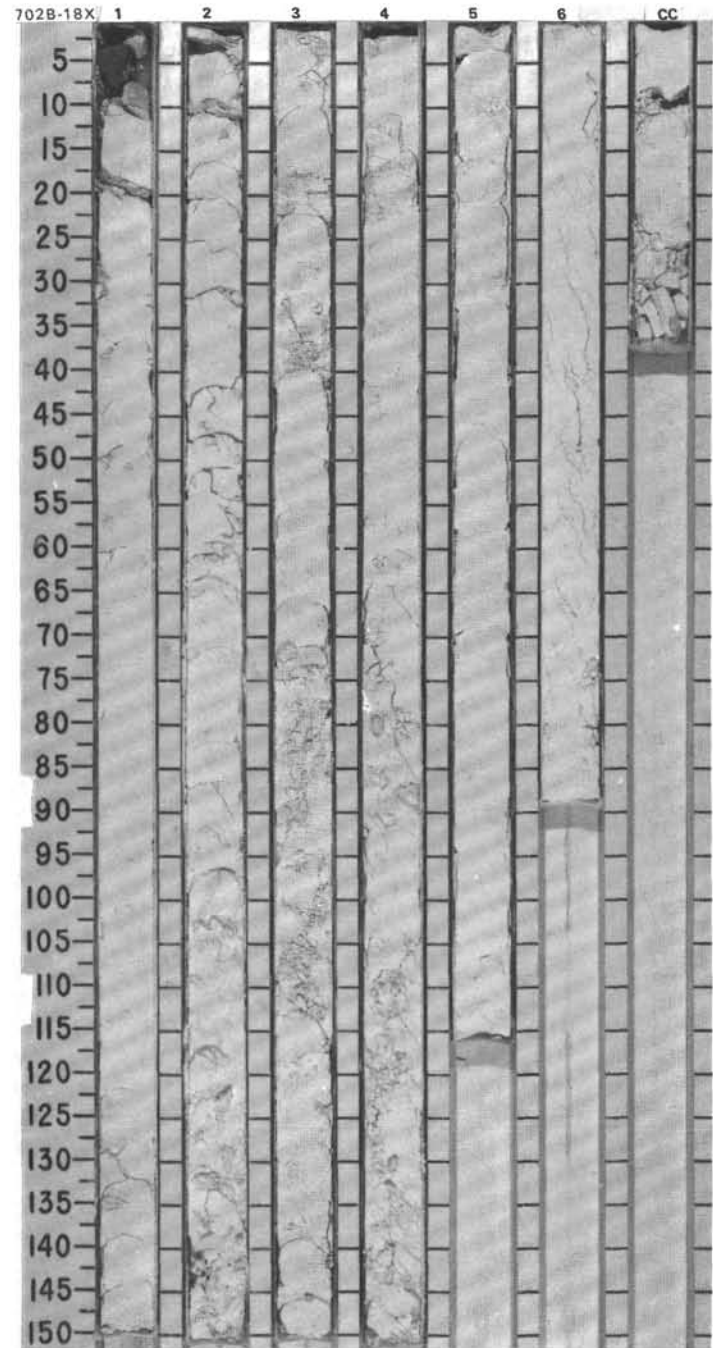
SITE 702 HOLE B CORE 16X CORED INTERVAL 3223.0-3232.5 mbsl; 139.3-148.8 mbsf

TIME-ROCK UNIT	BIOSTRAT. ZONE/ FOSSIL CHARACTER					PHYS. PROPERTIES	CHEMISTRY	SECTION	METERS	GRAPHIC LITHOLOGY	DRILLING DISTURB.	SED. STRUCTURES	SAMPLES	LITHOLOGIC DESCRIPTION																				
	FORAMINIFERS	NANNOFOSSILS	RADIOLARIANS	DIATOMS	SILICO- FLAGELLATES																													
MIDDLE EOCENE	A. primitiva Zone													<p>NANNOFOSSIL CHALK</p> <p>Drilling disturbance: Moderately to highly fragmented.</p> <p>Major lithology: Nannofossil chalk, pure white (no color code), micritic in part.</p> <p>Minor lithology: Foraminifer-bearing nannofossil chalk in 114-702B-16X, CC.</p> <p>SMEAR SLIDE SUMMARY (%):</p> <table border="1"> <tr> <td></td> <td>1, 77</td> <td>6, 82</td> <td>CC, 18</td> </tr> <tr> <td></td> <td>D</td> <td>D</td> <td>D</td> </tr> </table> <p>COMPOSITION:</p> <table border="1"> <tr> <td>Foraminifers</td> <td>5</td> <td>8</td> <td>12</td> </tr> <tr> <td>Nannofossils</td> <td>80</td> <td>80</td> <td>73</td> </tr> <tr> <td>Micrite</td> <td>15</td> <td>12</td> <td>15</td> </tr> </table>		1, 77	6, 82	CC, 18		D	D	D	Foraminifers	5	8	12	Nannofossils	80	80	73	Micrite	15	12	15
	1, 77	6, 82	CC, 18																															
	D	D	D																															
Foraminifers	5	8	12																															
Nannofossils	80	80	73																															
Micrite	15	12	15																															
LOWER MIDDLE EOCENE	NP 14-15																																	
	unzoned																																	
	Barren																																	
	Barren																																	
	Chronozone C20R																																	
	Chronozone C20R					$\phi=54.98$	$\rho_g=2.87$	1	0.5				*																					
	Chronozone C20R					$\phi=57.45$	$\rho_g=2.93$	2	1.0				*																					
	Chronozone C20R					$\phi=55.72$	$\rho_g=2.89$	3					*																					
	Chronozone C20R							4					*																					
	Chronozone C20R							5					*																					
	Chronozone C20R							6					*																					
	Chronozone C20R							7					*																					
	Chronozone C20R							CC					*																					



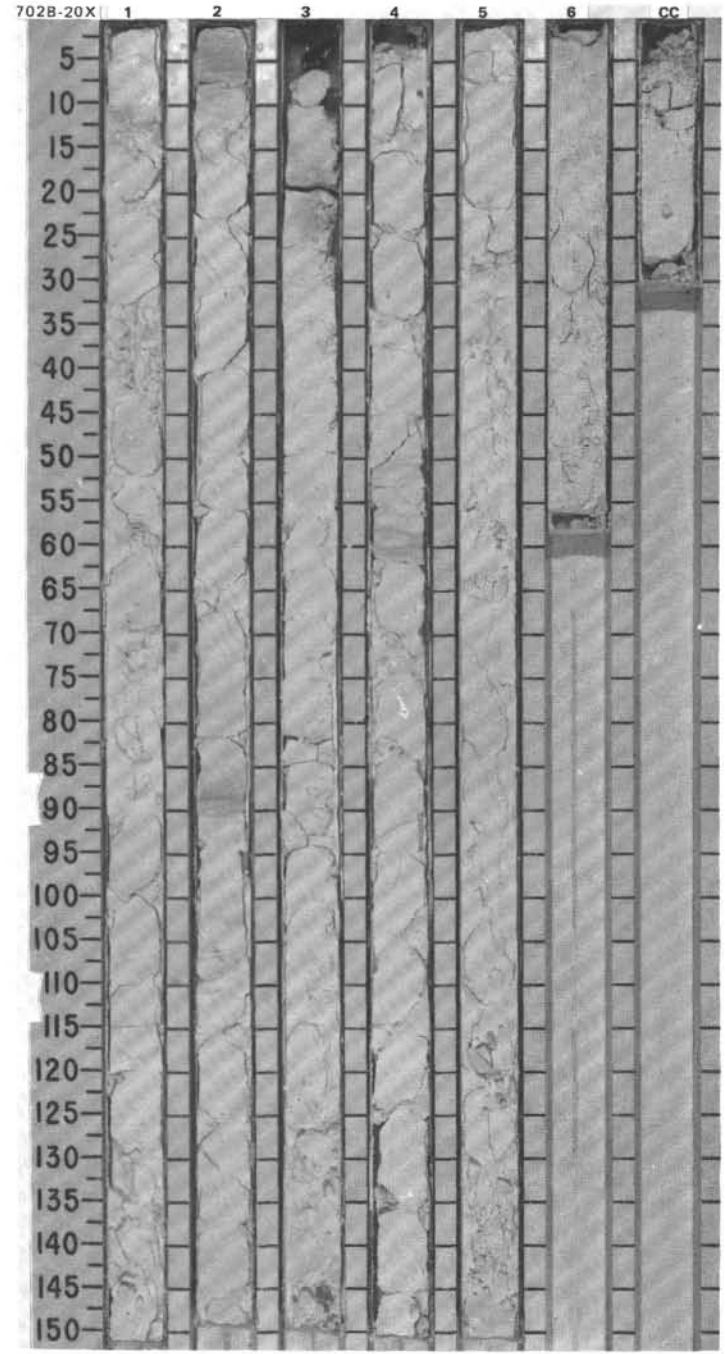
SITE 702 HOLE B CORE 18X CORED INTERVAL 3242.0-3251.5 mbsf; 158.3-167.8 mbsf

TIME-ROCK UNIT	BIOSTRAT. ZONE/ FOSSIL CHARACTER	SECTION	METERS	GRAPHIC LITHOLOGY	DRILLING DISTURB.	SED. STRUCTURES	SAMPLES	LITHOLOGIC DESCRIPTION														
LOWER EOCENE								<p>NANNOFOSSIL CHALK</p> <p>Drilling disturbance: Moderately to highly fractured.</p> <p>Major lithology: Nannofossil chalk, white (no color code). Mudstone clast in Section 1, 0-6 cm.</p> <p>SMEAR SLIDE SUMMARY (%):</p> <table> <tr><td>Foraminifers</td><td>1</td></tr> <tr><td>Nannofossils</td><td>94</td></tr> <tr><td>Radiolarians</td><td>Tr</td></tr> <tr><td>Sponge spicules</td><td>Tr</td></tr> <tr><td>Micrite</td><td>5</td></tr> </table> <p>COMPOSITION:</p> <table> <tr><td></td><td>3,66</td></tr> <tr><td>D</td><td></td></tr> </table>	Foraminifers	1	Nannofossils	94	Radiolarians	Tr	Sponge spicules	Tr	Micrite	5		3,66	D	
Foraminifers	1																					
Nannofossils	94																					
Radiolarians	Tr																					
Sponge spicules	Tr																					
Micrite	5																					
	3,66																					
D																						
UPPER LOWER EOCENE		1	0.5																			
	NP 13-16	2	1.0																			
unzoned (LOWER EOCENE)	Barren	3																				
	Barren	4																				
	Chronozone C21N	5																				
	$\phi = 52.85$ $\rho_g = 2.67$	6																				
	$\phi = 52.70$ $\rho_g = 2.88$	CC																				

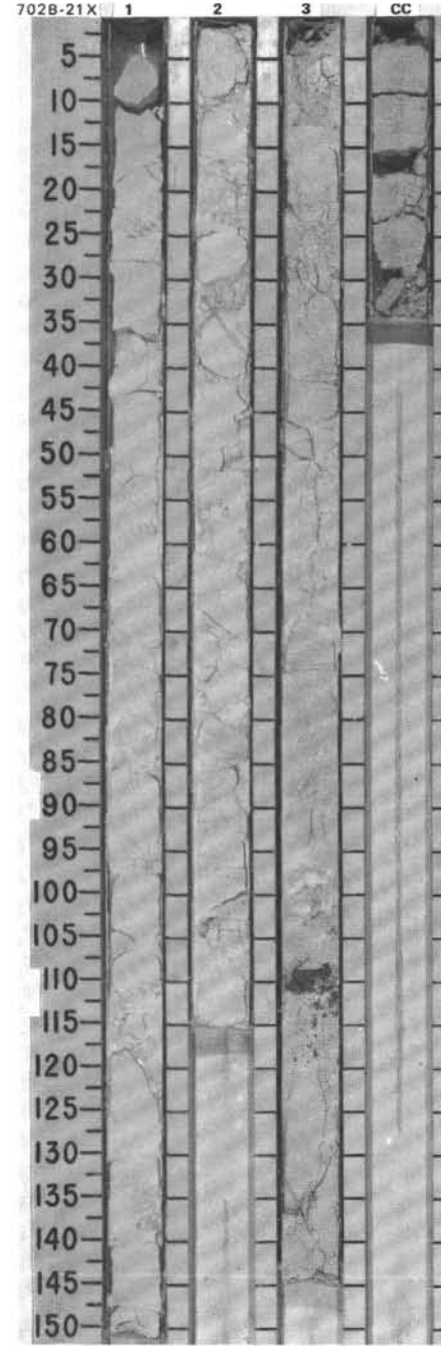


SITE 702 HOLE B CORE 20X CORED INTERVAL 3261.0-3270.5 mbsf; 177.3-186.8 mbsf

TIME-ROCK UNIT	BIOSTRAT. ZONE/ FOSSIL CHARACTER				PHYS. PROPERTIES	CHEMISTRY	SECTION	METERS	GRAPHIC LITHOLOGY	DRILLING DISTURB.	SED. STRUCTURES	SAMPLES	LITHOLOGIC DESCRIPTION												
	FORAMINIFERS	NANNOFOSSILS	RADIOLARIANS	DIAATOMS										SILICO- FLAGELLATES	PALEOMAGNETICS										
MIDDLE EOCENE	M. crater Zone				$\phi=49.42$		1	0.5					<p>NANNOFOSSIL CHALK</p> <p>Drilling disturbance: Moderately fractured.</p> <p>Major lithology: Nannofossil chalk (micrite-bearing in part, up to about 15%), white (no color code) to light gray (5Y 7/1). Bioturbation moderate in Section 1, 88-92 cm (<i>Planolites</i>), Section 4, 49-62 cm, and Section 5, 146-150 cm.</p> <p>Minor lithology: One mudstone clast in Section 3, 0-8 cm. Broken chert pieces in Section 3, 145-150 cm.</p> <p>SMEAR SLIDE SUMMARY (%):</p> <table style="margin-left: 20px;"> <tr><td></td><td>2, 6</td></tr> <tr><td></td><td>M</td></tr> </table> <p>COMPOSITION:</p> <table style="margin-left: 20px;"> <tr><td>Foraminifers</td><td>1</td></tr> <tr><td>Nannofossils</td><td>84</td></tr> <tr><td>Radiolarians</td><td>Tr</td></tr> <tr><td>Micrite</td><td>15</td></tr> </table>		2, 6		M	Foraminifers	1	Nannofossils	84	Radiolarians	Tr	Micrite	15
	2, 6																								
	M																								
Foraminifers	1																								
Nannofossils	84																								
Radiolarians	Tr																								
Micrite	15																								
LOWER MIDDLE EOCENE	P9				$\phi=49.42$		2	1.0																	
LOWER EOCENE	NP 14-15				$\phi=49.42$		3																		
UPPER LOWER EOCENE	Barren				$\phi=51.33$		4																		
	Barren				$\rho_g=2.84$		5																		
	Barren						6																		
							CC																		

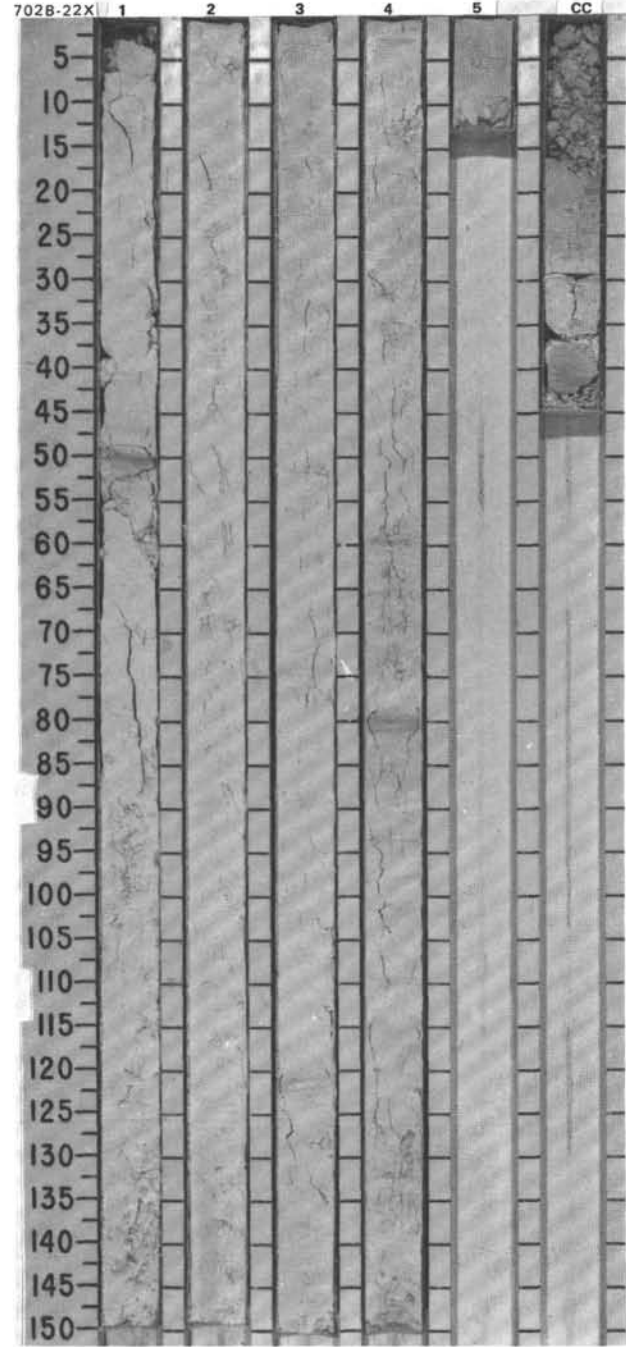


TIME-ROCK UNIT		BIOSTRAT. ZONE/ FOSSIL CHARACTER	FORAMINIFERS	NANNOFOSSILS	RADIOLARIANS	DIATOMS	SILICO- FLAGELLATES	PALEOMAGNETICS	PHYS. PROPERTIES	CHEMISTRY	SECTION	METERS	GRAPHIC LITHOLOGY	DRILLING DISTURB.	SED. STRUCTURES	SAMPLES	LITHOLOGIC DESCRIPTION																		
LOWER EOCENE	UPPER LOWER EOCENE																																		
<i>M. crater</i> Zone	P9			not examined	Barren	Barren	Barren				1	0.5					<p>NANNOFOSSIL CHALK</p> <p>Drilling disturbance: Moderately fractured.</p> <p>Major lithology: Nannofossil chalk, white (no color code), Faint bioturbation in Section 2, 81-115 cm, and Section 3, 0-112 cm (<i>Thalassinoides</i>, <i>Zoophycos</i>?, and <i>Planolites</i>).</p> <p>Minor lithology: "Slightly sandy" (because of foraminifer content in Section 3, 71-110 cm) micrite-bearing nannofossil chalk in Section 3, 76-77 cm, and 80 cm pieces at: Section 3, 110-112 cm.</p> <p>SMEAR SLIDE SUMMARY (%):</p> <table border="0"> <tr> <td></td> <td>1, 65</td> <td>3, 80</td> </tr> <tr> <td></td> <td>D</td> <td>D</td> </tr> </table> <p>COMPOSITION:</p> <table border="0"> <tr> <td>Volcanic glass</td> <td>Tr</td> <td>—</td> </tr> <tr> <td>Foraminifers</td> <td>3</td> <td>5</td> </tr> <tr> <td>Nannofossils</td> <td>89</td> <td>85</td> </tr> <tr> <td>Micrite</td> <td>8</td> <td>10</td> </tr> </table>		1, 65	3, 80		D	D	Volcanic glass	Tr	—	Foraminifers	3	5	Nannofossils	89	85	Micrite	8	10
	1, 65	3, 80																																	
	D	D																																	
Volcanic glass	Tr	—																																	
Foraminifers	3	5																																	
Nannofossils	89	85																																	
Micrite	8	10																																	
LNP 14										2	1.0																								
											3																								
											CC																								



SITE 702 HOLE B CORE 22X CORED INTERVAL 3280.0-3289.5 mbsl; 196.3-205.8 mbsf

TIME-ROCK UNIT	BIOSTRAT. ZONE/ FOSSIL CHARACTER					SECTION	METERS	GRAPHIC LITHOLOGY	DRILLING DISTURB.	SED. STRUCTURES	LITHOLOGIC DESCRIPTION																		
	FORAMINIFERS	NANNOFOSSILS	RAD/OLIVARIANS	DIATOMS	SILICO- FLAGELLATES							PALEOMAGNETICS	PHYS. PROPERTIES	CHEMISTRY															
LOWER EOCENE	UPPER LOWER EOCENE					1	0.5 1.0				<p>NANNOFOSSIL CHALK</p> <p>Drilling disturbance: Moderately fractured.</p> <p>Major lithology: Nannofossil chalk, white (10YR 8/1, 8/2). Bioturbation in Section 4, 55-92 cm.</p> <p>Minor lithology: Micrite-bearing nannofossil chalk, white (10YR 8/2) to light gray (5Y 7/1) in Section 1, 44-53 cm; Section 3, 74 and 120 cm; Section 4, 60-82 cm; Section 5, 0-13 cm; and CC, 0-38 cm. Micritic nannofossil chalk, very pale brown (10YR 8/3) in CC, 38-45 cm, with <i>Planolites</i> burrows.</p> <p>SMEAR SLIDE SUMMARY (%):</p> <table border="1"> <tr> <td></td> <td>1, 80</td> <td>4, 81</td> </tr> <tr> <td></td> <td>D</td> <td>D</td> </tr> </table> <p>COMPOSITION:</p> <table border="1"> <tr> <td>Clay</td> <td>—</td> <td>2</td> </tr> <tr> <td>Foraminifers</td> <td>5</td> <td>3</td> </tr> <tr> <td>Nannofossils</td> <td>85</td> <td>65</td> </tr> <tr> <td>Micrite</td> <td>10</td> <td>30</td> </tr> </table>		1, 80	4, 81		D	D	Clay	—	2	Foraminifers	5	3	Nannofossils	85	65	Micrite	10	30
	1, 80	4, 81																											
	D	D																											
Clay	—	2																											
Foraminifers	5	3																											
Nannofossils	85	65																											
Micrite	10	30																											
<i>P. wilcoxensis</i> Zone	M. crater Zone					2																							
NP 10-12	LOWER EOCENE P8]					3																							
	Barren					4																							
	Barren					5																							
	Barren					CC																							
	$\phi = 66.21$ $\rho_g = 4.15$																												

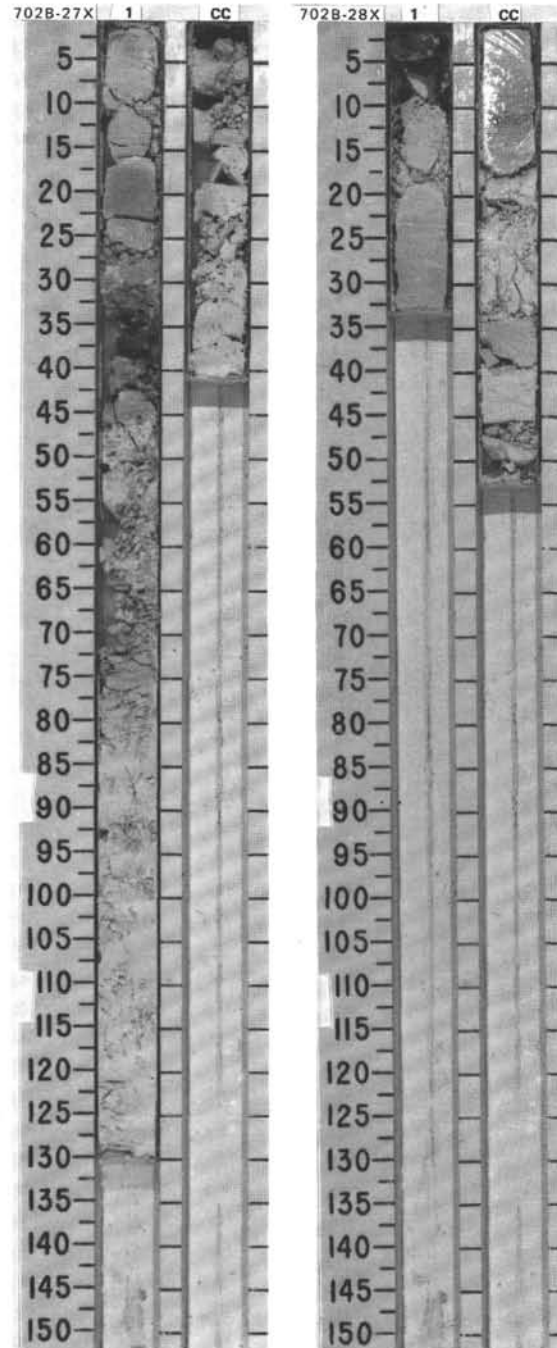


SITE 702 HOLE B CORE 27X CORED INTERVAL 3327.5-3337.0 mbsl; 243.8-245.3 mbsf

TIME-ROCK UNIT	BIOSTRAT. ZONE/ FOSSIL CHARACTER					CHEMISTRY	SECTION	METERS	GRAPHIC LITHOLOGY	DRILLING DISTURB.	SED. STRUCTURES	SAMPLES	LITHOLOGIC DESCRIPTION																						
	FORAMINIFERS	NANNOFOSSILS	RADIOLIARIANS	DIATOMS	SILICO- SUGELLATES									PALEOMAGNETICS	PHYS. PROPERTIES																				
UPPER PALEOGENE													<p>(MICRITIC) NANNOFOSSIL CHALK, INDURATED</p> <p>Drilling disturbance: Moderately fractured to drilling breccia.</p> <p>Major lithology: (Micritic) nannofossil chalk, indurated, white (no color code) to very indurated, light gray (5Y 7/1) in Section 1, 15-46 cm.</p> <p>SMEAR SLIDE SUMMARY (%):</p> <table style="margin-left: 20px;"> <tr> <td>1, 22</td> <td>CC,</td> </tr> <tr> <td>D</td> <td>D</td> </tr> </table> <p>COMPOSITION:</p> <table style="margin-left: 20px;"> <tr> <td>Volcanic glass</td> <td>Tr</td> <td>—</td> </tr> <tr> <td>Accessory minerals</td> <td>Tr</td> <td>—</td> </tr> <tr> <td>Foraminifers</td> <td>—</td> <td>Tr</td> </tr> <tr> <td>Nannofossils</td> <td>70</td> <td>70</td> </tr> <tr> <td>Radiolarians</td> <td>—</td> <td>Tr</td> </tr> <tr> <td>Micrite</td> <td>30</td> <td>30</td> </tr> </table>	1, 22	CC,	D	D	Volcanic glass	Tr	—	Accessory minerals	Tr	—	Foraminifers	—	Tr	Nannofossils	70	70	Radiolarians	—	Tr	Micrite	30	30
1, 22	CC,																																		
D	D																																		
Volcanic glass	Tr	—																																	
Accessory minerals	Tr	—																																	
Foraminifers	—	Tr																																	
Nannofossils	70	70																																	
Radiolarians	—	Tr																																	
Micrite	30	30																																	
UPPER PALEOGENE P5	NP 9		Barren	Barren	Barren	$\phi=45.44$	$R_0=2.85$				*																								

SITE 702 HOLE B CORE 28X CORED INTERVAL 3337.0-3346.5 mbsl; 253.3-262.8 mbsf

TIME-ROCK UNIT	BIOSTRAT. ZONE/ FOSSIL CHARACTER					CHEMISTRY	SECTION	METERS	GRAPHIC LITHOLOGY	DRILLING DISTURB.	SED. STRUCTURES	SAMPLES	LITHOLOGIC DESCRIPTION
	FORAMINIFERS	NANNOFOSSILS	RADIOLIARIANS	DIATOMS	SILICO- SUGELLATES								
UPPER PALEOGENE													<p>(MICRITIC) NANNOFOSSIL CHALK, INDURATED</p> <p>Drilling disturbance: Soupy to highly fragmented.</p> <p>Major lithology: (Micritic) nannofossil chalk, indurated, light gray (5Y 7/1) to greenish gray (5GY 6/1). <i>Planolites</i> in Section 1. <i>Zoophycos</i> and <i>Planolites</i> in CC, in indurated drilling biscuits.</p>
UPPER PALEOGENE P4	NP 8		Barren	Barren	Barren	$\phi=36.92$	$R_0=2.77$						

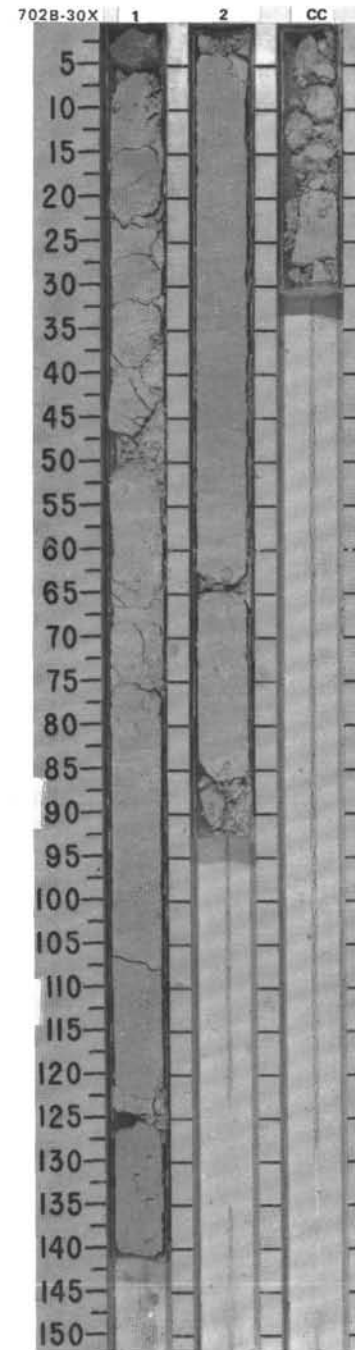
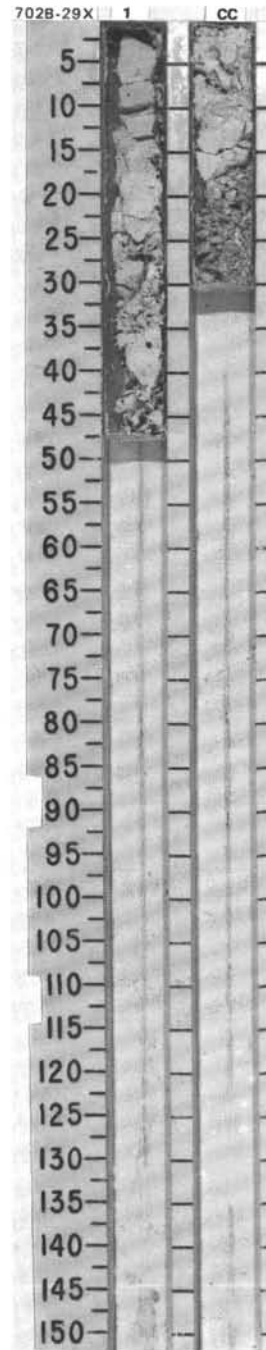


SITE 702 HOLE B CORE 29X CORED INTERVAL 3346.5-3356.0 mbsl; 262.8-272.3 mbsf

TIME-ROCK UNIT	BIOSTRAT. ZONE/ FOSSIL CHARACTER					CHEMISTRY	SECTION	METERS	GRAPHIC LITHOLOGY	DRILLING DISTURB. SED. STRUCTURES	SAMPLES	LITHOLOGIC DESCRIPTION
	FORAMINIFERS	NANNOFOSSILS	RADIOLARIANS	DIATOMS	SILICES- FLAGELLATES							
UPPER PALEOCENE	P4						1				*	(MICRITIC) NANNOFOSSIL CHALK, INDURATED Drilling disturbance: Drilling breccia. Major lithology: (Micritic) nannofossil chalk, indurated, white (no color code). Disseminated pebbles throughout Section 1 as drilling contamination. SMEAR SLIDE SUMMARY (%): 1, 25 D COMPOSITION: Foraminifers Tr Nannofossils 65 Radiolarians Tr Micrite 35
UPPER PALEOCENE	NP 8	Barten	Barten	Barten			0.5		X			

SITE 702 HOLE B CORE 30X CORED INTERVAL 3356.0-3361.0 mbsl; 272.3-277.3 mbsf

TIME-ROCK UNIT	BIOSTRAT. ZONE/ FOSSIL CHARACTER					CHEMISTRY	SECTION	METERS	GRAPHIC LITHOLOGY	DRILLING DISTURB. SED. STRUCTURES	SAMPLES	LITHOLOGIC DESCRIPTION
	FORAMINIFERS	NANNOFOSSILS	RADIOLARIANS	DIATOMS	SILICES- FLAGELLATES							
UPPER PALEOCENE	P4						1				*	MICRITE-BEARING NANNOFOSSIL CHALK Drilling disturbance: Moderately fractured to highly fragmented. Major lithology: Nannofossil chalk, micrite-bearing, white (no color code). Faint <i>Planolites</i> ?, <i>Zoophycos</i> , and composite <i>Planolites</i> traces in Section 1. Minor lithology: Micritic, foraminifer-bearing nannofossil chalk in Section 1, 100 cm. SMEAR SLIDE SUMMARY (%): 1, 18 1, 90 1, 100 D D M COMPOSITION: Quartz/feldspar 1 — — Foraminifers 6 — 12 Nannofossils 58 77 48 Micrite 35 23 40
UPPER PALEOCENE	NP 8	Barten	Barten	Barten			1.0					



SITE 702 HOLE B CORE 31X CORED INTERVAL 3361.0-3370.5 mbsl; 277.3-286.8 mbsf

TIME-ROCK UNIT	BIOSTRAT. ZONE/ FOSSIL CHARACTER					PHYS. PROPERTIES	SECTION	METERS	GRAPHIC LITHOLOGY	DRILLING DISTURB.	SED. STRUCTURES	SAMPLES	LITHOLOGIC DESCRIPTION
	FORAMINIFERS	NANNOFOSSILS	RADIOLARIANS	DIATOMS	SILICO- FLAGELLATES								
UPPER PALEOCENE													<p>(MICRITIC) NANNOFOSSIL CHALK, VERY INDURATED</p> <p>Drilling disturbance: Very disturbed to moderately fractured.</p> <p>Major lithology: (Micritic) nannofossil chalk, very indurated, light gray (5Y 7/1).</p> <p>Minor lithology: Chert nodule, gray (5Y 5/1), in Section 1, 82-88 cm.</p>
UPPER PALEOCENE P3b	NP 7-6	not examined				$\phi=38.19$	1						
			unzoned				CC						
			PALEOCENE										
			<i>Corbisena disymmetrica disymmetrica</i>										

SITE 702 HOLE B CORE 32X CORED INTERVAL 3370.5-3378.0 mbsl; 286.8-294.3 mbsf

TIME-ROCK UNIT	BIOSTRAT. ZONE/ FOSSIL CHARACTER					PHYS. PROPERTIES	SECTION	METERS	GRAPHIC LITHOLOGY	DRILLING DISTURB.	SED. STRUCTURES	SAMPLES	LITHOLOGIC DESCRIPTION
	FORAMINIFERS	NANNOFOSSILS	RADIOLARIANS	DIATOMS	SILICO- FLAGELLATES								
UPPER PALEOCENE													<p>NANNOFOSSIL CHALK, INDURATED, and MICRITE-BEARING CLAY-BEARING NANNOFOSSIL CHALK</p> <p>Drilling disturbance: Moderately fractured to highly fragmented.</p> <p>Major lithology: (Micritic) nannofossil chalk, indurated, white (5Y 8/1), in Section 1. Clay-bearing nannofossil chalk (micrite-bearing), light gray (5Y 7/1), in CC, 0-24 cm.</p> <p>Minor lithology: Pebbles (granodiorite, granite) as downhole contamination in Section 1, 0-21 cm. Limestone and chert, gray (5Y 6/1), in CC, 24-36 cm.</p> <p>SMEAR SLIDE SUMMARY (%):</p> <p style="margin-left: 40px;">CC, 20</p> <p style="margin-left: 40px;">D</p> <p>COMPOSITION:</p> <p style="margin-left: 20px;">Clay 10</p> <p style="margin-left: 20px;">Foraminifers 3</p> <p style="margin-left: 20px;">Nannofossils 77</p> <p style="margin-left: 20px;">Sponge spicules Tr</p> <p style="margin-left: 20px;">Micrite 10</p>
UPPER PALEOCENE P3b	NP 5-7	not examined				$\phi=13.34$	1						
			unzoned				CC						
			PALEOCENE										
			<i>Corbisena disymmetrica disymmetrica</i>										

